TURUN YLIOPISTON JULKAISUJA
ANNALES UNIVERSITATIS TURKUENSIS

SARJA - SER. D OSA - TOM. 1071

MEDICA - ODONTOLOGICA

ON GLUCOSE METABOLISM IN PATIENTS WITH THE m.3243A>G MUTATION

by

Markus Lindroos

TURUN YLIOPISTO
UNIVERSITY OF TURKU
Turku 2013

From the Department of Neurology and Turku PET Centre, University of Turku and Turku University Hospital, Turku, Finland

Research school membership: Turku Graduate School of Clinical Sciences

Supervised by

Professor Pirjo Nuutila, Turku PET Centre and the Department of Medicine, University of Turku and Turku University Hospital, Turku, Finland

and

Professor Kari Majamaa, the Department of Clinical Medicine, Neurology, University of Oulu, Oulu, Finland and the Department of Neurology, University of Turku and Turku University Hospital, Turku, Finland

Reviewed by

Professor John Vissing, Neuromuscular Research Unit, the Department of Neurology, Rigshospitalet, University of Copenhagen, Copenhagen, Denmark

and

Professor Ulla Ruotsalainen, the Department of Signal Processing, Tampere University of Technology, Tampere, Finland

Dissertation opponent

Professor Leif Groop, the Department of Clinical Sciences, Diabetes and Endocrinology, CRC at Skåne University Hospital, Lund University, Malmö, Sweden

ISBN 978-951-29-5395-0 (PRINT)
ISBN 978-951-29-5396-7 (PDF)
ISSN 0355-9483
Painosalama Oy, Turku, Finland 2013

To my family

ABSTRACT

Markus Lindroos

ON GLUCOSE METABOLISM IN PATIENTS WITH THE m.3243A>G MUTATION

The Department of Neurology and Turku PET Centre, University of Turku and Turku University Hospital, Turku, Finland
Annales Universitatis Turkuensis Ser. D
Painosalama Oy, Turku, Finland 2013

Background: The m.3243A>G mutation in mitochondrial DNA is the most common cause for mitochondrial diabetes. In addition, unexpected deaths related to the m.3243A>G associate with encephalopathy and cardiomyopathy. Failing mitochondrial respiratory chain in neurons, myocytes and beta cells is considered to underlie the multiorgan manifestations of the m.3243A>G.
Aims: The primary aim of the study was to characterize the organ-specific glucose metabolism in patients with m.3243A>G and secondly, to study patients with or without signs of diabetes, cardiomyopathy or encephalopathy. The insulin-stimulated glucose metabolism in brain, heart, skeletal muscle, adipose tissue and liver were measured with 2-deoxy-2-[^{18}F]fluoro-α-D-glucose in 15 patients and 14 controls. Brain oxygen metabolism was assessed with [^{15}O]oxygen and insulin secretion was modelled based on oral glucose tolerance test.
Results: The glucose oxidation in brain was globally decreased in patients with or without clinical encephalopathy. The insulin-stimulated glucose influx to skeletal muscle and adipose tissue was decreased in patients with or without diabetes as the hepatic glucose metabolism was normal. Impaired beta cell function and myocardial glucose uptake were associated with the high m.3243A>G heteroplasmy.
Conclusions: This cross-sectional study suggests that: 1) The ability of insulin to stimulate glucose metabolism in skeletal muscle and adipose tissue is weakened before

the beta cell failure results in mitochondrial diabetes. 2) Glucose oxidation defect is detected in otherwise unaffected cerebral regions in patients with the m.3243A>G, thus it likely precedes the clinical encephalopathy. 3) Uneconomical glucose hypometabolism during hyperinsulinemia contributes to the cardiac vulnerability in patients with high m.3243A>G heteroplasmy.

Keywords: The m.3243A>G mutation, glucose metabolism, mitochondria

TIIVISTELMÄ

Markus Lindroos

GLUKOOSIAINEENVAIHDUNTA m.3243A>G MUTAATION OMAAVILLA POTILAILLA

Neurologian oppiaine ja Valtakunnallinen PET-keskus, Turun yliopisto ja Turun yliopistollinen keskussairaala, Turku
Annales Universitatis Turkuensis Ser. D
Painosalama Oy, Turku, Finland 2013

Tausta: Mitokondriaalisen DNA:n m.3243A>G mutaatio on yleisin mitokondriaalisen sokeritaudin syy. Lisäksi m.3243A>G mutaatioon liittyvät odottamattomat kuolemat ovat yhteydessä aivo- ja sydänsairauteen. Mitokondriaalisen m.3243A>G mutaation aiheuttaman vian soluhengityksessä hermosoluissa, sydänlihassoluissa ja insuliinia erittävissä haimasoluissa ajatellaan johtavan tähän monielinsairauteen.
Tavoitteet: Väitöskirjatyön ensisijaisena tavoitteena oli määrittää eri elinten glukoosiaineenvaihduntaa m.3243A>G mutaation omavilla potilailla. Toissijainen tavoite oli tutkia potilaita, joilla ei ole tai joilla on merkkejä aivo-, sydän- tai sokeritaudista. Viidentoista potilaan ja neljäntoista verrokin glukoosin kudoksiin kulkeutuminen aivoissa, sydämessä, luurankolihaksessa, rasvakudoksessa ja maksassa mitattiin käyttäen 2-deoxy-2-[^{18}F]fluoro-α-D-glukoosi–positroniemissiotomografiaa insuliini-infuusion aikana. Aivojen hapen käyttö arvioitiin [^{15}O]-happea käyttäen ja insuliinineritys mallinnettiin sokerirasitustestin avulla.
Tulokset: Eri aivoalueiden glukoosin hapettuminen havaittiin vähentyneeksi, myös niillä potilailla, joilla ei ollut aivotaudin oireita. Insuliinin aktivoima glukoosinotto luurankolihakseen ja rasvakudokseen oli alentunut sekä sokeritautia sairastavilla että siltä säästyneillä potilailla, kun taas maksan glukoosiaineenvaihdunta todettiin tavanomaiseksi. Insuliinin eritys sekä sydänlihaksen glukoosin käyttö olivat vajavaisia, erityisesti potilailla, joilla on korkea m.3243A>G heteroplasmia-aste.

Päätelmät: Tämän poikkileikkaustutkimuksen perusteella: 1) Glukoosiaineenvaihdunnan insuliiniherkkyys vähenee rasvakudoksessa ja luurankolihaksessa jo ennen kuin haiman insuliinierityksen riittämättömyys johtaa mitokondriaaliseen sokeritautiin. 2) Koska glukoosin hapetus havaittiin alentuneeksi muuten oireettomilla aivoalueilla, niin se voi edeltää m.3243A>G potilaiden aivosairautta. 3). Epätaloudellisen alhainen glukoosin hyödyntäminen korkean insuliinipitoisuuden aikana rasittaa suuren m.3243A>G heteroplasmian omaavien potilaiden sydäntä.

Avainsanat: m.3243A>G pistemutaatio, glukoosiaineenvaihdunta

TABLE OF CONTENTS

ABSTRACT 4

TIIVISTELMÄ 6

TABLE OF CONTENTS 8

ABBREVIATIONS 11

LIST OF ORIGINAL PUBLICATIONS 13

1 INTRODUCTION 14

2 REVIEW OF THE LITERATURE 16
2.1 Human mitochondria 16
2.1.1 Mitochondrial DNA basic concepts 16
2.1.2 Maternal inheritance 18
2.1.3 Heteroplasmy and segregation 20
2.1.4 Mitochondrial structure and oxidative ATP production 21
2.2 Mitochondrial disease 25
2.2.1 Outlines of metabolic mitochondrial disease 25
2.2.2 Large-scale rearrangements in mtDNA 25
2.2.3 Point mutations in mtDNA 26
2.2.4 Mitochondrial disease due to mutations in nuclear DNA 27
2.2.5 Metabolic aspects of mitochondrial morphology 28
2.3 The m.3243A>G mutation in mtDNA 29
2.3.1 Clinical presentation of the m.3243A>G mutation 29
2.3.2 Epidemiology of the m.3243A>G mutation 31
2.3.3 Pathophysiology of the m.3243A>G mutation 32
2.3.3.1 Transcription failure 32
2.3.3.2 Electron transport chain deficiency 32
2.3.3.3 Carbohydrate and calcium metabolism 33
2.3.3.4 Glucose metabolism in models mimicking m.3243A>G disease 34
2.4 Brain metabolism and mitochondrial encephalopathy 36
2.4.1 Glucose metabolism in brain 36
2.4.1.1 Glucose as a neuronal substrate 36
2.4.1.2 Immediate carbohydrate oxidation in the brain 36
2.4.1.3 Glucose homeostasis and brain metabolism 37
2.4.1.4 Measuring human brain glucose metabolism 38
2.4.2 Mitochondrial encephalopathy 39
2.4.2.1 Clinical and pathological presentation 39
2.4.2.2 Imaging in mitochondrial encephalopathy 40
2.4.2.3 Brain metabolism in mitochondrial disease 41
2.5 Mitochondrial failure and adult-onset diabetes 41
2.5.1 Role of genetic background in adult-onset diabetes 41
2.5.2 Role of mitochondrial function in insulin secretion 43

2.5.3 Mitochondrial diabetes..... 44
2.5.3.1 Clinical presentation..... 44
2.5.3.2 Beta cell failure 45
2.6. The role of skeletal muscle in glucose homeostasis 46
2.6.1 Skeletal muscle metabolism 46
2.6.1.1 Nutritive metabolism in the skeletal muscle 46
2.6.1.2 Glucose transport to skeletal muscle during hyperinsulinemia 46
2.6.1.3 Insulin resistance and oxidative capacity..... 47
2.6.2 Metabolic aspects of mitochondrial myopathy 48
2.7 Mitochondrial and glucose metabolism in adipose tissue..... 49
2.7.1 Insulin action in adipose tissue..... 49
2.7.2 Adipogenesis and insulin resistance..... 50
2.7.3 Mitochondria in insulin-resistant adipocytes 51
2.8 The role of liver metabolism in glucose homeostasis…..... 51
2.8.1 Hepatic glucose metabolism and insulin resistance 51
2.8.1.1 Glucose metabolism in liver..... 51
2.8.1.2 Endogenous glucose production and diabetes 52
2.8.1.3 Measuring glucose influx to liver..... 53
2.8.2 Liver fat and hepatic failure in mitochondrial disease..... 54
2.9 Glucose utilization in human heart..... 55
2.9.1 Cardiac energetics..... 55
2.9.1.1 Myocardial substrate oxidation 55
2.9.1.2 Myocardial glucose uptake during hyperinsulinemia 56
2.9.2 Mitochondrial cardiomyopathy..... 57
2.9.2.1 General outlines 57
2.9.2.2 Cardiac manifestations of the m.3243A>G mutation 58
2.9.2.3 Pathophysiology of mitochondrial cardiomyopathy..... 58

3 AIMS OF THE STUDY..... 60

4 SUBJECTS AND STUDY DESIGN..... 61
4.1 Study subjects..... 61
4.2 Study design..... 62
4.2.1 General outlines..... 62
4.2.2 Performing PET during euglycemic hyperinsulinemia 63
4.2.3 Primary variables and power calculations 64
4.3 Safety and ethical considerations 65

5 METHODS 66
5.1 Assessment of the mutation heteroplasmy 66
5.2 Glucose tolerance test and the indices of the beta cell function 66
5.3 Magnetic resonance imaging and spectroscopy 67
5.3.1 Brain magnetic resonance imaging and spectroscopy 67
5.3.2 Cardiac magnetic resonance imaging..... 68
5.3.3 Abdominal fat depots..... 69
5.3.4 Assessment of liver fat content with [^{1}H]MRS..... 69
5.4 Indirect calorimetry..... 69
5.5 Euglycemic hyperinsulinemia..... 70
5.6 PET-imaging 71
5.6.1 Production of PET tracers 71

5.6.2 Image acquisition..... 71
5.6.3 Quantification of the PET data 72
5.6.3.1 Tissue glucose uptake rate 72
5.6.3.2 Muscle and brain perfusion 73
5.6.3.3 Brain oxygen metabolism..... 74
5.6.4 Tissue analysis..... 75
5.6.4.1 Brain..... 75
5.6.4.2 Myocardium, skeletal muscle, liver and adipose tissue 76
5.7 Biochemical analyses and cytokines..... 76
5.8 Statistical methods..... 77
5.8.1 General analysis..... 77
5.8.2 Statistical approach to multiple regions of interest in brain..... 78
5.8.3 Statistical parametric mapping approach..... 79

6 RESULTS..... 81
6.1 Feasibility of the study protocol (I-IV)..... 81
6.2 Brain metabolism (I)..... 81
6.2.1 Clinical encephalopathy and white matter [^{1}H]MRS 81
6.2.3 Oxidative glucose metabolism in the brain..... 82
6.3 Metabolic characteristics related to insulin secretion and action (II-IV) 85
6.4 Insulin secretion and beta cell function (II) 87
6.5 Skeletal muscle glucose uptake and perfusion (II)..... 90
6.6 Adipose tissue metabolism and adipocytokines (III)..... 92
6.7 Liver metabolism (III)..... 94
6.8 Cardiac glucose uptake (IV)..... 95

7 DISCUSSION..... 99
7.1 Synopsis 99
7.2 Brain glucose oxidation in the presence of the m.3243A>G mutation..... 100
7.3 Insulin secretion in patients with the m.3243A>G mutation 103
7.4 Skeletal muscle insulin resistance in mitochondrial diabetes..... 105
7.5 Adipose tissue metabolism during hyperinsulinemia 108
7.6 The role of liver metabolism in mitochondrial diabetes..... 110
7.7 Metabolic aspects of mitochondrial cardiomyopathy 112

8 CONCLUSIONS..... 115

9 ACKNOWLEDGEMENTS..... 117

10 REFERENCES..... 119

ORIGINAL PUBLICATIONS..... 145

ABBREVIATIONS

[^{15}O]H_2O	[^{15}O]-water
[^{18}F]FDG	2-deoxy-2-[^{18}F]fluoro-α-D-glucose
[^{1}H]MRS	[^{1}H] magnetic resonance spectroscopy
ADP	adenosine- 5'-diphosphate
ANOVA	analysis of variance
ATP	adenosine- 5'-triphosphate
BMI	body mass index
BSR	basal insulin secretion rate
CNS	central nervous system
CoA	coenzyme A
COX	cytochrome c oxidase
Cr	creatine
CSF	cerebrospinal fluid
DNA	deoxyribonucleic acid
EE	energy expenditure
EEG	electroencephalography
EGP	endogenous glucose production
ETC	electron transport chain
FAD	flavin adenine dinucleotide
FFA	free fatty acid
GIS	glucose-induced insulin secretion
GK	glucokinase
GLUT	glucose-specific transporter protein
Hb-$A1_C$	glycosylated haemoglobin
HK II	hexokinase II
IGI	insulinogenic index
KO	knockout
LHON	Leber's hereditary optic neuropathy
LVGU	left ventricular glucose uptake
LVH	left ventricular hypertrophy
LS	Leigh Syndrome
MELAS	mitochondrial encephalomyopathy, lactic acidosis, and stroke-like episodes
MERRF	myoclonic epilepsy with ragged red fibres
MIDD	maternally inherited diabetes and deafness
MODY	maturity-onset diabetes of the young
MRI	magnetic resonance imaging
MT-ATP	mitochondrial ATP synthase F0 subunits encoding genes
MT-COX	mitochondrial cytochrome c oxidase subunits encoding genes
MT-CYB	mitochondrial cytochrome b encoding gene
MT-ND	mitochondrial NADH dehydrogenase subunits encoding genes
MT-TL1	mitochondrially encoded tRNA leucine 1 (UUA/G)

mtDNA	mitochondrial DNA
NAA	N-Acetyl-L-aspartic acid
NAD	nicotinic acid adenine dinucleotide
NARP	neuropathy, ataxia and retinitis pigmentosa
OGTT	oral glucose tolerance test
OXPHOS	oxidative phosphorylation
PDH	pyruvate dehydrogenase
PEO	progressive external ophthalmoplegia
PET	positron emission tomography
PGC-1	PPAR gamma coactivator 1
POLG	mitochondrial DNA polymerase gamma
PPAR	peroxisome proliferator-activated receptor
rCBF	regional cerebral blood flow
$rCMRO_2$	regional cerebral metabolic rate of oxygen
rGMR	regional glucose metabolic rate
RNA	ribonucleic acid
ROI	region of interest
RRF	ragged red fibre
SD	standard deviation
SV	stroke volume
TE	echo time
TFAM	mitochondrial transcription factor A
TNF- α	tumour necrosis factor α
TR	repetition time
VO_2 max	maximal oxygen uptake
WPW	Wolff– Parkinson–White

LIST OF ORIGINAL PUBLICATIONS

This thesis is based on the following original publications, which are referred to in the text by the corresponding roman numerals I-IV. Unpublished data are also presented.

I **Lindroos MM**, Borra RJ, Parkkola R, Virtanen SM, Lepomäki V, Bucci M, Virta JR, Rinne JO, Nuutila P, Majamaa K. Cerebral oxygen and glucose metabolism in patients with mitochondrial m.3243A>G mutation. Brain 2009: 132; 3274–3284. Reprinted in agreement with Oxford University Press.

II **Lindroos MM,** Majamaa K, Tura A, Mari A, Kalliokoski KK, Taittonen MT, Iozzo P, Nuutila P. m. 3243A>G mutation in mitochondrial DNA leads to decreased insulin sensitivity in skeletal muscle and to progressive β-cell dysfunction. Reprinted by permission of the American Diabetes Association. From Diabetes, Vol. 58, 2009;543-549.

III **Lindroos MM,** Borra RJ, Mononen N, Lehtimäki T, Virtanen KA, Lepomäki V, Guiducci L, Iozzo P, Majamaa K, Nuutila P. Mitochondrial diabetes is associated with insulin resistance in subcutaneous adipose tissue but not with increased liver fat content. Journal of Inherited Metabolic Disease 2011: 34; 1205-1212. Reprinted with kind permission from Springer Science and Business Media

IV **Lindroos MM,** Pärkkä JP, Taittonen MT, Iozzo P, Kärppä M, Hassinen I, Knuuti J, Nuutila P, Majamaa K. Myocardial glucose uptake in patients with the mitochondrial m.3243A>G mutation in mitochondrial DNA. Submitted.

1 INTRODUCTION

Disorders arising from mutations in the maternally inherited mitochondrial deoxyribonucleic acid (mtDNA) frequently affect the central nervous system (CNS), cardiac muscle and other organs with high energy needs. These mutations in mtDNA are heteroplasmic, i.e. the proportion of the mutated mtDNA varies across tissues, in part contributing to heterogeneous clinical phenotypes (Mariotti et al. 1995). Decreased respiratory chain activity and increased glucose utilization due to the compensatory rise in anaerobic adenosine-5'-triphosphate (ATP) production characterizes metabolism in cultured cells harbouring mutated mtDNA (de Andrade et al. 2006). The m.3243A>G point mutation is the most common pathogenic mutation in mtDNA (Majamaa et al. 1998; Man et al. 2003). It was first associated with the classical phenotype including mitochondrial encephalomyopathy, lactic acidosis and stroke-like episodes (MELAS; Goto et al. 1990). The lactate is elevated both in blood and cerebrospinal fluid (CSF) in these patients (Kaufmann et al. 2004). The full-blown MELAS syndrome is a rare manifestation in adults with m.3243A>G, while other manifestations, such as diabetes mellitus, sensorineural hearing impairment and left ventricular hypertrophy (LVH) are more common (Majamaa-Voltti et al. 2006). The involvement of mtDNA mutations in the hereditary forms of diabetes is evident (Whittaker et al. 2007). The m.3243A>G mutation in mtDNA accounts for ~1% of adult-onset diabetes and is the most common cause of mitochondrial diabetes (Katulanda et al. 2008). This mutation is highly diabetogenic as most of its carriers develop diabetes during their lives (Guillausseau et al. 2001). Interestingly, also in the common form of adult-onset diabetes, changes in respiratory chain function in key tissues contributing to the glucose homeostasis have been suggested to underlie both the decrease in the insulin action in hepatic, adipose and muscle tissues and to diminish the glucose sensitivity of the pancreatic beta cells already before the onset of type 2 diabetes (Phielix et al. 2008; Patti and Corvera. 2010). This renders the m.3243A>G mutation as a potential pathogenic model to study the role of mitochondrial failure in diabetes.

Insulin action in metabolic active tissues important for the glucose homeostasis, such as the liver, adipose tissue and to some extent the skeletal muscle has not been studied in detail in patients with the m.3243A>G mutation. Most but not all patients with the m.3243A>G display defects in glucose-induced insulin secretion (GIS)(Velho et al. 1996; Hosszufalusi et al. 2009; Brändle et al. 2001). Patients with m.3243A>G also show a decreased oxidation capacity in their skeletal muscles as well as in isolated myocytes harbouring the mutation (Jeppesen et al. 2006; Vydt et al. 2007; Silvestri et al. 2000). The possible threshold effect of the heteroplasmy to insulin secretion or action has not been clarified. In the heart, the phosphocreatine to ATP ratio has been shown to be decreased, somewhat resembling the findings in more common diseases such as diabetes and sporadic LVH (Lodi et al. 2004). Apart from the genetic aetiology and the biochemical defect in isolated cells the metabolic pathophysiology of mitochondrial encephalopathies, diabetes and cardiomyopathy have been poorly elucidated in these patients. No controlled studies aiming to quantify cerebral glucose and oxygen metabolism have been carried out in order to understand the metabolic encephalopathy in patients carrying the m.3243A>G mutation. The purpose of this cross-sectional study was firstly, to quantify regional glucose and oxygen metabolism in the brain in patients harbouring the m.3243A>G mutation using positron emission tomography (PET). Secondly, the GIS was measured and modelled after glucose ingestion. Thirdly, the insulin-stimulated glucose uptake rate was assessed in skeletal muscle, subcutaneous adipose tissue, liver and myocardium by tracking the injected glucose analogue-tracer in the tissues with PET scanning during insulin infusion. The results of the organ specific glucose metabolism were then reported in the context of other manifestations, such as brain atrophy, glucose tolerance, physical activity, adipocytokine levels, liver fat content and the measures of left ventricle function.

2 REVIEW OF THE LITERATURE

2.1 Human mitochondria

2.1.1 Mitochondrial DNA basic concepts

The presence of DNA within mitochondria was described in 1960s (Nass and Nass 1963). The mitochondrial DNA (mtDNA) is a circular, double-stranded structure of 16,569 base pairs, which is organized in discrete dynamic protein-rich nucleotides within the mitochondrial network (Figure 1)(Andrews et al. 1999; Garrido et al. 2003). Mitochondria are polyploid organelles, each mitochondrion containing two to ten copies of its DNA. Mitochondrial DNA is considered to be a remnant from the protobacteria that populated eukaryotic cells about 1.5 billion years ago. During the evolution the mitochondrial mtDNA became a compact molecule with contiguous coding sequences containing no introns or repeats. The continuous replication of mtDNA is seemingly independent of cell cycle i.e. relaxed (Bogenhagen and Clayton. 1977). The mitochondria may replicate their DNA and divide in response to the energy needs of the cell (Hock and Kralli. 2009). The replication of mtDNA proceeds by a strand-coupled mechanism. It relies on nuclear-encoded proteins, such as mitochondrial DNA polymerase gamma (POLG), mitochondrial helicase Twinkle and the mitochondrial single-stranded DNA binding protein. Also the mitochondria specific topoisomerases and ribonucleic acid (RNA) polymerase are involved (Mao and Holt. 2009; Pohjoismäki et al. 2010). The differences in replication rates between mutant and wild-type mtDNA have been proposed to partly explain the late onset and progression in some mitochondrial disorders (Chinnery and Samuels. 1999).

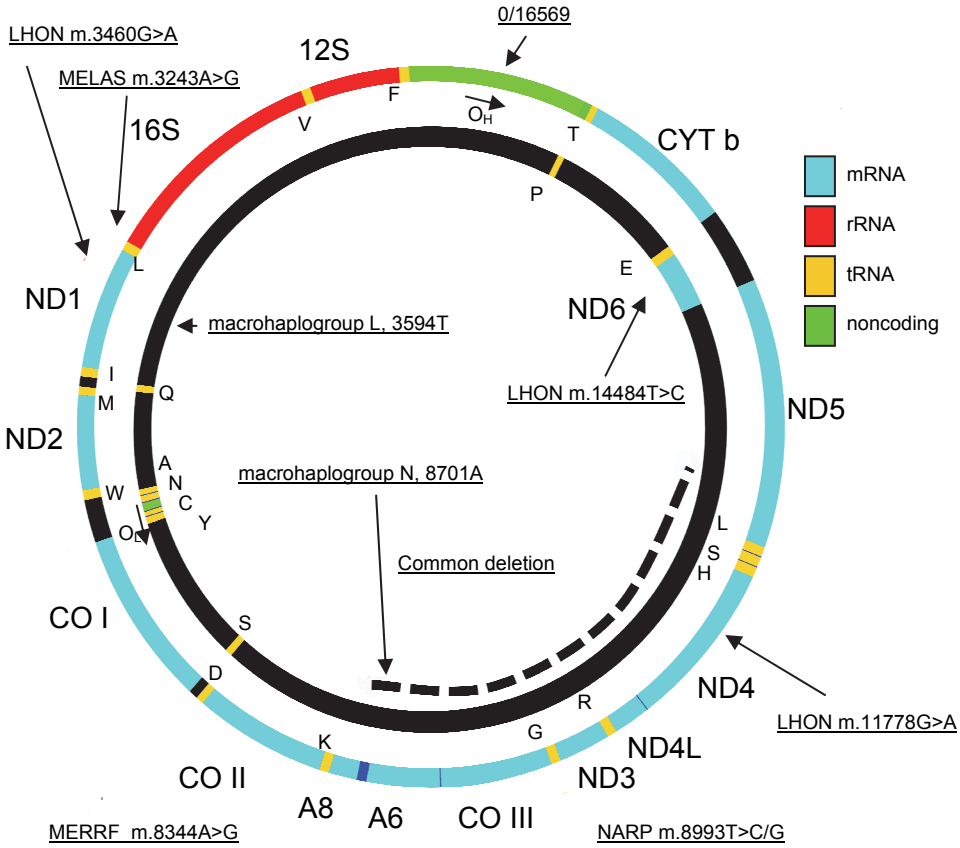

Figure 1. Mitochondrial DNA. The location of the genes, encoding respiratory chain complex protein subunits are shown. The ND1-6 and ND4L (complex I), CYT b (complex III), CO I–III (complex IV) and A6 and 8 (complex V, ATP synthase). Non-coding control region encompasses the heavy-strand and light-strand promoter proteins and includes the heavy strand (outer ring) origin of replication (O_H). Location of some of the well known mitochondrial point mutations and their classical presentations are indicated: m.3243A>G, mitochondrial encephalomyopathy, lactic acidosis, and stroke-like episodes (MELAS), m.11778 G>A, 14484 T>C and m.3460G>A, Leber's hereditary optic neuropathy (LHON), 8344A>G, myoclonic epilepsy with ragged red fibres (MERRF), 8993T>C/G neuropathy, ataxia and retinitis pigmentosa (NARP). The site of common deletion, which is a frequent cause of Kearns-Sayre syndrome and progressive external ophthalmoplegia (PEO) is shown with a broken line. As an example two haplogroup markers are shown: macrohaplogroup L, 3594T (L0, L1, L2) versus 3594C (L3, M, N), macrohaplogroup N, 8701A (versus M and L0-3, 8701G) plus 10398A (10398A for European lineages T/W/X/K2, and L/J/I/K1 are 10398G). mRNA = messenger RNA, rRNA = ribosomal RNA, and tRNA = transfer RNA.

Mitochondrial DNA has a slightly different genetic code as compared to nuclear DNA and the expression of the different code relies on the mitochondrial coded ribosomal RNAs 12S and 16S and to 22 transfer RNAs (Barrell et al. 1979; Clayton. 2000). Nuclear-encoded transcriptional factors, such as mitochondrial transcription factor A (TFAM) and B2 (TFB2M) co-operate with mitochondrial monomeric RNA polymerase and associate with promoters of the C-rich light-strand and the G-rich heavy-strand in the 1121-nucleotide non-coding control region. These three proteins are essential for basal transcription of human mtDNA. The mitochondrial transcription termination factor (MTERF) protein family regulates transcription termination and is needed for the proper translation (Litonin et al. 2010). The remaining 13 mitochondrial genes are transcribed to messenger RNAs to be further translated to form polypeptide subunits, which are structurally involved in proton-translocation in the oxidative respiratory chain (Figure 1 and 2). These are the mitochondrial nicotinic acid adenine dinucleotide (NAD) dehydrogenase subunits 1-6, 4L encoding genes (MT-ND1–6, L4), which encode seven of the 45 polypeptides of the respiratory chain complex I, cytochrome b encoding gene (MT-CYB), which encodes one of the 11 subunits of the complex III, mitochondrial cytochrome c oxidase subunits encoding genes (MT-COX1–3), which encode three of the 13 polypeptides in the complex IV, additionally mitochondrial ATP synthase F0 subunits encoding genes (MT-ATP6 and 8) encode two of the sixteen subunits in the complex V (Figure 1).

2.1.2 Maternal inheritance

In contrast to the nuclear genes, the mitochondria and the mtDNA originate from mother's oocyte. Therefore only the daughters transmit the mtDNA to the next generation (Giles et al. 1980). Thus, maternal inheritance is an important clue to the diagnosis of mtDNA-related disorders. Human sperm contains hundreds of mtDNA copies per cell and the number is probably downregulated in mammalian spermatogenesis (Rantanen et al. 2001). Thereby it becomes diluted when it is combined with the ca. 100,000-200,000 mtDNA copies from the oocyte (Chen et al.

1995). Furthermore, during spermatogenesis the sperm mitochondrial outer membrane proteins become ubiquitinated and just after fertilization the paternal mtDNAs are selectively recognized and removed (Nishimura et al. 2006). The analyses of infants born after intracytoplasmic sperm injection have clearly failed to identify paternal mtDNA with methods capable of detecting levels as low as 0.001% (Marchington et al. 2002). However, in mammal interspecific crosses the sperm mtDNAs can occasionally persist (Kaneda et al. 1995). There is at least one verified case of the paternal inheritance in humans. This was a patient with mitochondrial myopathy and a paternal inherited mtDNA with microdeletion in ND2 found only in muscle. In addition, this case also proved that mtDNA molecules may recombine as few of the maternal and paternal mtDNAs had recombined in the muscle (Kraytsberg et al. 2004). This case has then been proven to be the exception that confirms the maternal inheritance rule as subsequent studies have not found more evidence of the paternal inheritance of mtDNA (Taylor et al. 2003a).

The mtDNA sequence is well-conserved from one generation to another and intra- and intermolecular recombination in mtDNA seldom occurs (D'Aurelio et al. 2004). This lack of recombination and the strict maternal inheritance makes the mtDNA a useful tool in population studies, where it enables to track the maternal line through generations (Giles et al. 1980; Elson et al. 2001). On the other hand, the mutation rate in mtDNA is several times higher than that in the nuclear DNA giving the mtDNA its characteristic polymorphic variation (Finnilä et al. 2001). Mitochondrial DNA is highly polymorphic, and any two individuals differ with tens of base pairs on average (Finnilä et al. 2001). Based upon combinations of polymorphisms in the mtDNA accumulated since the last common mtDNA ancestor, the mtDNA molecules can be sorted to different haplotypes (Figure 1). Using these haplotypes the mutational history of human mtDNA as well as the geographical maternal line can be reconstructed as a single sequential mutational tree (Pierron et al. 2011). Interestingly, some of the geographic variation in mtDNA between populations is poorly explained by random fluctuation. Therefore, part of the non-random mtDNA variation has been suggested to

result from natural selection as the population has adapted to environmental factors such as temperature (Ruiz-Pesini et al. 2004). Haplotypes are arranged to haplogroups by convention and may have importance in genetic counselling. This is because some of the pathogenic mitochondrial mutations have a lower or higher tendency to generate disease manifestations i.e. low or high penetrance if they coexist with a certain haplogroup in mtDNA (Hudson et al. 2007).

2.1.3 Heteroplasmy and segregation

Each human cell has hundreds to thousands of mtDNAs. Usually, all mtDNA molecules in a cell or tissues are identical, a condition known as homoplasmy. However, mutations in mtDNA are characterized by the coexistence of wild type and mutant mtDNA in various proportions within each cell and intraindividually in various tissues. This situation is called heteroplasmy (Whittaker et al. 2009). In cell division, the human wild type and mutant mtDNAs are passed into daughter cells apparently at random. Thus the degree of heteroplasmy may shift and the phenotype may change accordingly. This mechanism resulting in an arbitrary ratio of wild type and mutant mtDNA into the two daughter cells is called mitotic segregation (Brown et al. 2001; Jenuth et al. 1996). A similar random drift partly explains the variation in heteroplasmy between generations, among offspring of the same mother, in various tissues or between individual muscle fibres in one individual (Elson et al. 2001). The term genetic bottleneck refers to a restriction in the number of mitochondrial genomes transmitted between generations. The number of mtDNA copies passed along from mother to child is small, five to 200 copies (Kaneda et al. 1995). Thus at the population level, new mtDNA mutations become segregated in few generations to relatively near homoplasmy and are likely to be exposed rapidly to natural selection (Cree et al. 2008). Otherwise the lack of recombination in combination with biparental inheritance pattern would allow deleterious mitochondrial mutations with a replicative advantage to rapidly spread throughout the population. Therefore it has been speculated that natural selection may prefer a uniparental, i.e. the maternal inheritance pattern of mtDNA (Korpelainen. 2004). Whether the genetic bottleneck

takes place during early oogenesis through the random segregation of the estimated 100,000-200,000 mtDNA molecules in human oocytes or rather during postnatal folliculogenesis is not entirely clear (Cree et al. 2008; Wai et al. 2008). Purifying selection in transmission of mammalian mitochondrial DNA occurs in the female germ line. This reduces the impact of severe mutations at the population level (Fan et al. 2008; Stewart et al. 2008). The clinical implications of the segregation and purifying mechanism are that in case of heteroplasmic mutations a high proportion of mutant load in the mother relatively rarely results in a severe defect in the off-spring. It has been shown that the maternal transmission rate of a disease may be under 5% in case of large scale mtDNA deletions (Chinnery et al. 2004).

2.1.4 Mitochondrial structure and oxidative ATP production

The histological appearance of the mitochondria is a double-membrane organelle with faint, thread-like granular appearance located in cytoplasm. The mitochondrial shape, DNA organisation and proteome expression are highly tissue specific (Pohjoismäki et al. 2009; Mootha et al. 2003). In general, *the outer mitochondrial membrane* includes transport system proteins, such as protein pores permeable up to 5000 dalton, the translocase-of-the-outer-membrane for active transport of larger proteins, proteins for fatty acids elongation and transport, mitochondrial fusion proteins, and enzymes, such as monoamine oxidase (Li et al. 2009). *The intermembrane milieu* resembles the cytoplasm and it includes enzymes, such as creatine kinase. *The inner mitochondrial membrane* is protein rich containing more than 100 different polypeptides, including the megadalton complexes of the electron transport chain (ETC) and the ATP synthase, altogether equalling 1 protein to 15 membrane phospholipids (Figure 2). The inner mitochondrial membrane lacks porins and is highly impermeable to all molecules including small charged ions. Therefore transporters, such as the translocases of the inner membrane are required to supply the nuclear encoded proteins into the mitochondrial matrix (Sirrenberg et al. 1996). *The intramitochondrial space*, i.e. the mitochondrial matrix, contains approximately 2/3 of the over one thousand mitochondrial proteins, such as the enzymes of citric acid cycle, beta-oxidation and

ribosomes as well as tRNAs and mtDNAs (Figure 2)(The MitoP2 database, http://www.mitop.de; Zhang et al. 2008; Li et al. 2009).

In the mitochondrion, the citric acid cycle oxidizes the acetyl coenzyme A (acetyl-CoA) derived from glucose or fatty acids and reduces the cofactors NAD and flavin adenine dinucleotide (FAD), which then provide electrons for the ETC (Figure 2) (Sazanov and Jackson. 1994). ETC transfers the electrons through a series of tightly coupled and controlled oxidation–reduction reactions into the molecular oxygen. This transfer is coupled to proton export across the inner membrane. Thus, the ETC ultimately converts the energy from plant hydrocarbons into a hydrogen gradient across the inner mitochondrial membrane (Rich. 2003). The potential energy in this electrochemical gradient is then allocated to synthesize ATP from adenosine- 5'-diphosphate (ADP) via complex V or to heat production via mitochondrial proteins, which uncouple the proton influx from ATP synthesis (Saraste. 1999; Azzu and Brand. 2010). The importance of the mitochondrial proton gradient for natural selection becomes evident when the present mitochondrial genome is compared with the α-protobacterial genome. Approximately 99% of the protomitochondrial protein coding genes have disappeared or have been incorporated into the nuclear DNA and at present, all the proteins expressed by the human mtDNA are structural subunits closely linked to proton transport in complexes I, III and IV and V (Adams and Palmer. 2003).

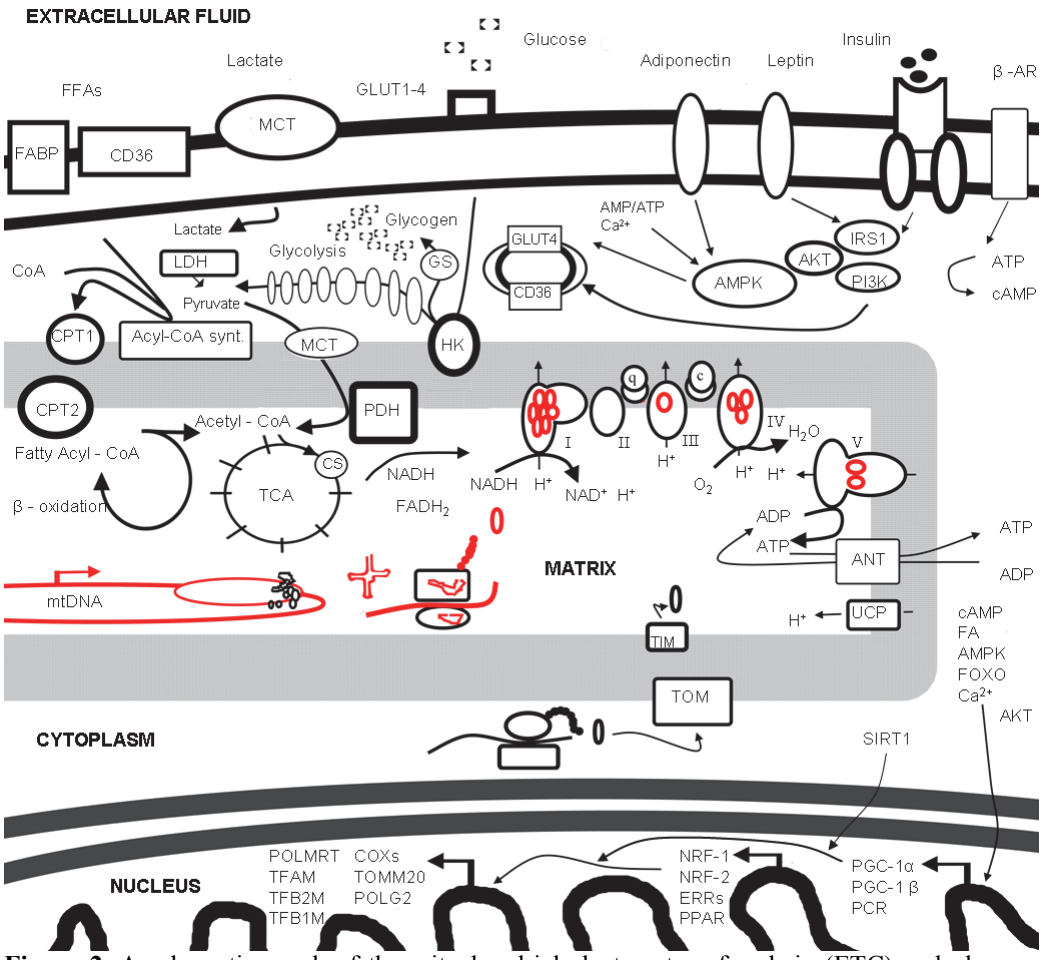

Figure 2. A schematic graph of the mitochondrial electron transfer chain (ETC) and glucose metabolism in the cell. Protein encoding genes in mitochondrial DNA (red) are transcribed to messenger RNAs (red) to be further translated in ribosomes with help of mitochondrial transfer and ribosomal RNAs (red) to form polypeptide subunits (red), which are structurally involved in proton-translocation in the oxidative respiratory chain (red). Respiratory chain complexes are indicated with I-V. Fatty acid (FA) transport is facilitated to cytosol via transport proteins such as translocase / the homologue of human CD36 (FAT/CD36), plasma membrane associated binding protein (FABPpm), and possibly via transport protein (FATP). Acyl-coenzyme A (CoA) is added and the hydrocarbons are further transported to mitochondria via respective transporters such as carnitine palmitoyltransferases I and II (CPT1 and 2) and carnitine-acylcarnitine translocase. Acetyl-CoAs are repetitively removed and ATP is generated in the beta-oxidation. Transmembrane glucose transporters (GLUT1-4). GLUT4 and CD36 are translocated to cell surface in response to insulin or exercise. In cytosol hexokinase (HK) converts glucose to glucose-6-phosphate (G6P), which is the first step of both glycogen synthesis and glycolysis. G6P enters the anaerobic glycolysis, which produces pyruvate, lactate and ATP. Lactate and pyruvate transport across mitochondrial and plasma membrane is facilitated by monocarboxylate transporters (MCTs). Citrate synthase (CS) is the pace-making first step of the tricarboxylic acid (TCA) cycle. Pyruvate dehydrogenase transforms pyruvate to acetyl-CoA which enters to TCA cycle. TCA cycle oxidizes the acetyl-CoA and reduces

nicotinamide adenine dinucleotide (NAD) and flavin adenine dinucleotide (FAD). NADH and $FADH_2$ then provide electrons into molecular oxygen (oxidation) via complex I and II and the rest of the ETC. This electron flow to oxygen is coupled with proton pumping through the inner mitochondrial membrane and a hydrogen gradient is established. This gradient i.e. membrane potential can be dissipated to heat by uncoupling proteins (UCP) or converted to ATP by ATP synthase (V). ADP and ATP are exchanged between the mitochondrial matrix and the cytoplasm via Adenine nucleotide translocator (ANT). Different physiological signals such as cold, muscle contraction, insulin, starvation may activate mitochondrial proliferation. This proliferation is regulated by activating different promoters in the coactivator genes such as PGC-1α. Their transcripts in turn *trans* activate an array of transcription factors such as NRF-1, which in turn increases expression of proteins needed for mitochondrial structure, metabolism and mtDNA processing. Such proteins include for instance COX17, TOM20, TFAM and POLG. SIRTs exert post transcript activation of PGC-1α in response to starvation. Adiponectin and leptin bind to their plasmamembrane receptors and activate intracellular pathways. GS = Glycogen synthase. TIM = Translocase of the inner membrane. TOM = Translocase of the outer membrane. IRS1 = insulin receptor substrate 1, AMPK = AMP-activated protein kinase, SIRT1 = silent information regulator T1, peroxisome proliferator-activated receptor (PPAR) gamma co-activator 1α (PGC-1α). β-AR = β-Adrenergic Receptor. LDH = lactate dehydrogenase. AKT = Protein Kinase B, FA =Fatty acid, NRF1 and 2 = Nuclear Respiratory Factors 1 and 2, PI3K = Phosphatidylinositol 3-kinases, cAMP= Cyclic adenosine monophosphate. FOXO = Forkhead box proteins O, ERR = Estrogen related receptor.

2.2 Mitochondrial disease

2.2.1 Outlines of metabolic mitochondrial disease

The first case report on a mitochondrial disease was a patient with a notable increase in basal metabolic rate and lack of coupling of oxidation and phosphorylation in muscle mitochondria (Luft et al. 1962). However, it became early evident that the failing respiratory chain function is the hall mark of mitochondrial diseases (Willems et al. 1977). Besides the respiratory chain, biochemical defects in other major steps of mitochondrial metabolism were identified. These include the enzymes limiting substrate utilization, (Blass et al. 1970) substrate transport (DiMauro and DiMauro. 1973) and turnover in Krebs cycle (Petrova-Benedict et al. 1987). Since 1988 these protein deficiencies have found their mutation counterparts in the human genome (Holt et al. 1988; Bourgeron et al. 1994; Monnot et al. 2009; Anichini et al. 2010).

2.2.2 Large-scale rearrangements in mtDNA

Variable mutations in mtDNA lead to respiratory chain failure. Large-scale rearrangements, more particularly a large single deletion was the first mutation to be associated with mitochondrial disease (Holt et al. 1988). From all the large-scale rearrangements, the single deletions have the highest prevalence estimates near to 1.6 per 100 000 in an adult population (Remes et al. 2005). Approximately one-third of the mtDNA deletions involve an identical 4977 base-pair segment, often referred to as the common deletion (Figure 1). Single duplications and several duplications or deletions in mitochondrial tRNAs or protein-coding genes are not as prevalent (Poulton et al. 1989). Large-scale rearrangements of mtDNA are nearly sporadic and were previously believed to be the result of the clonal amplification of a single mutational event in the oocyte (Chen et al. 1995; Chinnery et al. 2004). Besides the common Kearns-Sayre syndrome including ptosis, progressive external ophthalmoplegia (PEO) and salt-and-pepper like retinal pigmentary change before the age of twenty, the clinical phenotypes associated with large deletions recapitulate many manifestations generally encountered in patients with mitochondrial disease. At least, short stature, encephalopathy, diabetes,

ataxia, and also cardiomyopathy, conduction block, myopathy, retinal degeneration and hearing loss have been reported (Aure et al. 2007).

2.2.3 Point mutations in mtDNA

The human mtDNA mutation rate is high, about 2.5 substitutions per site per million years, which is 10 and 20 times higher than that in the nuclear DNA rendering the point mutations in mtDNA relatively common (Pärsons et al. 1997). Most of the 150 point mutations associated with human disease lead ultimately to respiratory chain failure primary through the transfer RNA encoding genes, which then change the translation of other genes. In addition, several rare pathogenic mutations in the protein encoding genes or ribosomal RNA genes have been identified (http://www.mitomap.org/). The most common pathogenic heteroplasmic point mutations affecting the respiratory chain are associated with specific phenotypes characteristic of mitochondrial disease. Often the degree of heteroplasmy determines largely the severity of the biochemical failure and disease. These characteristic phenotypes of mitochondrial disease include for instance MELAS (m.3243A>G), myoclonic epilepsy and ragged red fibres (MERRF, m.8344A>G), and neuropathy, ataxia and retinitis pigmentosa (NARP, m.8993T>C)(Figure 1)(Hirano and Pavlakis. 1994; Shoffner et al. 1990; Mäkela-Bengs et al. 1995). However, a variety of other phenotype-genotype associations have been ascribed to these characteristic heteroplasmic point mutations in mtDNA (Austin et al. 1998; Tatuch et al. 1992; Chinnery et al. 1997; Majamaa et al. 1998).

Part of the mtDNA point mutations leading to deficient ETC activity are homoplasmic. For an unknown reason the manifestations associated with homoplasmic mutations have typically an extremely variable penetrance. Classical nearly pathognomonic clinical presentations for homoplasmic mutations in mtDNA genes include: Leber's hereditary optic neuropathy (LHON) in the protein subunit encoding genes of the complex I, (MT-ND4, m.11778G>A; MT-ND1, m.3460G>A and MT-ND6, m.14484T>C), maternally inherited Leigh syndrome (LS) and progressive necrotising

encephalopathy and non-syndromic or aminoglycoside-induced sensorineural hearing loss (rRNA m.1555A>G for sensorineural hearing loss)(Wallace et al. 1988; Puomila et al. 2007; Limongelli et al. 2004; Yamasoba et al. 2002; Estivill et al. 1998).

2.2.4 Mitochondrial disease due to mutations in nuclear DNA

Mutations in nuclear DNA disturbing the structure, translation or assembly of respiratory chain proteins or replication and maintenance of mtDNA result in biochemical defects and phenotypes characteristic of mitochondrial disease. Notably, the majority of the respiratory chain proteins are encoded by nuclear DNA, translated in cytosol and transported into the mitochondrion (Figure 2). As the corresponding mutations in mtDNA the nuclear DNA mutations in genes encoding structural subunits of the respiratory chain complexes I,II, IV and V or their assembly proteins, including coenzyme Q(10) biosynthesis, become commonly manifest in early childhood. These mutations are associated with severe respiratory chain deficiency. LS or other severe forms of encephalopathy are the most common phenotype (Loeffen et al. 1998b; Bourgeron et al. 1995; Zhu et al. 1998; Lopez et al. 2006; Cizkova et al. 2008). A variety of mutations in nuclear genes encoding proteins needed for mtDNA translation or maintenance (including ANT1 gene) or replication (including deoxyribonucleoside kinases and other mitochondrial proteins maintaining deoxyribonucleoside triphosphate pools) of mtDNA usually lead to more subtle respiratory chain defects and become manifest later in life. The characteristic manifestations, such as encephalopathy, lactic acidosis, hepatopathy, myopathy and PEO resemble those of mtDNA mutations (Coenen et al. 2004; Smeitink et al. 2006; Fratter et al. 2010; Kaukonen et al. 2000; Van Goethem et al. 2001; Naviaux and Nguyen. 2004; Mandel et al. 2001; Saada et al. 2001; Zanna et al. 2008; GeneReviews: POLG-Related Disorders[Internet]; Parini et al. 2009). Most of these mutations lead to depletion of mtDNA and some to accumulation of deletions in mtDNA. At present, an increasing number of mutations in proteins involved in mitochondrial protein import are added to the list of metabolic mitochondrial diseases because they ultimately lead to the respiratory chain failure and resembling phenotypes (Tranebjaerg et al. 2001;

Takakubo et al. 1995; Magen et al. 2008). Finally, molecular genetics fails to detect a mutation possibly in one half of the adult patients affected by biochemical and clinical mitochondrial disease (Zeviani and Di Donato. 2004).

2.2.5 Metabolic aspects of mitochondrial morphology

In general, insulin, cold, exercise, nutrients, extra mitochondrial calcium and starvation have an impact on the overall mitochondrial biogenesis and metabolism (Hock and Kralli. 2009). It is characteristic of mitochondria to change shape, move and form new networks within the cell with nucleoids able to divide and redistribute within the mitochondrial network (Pohjoismäki et al. 2009; Amchenkova et al. 1988; Garrido et al. 2003; Hollenbeck and Saxton. 2005). Mitochondria continuously replicate their DNA, divide, react to extra-mitochondrial calcium changes and change their crista morphology, and move within the cell (Bereiter-Hahn and Voth. 1994; Yi et al. 2004). The morphology of mitochondrial network and inner membrane cristae also reflect the physiological variation in mitochondrial respiration and nutritive status (Hackenbrock. 1966; Scalettar et al. 1991; Plecita-Hlavata et al. 2008). A change in mitochondrial morphology and metabolism is also commonly seen in mitochondrial disease (Zanna et al. 2008; Kollberg et al. 2009; Kärppä et al. 2005; Carta et al. 2000). Much of the regulation of mitochondrial metabolism is exerted through transcription enhancing factors, such as nuclear respiratory factors 1 and 2, which bind to several nuclear mitochondrial gene promoters, such as respiratory complex subunits, TFAM, TFB2M, POLG subunits, mitochondrial fusion proteins, protein import complex genes. Thus the transcription and replication of mtDNA and ETC and the recruiting of the structural proteins needed for mitochondrial growth co-occur. The transcription enhancing factors in their turn are regulated by nuclear coactivators, such as PPAR gamma coactivator 1-α (PGC-1α), the promoter of which receives an array of positive and negative physiological signals from AKT, cAMP, Ca^{2+}, AMPK and fatty acids (Figure 2). The activation of PGC-1α and other nuclear coactivators also commonly induces gene expression needed for enhanced mitochondrial fatty acid oxidation, glucose

transport and uncoupling. The co-activators can be further induced by posttranslational regulation factors like Sirtuin 1 (Hock and Kralli. 2009).

It has been recently shown that experimental manipulation of mitochondrial proteins which control the morphology and fission-fusion, such as mitofusin exert also an impact on membrane potential and glucose metabolism in insulin responsive organs and on apoptosis in beta cells (Sebastian et al. 2012; Pich et al. 2005; Molina et al. 2009; John et al. 2005; Park et al. 2008a). In addition to the nuclear DNA mutations listed above, the aberrant mitochondrial respiration is associated with a loss of fusion function due to the mutations in genes encoding the involved proteins, such as the dynamin-related GTPase-like OPA1 protein (Zanna et al. 2008). Furthermore, mutations in mitofusin-2 gene repress mitochondrial fusion and the respiratory chain function and lead to Charcot–Marie–Tooth neuropathy and defects in central nervous system (Loiseau et al. 2007; Del Bo et al. 2008). Interestingly, obesity may impair the function of mitofusin-2 (Bach et al. 2005). Also mutations in monogenic forms of Parkinson's disease occur in genes that contribute to mitochondrial morphology (Deng et al. 2008). Finally, changes in mitochondrial morphology in affected organs have been commonly reported in various common diseases, such as diabetes, heart failure and neurodegenerative diseases. (Patti and Corvera. 2010; Ong and Hausenloy. 2010; Liang et al. 2008). At present, however the causal significance of these morphological mitochondrial changes in human disease has remained inconclusive.

2.3 The m.3243A>G mutation in mtDNA

2.3.1 Clinical presentation of the m.3243A>G mutation

The m.3243A>G mutation in the gene (MT-TL1) encoding transfer RNALeu(UUR) was the first mutation to be associated with mitochondrial encephalopathy characterized by seizures and dementia, lactic acidosis, and stroke-like episodes (MELAS), which in turn was described as a syndrome only a few years earlier (Goto et al. 1990; Pavlakis et al. 1984). The MELAS phenotype and m.3243A>G have a high

concordance (Hirano and Pavlakis. 1994). At present, several other mutations have been associated with the MELAS syndrome. Another common cause is the m.3271T>C mutation. In addition to the several point mutations in the MT-TL1 gene, mutations in other mitochondrial transfer RNA genes as well as in genes coding structural subunits in various respiratory chain complexes have been associated with the MELAS syndrome (Ruiz-Pesini et al. 2007; http://www.mitomap.org/). Furthermore, MELAS overlap syndromes have been described in the carriers of the mutations in respiratory chain subunit encoding genes. Especially the mutations in the MT-ND5 gene can result in MELAS and other phenotypes, such as the MELAS- LS, MELAS- LHON, MELAS-MERFF overlap syndromes (Santorelli et al. 1997; Chol et al. 2003; Pulkes et al. 1999; Naini et al. 2005). The reasons for the phenotype-genotype variation are poorly understood (van Eijsden et al. 2008).

The characteristic MELAS syndrome is a rather uncommon manifestation in the carriers of m.3243A>G. More prevalent manifestations of m.3243A>G include myopathy 27%, diabetes mellitus 48%, pigmentary retinopathy 15%, sensorineural hearing impairment 67%, dementia 27%, epilepsy 18%, short stature 42%, neuropathy 15%, ataxia 9% and myoclonus 8% (Chinnery et al. 1997; Majamaa-Voltti et al. 2006). Cardiac manifestations and migraine are also common in patients with m.3243A>G. (Majamaa et al. 1998; Uusimaa et al. 2007). In general, the tissues with high energy needs, i.e. the visual and auditory systems, neuronal tissue, heart, skeletal and smooth muscle, beta cells, kidney and liver appear to be the organs richest in the respiratory chain complexes and most vulnerable to the abnormal energy metabolism in mitochondrial diseases (Triepels et al. 1998; Loeffen et al. 1998a; Loeffen et al. 1999). However, in spite of the rich mitochondrial content in kidney and liver, renal manifestations, hepatopathy or other gastroenterological manifestations, such as recurrent vomiting, recurrent pancreatitis and gastrointestinal dysmotility are relatively uncommon manifestations in patients with the m.3243A>G mutation (Narbonne et al. 2004; Hotta et al. 2001; Majamaa-Voltti et al. 2006). Intriguingly, studies in patients with another mitochondrial translation defect have led to propose that the hepatic

manifestation paradox might be due to the differences in the organization of the mitochondrial translation proteins system in different tissues (Antonicka et al. 2006).

The level of heteroplasmy determines in part the severity of the phenotype. More severe phenotype is associated with higher m.3243A>G heteroplasmy as is the case for many other point mutations and large scale deletions in mtDNA (Chinnery et al. 1997; Jeppesen et al. 2006; Aure et al. 2007). Because of ongoing mitochondrial and cellular division the mutation load may show considerable variation among the tissues in each individual. In addition, for partly unknown reasons the heteroplasmy levels of m.3243A>G in various tissues have not a fully random hierarchy (Chinnery et al. 1999). The m.3243A>G mutation heteroplasmy may not impair respiratory chain function unless it exceeds a certain threshold. This threshold effect for the biochemical defect can be easily demonstrated *in vivo* in cybrid cells or fibroblasts (Jeppesen et al. 2006; James et al. 1996; DiFrancesco et al. 2008). The typical threshold level may vary in different tissues. Intriguingly, homoplasmic mutations in mtDNA leading to serious defects in oxidative phosphorylation (OXPHOS) often give rise to symptoms in one characteristic tissue, such as in the optic nerve in patients with the m.11778G>A mutation (Wallace et al. 1988; Sue et al. 1999). Therefore factors other than tissue heteroplasmy and the ensuing OXPHOS defect in cells likely explain much of the phenotype-genotype variation in mitochondrial disease.

2.3.2 Epidemiology of the m.3243A>G mutation

The prevalence of respiratory chain diseases due to mtDNA mutations has been initially estimated to be about 1 in 5,000. The prevalence of the m.3243A>G mutation was relatively high in a population-based study in Finland with 16.3 carriers per 100,000 (Majamaa et al. 1998; Uusimaa et al. 2007). However, the frequency has been even higher in other population-based studies performed on Caucasian populations (Elliott et al. 2008; Manwaring et al. 2007). The m.3243A>G mutation has been estimated to be the most common pathogenic mtDNA mutation. The m.3243A>G mutation is thus slightly more prevalent than the m.11778G>A mutation causing the LHON (Elliott et al. 2008;

Manwaring et al. 2007; Man et al. 2003; Schaefer et al. 2008; Darin et al. 2001; Puomila et al. 2007). In case of mitochondrial disease caused by homoplasmic point mutations and Complex I deficiency, the nuclear genetic background, sex and at least smoking affects the penetrance of phenotypes such as LHON (Cock et al. 1998; Hudson et al. 2005; Tsao et al. 1999; Puomila et al. 2007; Kirkman et al. 2009). In addition, variation of mtDNA haplogroups may modulate OXPHOS and explain why some patients with certain haplogroups have a high risk for LHON (Hudson et al. 2007). However, it has not been proved that the mtDNA haplogroups, nuclear genetic background, sex or environmental factors would explain the variation in disease manifestation in patients with m.3243A>G (Torroni et al. 2003).

2.3.3 Pathophysiology of the m.3243A>G mutation

2.3.3.1 Transcription failure

The nucleotides between positions 3230-3304 in mtDNA encode transfer RNA, which transfers the amino acid leucine to the polypeptide chain at the ribosome during translation. Defects in mitochondrial protein synthesis and respiratory activity are a constant observation in cellular models containing mutated mtDNA similar to the observation in other mutations in mtDNA transfer RNA genes. The m.3243A>G mutation has an impact on mitochondrial translation efficiency and on the termination of transcription (Kirino et al. 2004; King et al. 1992; Suomalainen et al. 1993; Flierl et al. 1997). As a result the assembly of complexes I, IV and V are almost totally lost in the cybrids harbouring homoplasmic m.3234A>G mutation (Sasarman et al. 2008). This translation defect may be modestly overcome by increasing the availability of leucyl-transfer RNA synthetase or elongation factors (Sasarman et al. 2008; Li and Guan. 2010).

2.3.3.2 Electron transport chain deficiency

The major biochemical defect in cells with m.3243A>G is the failing complex I activity in the mitochondrial electron-transport chain. This has been well-

documented in fibroblasts, myocytes, neurons and cybrid cells (James et al. 1996; Vydt et al. 2007; Sparaco et al. 2003; Li and Guan. 2010). The activity of complex I in the affected tissues has shown an inverse correlation with mutation heteroplasmy is some studies. On the other hand, low activity of the other complexes, particularly complex IV, has been reported in some tissues such as the skeletal muscle (Goto et al. 1992; Mariotti et al. 1995; Vydt et al. 2007). Complex I and IV gene expression may be compensatory induced in the presence of m.3243A>G (van Eijsden et al. 2008). The low complex IV activity in myocytes of patients with m.3243A>G is associated with two paradoxes. Firstly, COX stain is predominantly positive indicating the presence of the protein complex and, secondly, in the few COX-negative fibres the lack of staining is not due to the lack of wild type mtDNA at the site (Durham et al. 2007). A marked complex I deficiency is a rather constant finding also in other mitochondrial disorders. This is due to the disease-associated mutations in several structural subunit genes and in the assembly factor genes needed for complex I. Such mutations are found for instance in patients with the severe LS or childhood MELAS. In addition, neonatal deaths due to mitochondrial transfer RNA mutations leading to the near absence of the complex I activity emphasize the importance of the complex I function in humans (McFarland et al. 2002; Malfatti et al. 2007). Then again, mutations leading to the complex I deficiency and transfer RNA synthesis defects have also been associated with much milder phenotypes (Taylor et al. 2003b; Brown et al. 2000). Finally, the predictory value of detecting isolated complex I deficiency in muscle mitochondria for the disease manifestations is less than that of muscle ATP generating capacity, muscle histochemistry or the level of blood lactate in patients with the m.3243A>G mutation (Wibrand et al. 2010; Janssen et al. 2008).

2.3.3.3 Carbohydrate and calcium metabolism

The homoplasmic m.3243A>G mutation in cybrid cell leads to decreased glucose oxidation, increased anaerobic glycolysis and several-fold accumulation of extracellular pyruvate and lactate. A slight increase in citrate synthase activity, a 50-

80% decrease in oxygen consumption and a 90% decrease in ATP synthesis is observed in the presence of homoplasmic m.3243A>G mutation. (King et al. 1992; Pallotti et al. 2004). Due to the increase in anaerobic metabolism a ~2 fold rise in net glucose uptake is observed in these cells (de Andrade et al. 2006). The mitochondrial membrane potential is decreased resulting in the low oxidative ATP production (Sandhu et al. 2005; de Andrade et al. 2006; James et al. 1996; Antonicka et al. 1999). Interestingly, an augmented PGC-1α or β expression in cells harbouring the m.3243A>G mutation is able to increase the complex I activity and oxygen uptake (Srivastava et al. 2009). Some cell lines present progressive decline in oxygen consumption due to the m.3243A>G mutation after a low heteroplasmy threshold of around 21% (van den Ouweland et al. 1999). Impaired respiratory chain function does not only affect the hydrocarbon oxidation rate but also calcium signalling due to the decrease in mitochondrial membrane potential (de Andrade et al. 2006). Finally, based on cybrid studies, glutamate turnover and synthesis rate are likely to be decreased in the tissues affected by the m.3243A>G mutation (DiFrancesco et al. 2008).

2.3.3.4 Glucose metabolism in models mimicking m.3243A>G disease

Mitochondrial disease traditionally lacks animal models. Different cellular models compromised for their mitochondrial function mimic the metabolic changes observed in m.3243A>G cybrids or fibroblast. Cells survive without mitochondria and mtDNA by increasing glucose uptake and anaerobic glycolysis (de Andrade et al. 2006; Soejima et al. 1996). Further, abolishing the mitochondrial membrane potential with valinomycin provokes an increased 2-deoxy-2-[^{18}F]fluoro-α-D-glucose ([^{18}F]FDG) uptake in cancer cells. A similar compensatory anaerobic rise in glucose uptake by blocking the mitochondrial respiration with sodium azide can be demonstrated in cultured myocytes (Brown et al. 2008). On the other hand, various cell types including neurons are able to compensate complex I deficiency and maintain some of the mitochondrial membrane potential using ATP from anaerobic glycolysis and the reverse mode of F1Fo-ATP synthase (complex V, de Andrade et al. 2006; Abramov et

al. 2010). It is well-known that carbohydrates other than glucose limit compensatory anaerobic glycolysis and the viability of cells with respiratory chain defects (De Lonlay et al. 2002). Interestingly, no data on fatty acid metabolism, which is the essential substrate for heart and skeletal muscle, in cells harbouring the m.3243A>G mutation or mimicking models are available. It is also rather unclear how the nuclear and wild type mtDNA transcriptions are influenced by the m.3243A>G mutation, in different tissues. However, both nuclear and mtDNA gene transcripts for the ETC and glycolytic pathway may be somewhat upregulated in the heart, liver and in the skeletal muscle (Heddi et al. 1999; Srivastava et al. 2009; Durham et al. 2007). Nevertheless, changes in the expression of nuclear-encoded subunits of the respiratory chain and the proteins of the cell cycle have been reported both in the absence of mtDNA and in the presence of various mitochondrial mutations including m.3243A>G (Mineri et al. 2009; Cortopassi et al. 2006). Rodents with mutations in NADH-ubiquinone oxidoreductase Fe-S (Complex I) proteins develop encephalopathy and high lactate resembling LS or a severe MELAS phenotype. Decreased oxygen consumption in liver is present in these animals (Kruse et al. 2008). However, these animals do not develop diabetes or ragged red fibres (RRFs) characteristic for the m.3243A>G mutation. On the other hand RRFs are not present in all common mitochondrial diseases disturbing complex I activity such as LHON (Cortelli et al. 1991). A conditional tissue specific mutation expression in the gene encoding the TFAM, a transcription factor, creates a mouse model, where the affected tissues possibly best resemble mitochondrial disease due to the m.3243A>G mutation. These mice show decrease in complex I, III and IV activity, encephalopathy and myopathy with RRFs and COX deficiency mimicking most mitochondrial diseases (Li et al. 2000; Wang et al. 1999). The tissue-specific knockout (KO) of the nuclear TFAM gene in pancreas in mice presents a defect in insulin secretion, abnormal mitochondria in islets cells and develops later beta cell loss and diabetes (Silva et al. 2000). Unfortunately, the global TFAM KO is lethal *in utero* (Larsson et al. 1998).

2.4 Brain metabolism and mitochondrial encephalopathy

2.4.1 Glucose metabolism in brain

2.4.1.1 Glucose as a neuronal substrate

The basal human brain metabolism has been well-characterized by analyzing arterial and internal carotid vein differences for various metabolites. Studies using this method have clearly shown that human brain is an active net consumer of glucose and oxygen. It has been estimated that 95% of the glucose extracted by the brain is oxidized in the brain providing about 90% of the energy consumed by the human brain (Graham et al. 2002; Dalsgaard et al. 2002). Most of the glucose oxidation occurs in neurons of the cortical grey matter. The normal molecular ratio of the oxygen to glucose consumption is near to six and may be slightly decreased due to the high lactate availability and oxidation during intense exercise (Dalsgaard et al. 2004). Also a small fraction of free fatty acids (FFAs) is taken up and metabolized in human brain (Dalsgaard et al. 2002; Karmi et al. 2010). Extensive data suggest that these alternative substrates are preferentially metabolized by astrocytes and not by neurons or oligodendrocytes (Hertz et al. 2007; Wyss et al. 2009). In basal conditions the non-neuronal oxygen consumption occurs mainly in astrocytes. Oxygen consumption in astrocytes is proportional to their proportion of all cortical cells being as high as 30% (Hertz et al. 2007). The astrocytic oxidative capacity per cell is therefore comparable to that in neurons, which is further supported by the similar mitochondrial volume fraction in the two cell types (Pysh and Khan. 1972).

2.4.1.2 Immediate carbohydrate oxidation in the brain

The ATP in neurons is needed for the maintenance of membrane potential, the synaptic activity and to balance the rapid initial rise in extracellular potassium after an action potential (Brown et al. 2003; Dienel et al. 2007). An increase in energy needs due to sensory or mental activation provokes a temporal fall in the basal oxygen to glucose metabolism ratio due to the temporary increase in anaerobic

glycolysis in order to balance the rapid ATP decrease during physiological demand (Dienel et al. 2007). This is followed by a compensatory increase in carbohydrate oxidation (Gjedde and Marrett 2001; Dienel et al. 2007). The endogenous glycogen storage is relatively small and predominately located in astrocytes in the brain (Cruz and Dienel 2002; Ghosh et al. 2005). The anatomical correlates for this instant energy reservoir are the glycogen storages within the thin peripheral astrocytic processes, which envelope the peripheral projections of the neurons (Hertz et al. 2007). A shortage in oxygen or glucose leads to rapid depletion of this glycogen store. Persisting oxygen depletion leads to insufficient ATP supply of the brain, the electrical activity vanishes and the neuronal death ensues in few minutes (Brown et al. 2003; Allen et al. 1989). This in mind, it is not surprising that the regional metabolism in the brain is tightly coupled with the vascular supply of nutrients and oxygen (Paulson et al. 2010; Roland et al. 1987). The autoregulation of the brain perfusion pressure is part of this characteristic coupling. Further, the coupling of perfusion to glucose and oxygen metabolism in various brain regions and during different activation patterns is tight. This coupling, however can be overcome by a forced increase or decrease in the blood flow, implicating that the coupling ultimately is a blood flow response to the metabolic needs in the different neuron populations in the brain (Långsjö et al. 2005; Kuroda et al. 2006).

2.4.1.3 Glucose homeostasis and brain metabolism

The mammalian brain, cerebellum excluded, expresses only insulin insensitive glucose-specific transporter proteins 1 and 3 (GLUTl and GLUT3, Choeiri et al. 2002). Accordingly, acute hyperinsulinemia induces only minor changes in human brain glucose uptake (Hirvonen et al. 2011; Cranston et al. 1998). In contrast with insulin sensitive glucose transporters, insulin receptors are expressed at high levels in various brain areas and cell types (Baron-Van Evercooren et al. 1991). A role for neural insulin receptors in mammal metabolism is suggested by creating neuron-specific insulin receptor KO mice, which present diet-dependent susceptibility to obesity, and hypogonadism (Bruning et al. 2000). The density of glucose transporter proteins

reflects mainly the metabolic activity in various brain regions (Choeiri et al. 2002). Deficiency in the main glucose transporter, the GLUT1, leads to early encephalopathy and to a widespread glucose hypometabolism in the brain (Pascual et al. 2002). Diabetes or hyperglycaemia does not markedly change the glucose uptake rate in the brain. However GLUT1 may become downregulated and the glucose content is increased in various brain regions (Lutz and Pardridge. 1993; Heikkilä et al. 2009; Hasselbalch et al. 2001). A high availability of ketones, FFAs and lactate might potentially decrease glucose utilization and increase the oxidation and the turnover of alternative hydrocarbons in the brain (Dalsgaard et al. 2004; Pan et al. 2000; Bentourkia et al. 2009; LaManna et al. 2009; Chiry et al. 2006).

2.4.1.4 Measuring human brain glucose metabolism

Human data from arterio-venous difference studies as well as glucose uptake measured with 1-[^{11}C]D-glucose and [^{18}F]FDG-PET combined with brain perfusion or oxygen metabolism data have shown that a quantification of glucose uptake in different brain areas is accurate with dynamic [^{18}F]FDG-PET scans if simultaneous arterial sampling is used (Dalsgaard et al. 2002; Graham et al. 2002; Frackowiak et al. 1988). Both [^{18}F]FDG and glucose transport across the cell membrane are facilitated by the predominant GLUT1 transporter in the brain (Pascual et al. 2002; Rayner et al. 1994; Choeiri et al. 2002; Patlak and Blasberg. 1985). GLUT1 is the major facilitator of transmembrane transport of glucose both into the neurons and astrocytes (Chiry et al. 2006). In the cytoplasm [^{18}F]FDG and glucose are phosphorylated by a hexokinase. At this point, the metabolism of [^{18}F]FDG ceases except for very slow dephosphorylation. Thus, the accumulation rate of [^{18}F]FDG into the tissue is linearly proportional to the regional metabolic rate of glucose (rGMR). Minor differences may be attributed to the different transport and phosphorylation rate of the 2 hexoses in the tissue. The correction factor accounting for these differences is termed the lumped constant (LC, Graham et al. 2002; Reivich et al. 1985).

2.4.2 Mitochondrial encephalopathy

2.4.2.1 Clinical and pathological presentation

The full-blown mitochondrial encephalomyopathy, stroke-like episodes or epilepsy are rare CNS manifestations in adults with m.3243A>G (Majamaa et al. 1998). Mild to moderate cognitive decline is more common. Migraine and ataxia are also common traits in patients with m.3243A>G (Majamaa-Voltti et al. 2006; Fromont et al. 2009). The cognitive dysfunction has been attributed to the posterior regions of the brain as visuoconstructive problems dominate (Majamaa-Voltti et al. 2006). In addition, impairment in more frontally located cognitive functions, such as sustained attention, verbal memory and abstract reasoning have been recently reported in patients with m.3243A>G (Fromont et al. 2009). The clinical course of the encephalopathy is progressive in patients with m.3243A>G. Also the electrical activity in electroencephalography (EEG) gradually becomes slower in the occipito-parietal regions in patients with m.3243A>G and without stroke-like episodes during the follow-up (Majamaa-Voltti et al. 2006).

Neuropathological studies have described widespread infarct-like lesions in the cerebral cortex and gliosis and demyelinisation in the cerebral and cerebellar white matter in patients with m.3243A>G and stroke-like episodes (Tanahashi et al. 2000; Betts et al. 2006). Characteristic features also include basal ganglia calcifications, local and diffuse atrophy and necrosis without intravascular thrombosis or embolus in intracerebral arteries (Sue et al. 1998). Conclusive neuropathological studies including mildly affected carriers of the m.3243A>G are lacking. On the other hand, common neurodegenerative pathology, such as senile plaques, neurofibrillary tangles or Lewy bodies are rare also in patients with severe manifestations. The ultrastructural assessments show typically numerous abnormally enlarged mitochondria, which are aggregated in blood vessels (Tanahashi et al. 2000; Betts et al. 2006). These findings together with the severe COX deficiency co-occuring with high heteroplasmy in the walls of the blood vessels have lead some authors to suggests that an angiopathy due to mitochondrial dysfunction may cause the stroke-like episodes (Tanahashi et al. 2000;

Betts et al. 2006). However, the distribution of affected blood vessels has not shown a clear correlation between affected and spared brain regions speaking against the mitochondrial angiopathy hypothesis. In contrast, reduced staining for mtDNA-encoded subunits of the respiratory chain, has been confirmed in patients with m.3243A>G in the affected and non-affected brain cortex. This indirectly suggests that focal lesions in MELAS might be due to OXPHOS failure in neurons (Sparaco et al. 2003). Finally, the origin of the encephalopathy including the stroke-like lesions remains obscure (Tanahashi et al. 2000; Betts et al. 2006).

2.4.2.2 Imaging in mitochondrial encephalopathy

Neuroimaging data on patients with m.3243A>G is mainly derived from clinical reports including a handful of patients who have experienced acute stroke-like episodes. These studies have usually reported an absence of ischemia as the perfusion has been normal (Nariai et al. 2001). The stroke-like events are typically associated with asymmetric lesions located in the occipital and parietal lobes mimicking ischemia but not respecting the major vascular territories. Diffusion-weighted or other magnetic resonance imaging (MRI) has revealed that these lesions may evolve and disappear during follow-up. In discordance with the non-vascular distribution of the lesions, the oedema in acute lesion displays characteristics of vasogenic-extracellural rather than cytotoxic-intracellular tissue breakdown (Abe et al. 2004; Yoneda et al. 1999; Ohshita et al. 2000). Besides the stroke-like lesions, non-quantitative single photon emission computed tomography (SPECT) has shown both patterns of normal or asymmetric hypoperfusion in the parieto-occipital region of patients with m.3243A>G (Suzuki et al. 1996; Ito et al. 2008; Thajeb et al. 2005). In contrast with rather occasional stroke-like lesions, mild brain atrophy is frequent in patients with the m.3243A>G mutation (Majamaa-Voltti et al. 2006; Suzuki et al. 1996; Sue et al. 1998; Fromont et al. 2009). Besides the cerebellar and cerebral atrophy, relatively commonly reported non-acute radiological findings include basal ganglia calcifications and unspecific focal lesions in the grey matter in the parietal and occipital lobes and cerebellum (Sue et al. 1998).

2.4.2.3 Brain metabolism in mitochondrial disease

A relative decrease in glucose metabolism with possible preference for occipital and temporal lobes has previously been found in patients with mitochondrial disease (Damian et al. 1998; Molnar et al. 2000). However, the most commonly reported metabolic findings in patients with m.3243A>G are low N-Acetyl-L-aspartic acid (NAA) signal and accumulation of lactate in the focal stroke-like lesions (Fromont et al. 2009; Castillo et al. 1995). The voxel-vice [^{1}H] magnetic resonance spectroscopy ([^{1}H]MRS) lactate measurements in CSF in the lateral ventricle have also been linearly related to the m.3243A>G mutation heteroplasmy and to the symptoms in a large study population (Kaufmann et al. 2004). More elusive data on metabolic disturbances in the brain have been obtained using quantitative PET approach in all together 13 patients that had mitochondrial disease confirmed in muscle biopsy. These two studies have shown a rather well-preserved rGMR but a shift from aerobic glucose oxidation to anaerobic glycolysis as the oxygen consumption was markedly decreased in the patients (Frackowiak et al. 1988; Shishido et al. 1996). However, no quantitative data on glucose and oxygen metabolism in the unaffected brain regions are available in mitochondrial disease.

2.5 Mitochondrial failure and adult-onset diabetes

2.5.1 Role of genetic background in adult-onset diabetes

Twin studies propose that the risk of type 2 diabetes is inherited. These studies also propose that the diabetes becomes manifest only in subjects who are genetically predisposed to insulin resistance and who also possess defective beta cells rendering them unable to compensate for a decrease in insulin action (Beck-Nielsen et al. 2003). Defects in insulin sensitivity and beta cell function are common in the healthy offspring of patients with type 2 diabetes (Natali et al. 2010; Karlsson et al. 2006). Prospective studies show that the whole-body insulin resistance and alternation in the GIS precede diabetes onset by several years (Ahren. 2009). A 25-year follow-up of 155 children of couples who both had type 2 diabetes showed that decreased insulin sensitivity precedes diabetes at least by ten years (Martin et al. 1992). A follow-up

study including two hundred non-diabetic Pima Indians, a population at a high risk of inherited diabetes, has shown that an early insulin resistance is the major, and an impaired acute insulin response is the minor diabetes precursor (Lillioja et al. 1993). Peripheral insulin resistance also independently predicts later cardiovascular disease and is strongly associated with the other risk factors for cardiovascular disease already in adolescents (Moran et al. 2008; Kekäläinen et al. 1999; Raitakari et al. 1995). The few genetic factors that have been associated repeatedly but not unambiguously with insulin sensitivity include the Pro(12)Ala polymorphism in the PPAR-gamma2 gene, which is protective in obese subjects, and the mtDNA variant m.16189T>C (Vänttinen et al. 2005; Poulton et al. 1998; Park et al. 2008b).

Monogenetic diabetes is characterized by high penetrance. Several mutations in the proximity of nuclear transcription factor like genes predispose to type 2 diabetes but they may also cause a monogenetic form of diabetes, the maturity-onset diabetes of the young (MODY, Love-Gregory et al. 2004; Holmkvist et al. 2006; Grant et al. 2006; Silander et al. 2004; Steinthorsdottir et al. 2007). The most common cause of MODY is a defect in glucokinase gene, which interferes with the glucose metabolism both in hepatocytes and beta cells (MODY 2, Velho et al. 1992; Lorini et al. 2009). Several other mutations underlying the MODY phenotype affect transcription factors, for instance the hepatocyte nuclear factor and impair beta cell function (Yamagata et al. 1996; Stride and Hattersley. 2002). The gain of function mutations in ATP-sensitive inward rectifier potassium channel 11 encoding gene, which causes neonatal diabetes, as well as the different types of mitochondrial diabetes are other forms of monogenic diabetes (Pearson et al. 2006).

Association studies have shown that the common type 2 diabetes is a polygenetic disease. Each mutation associated with type 2 diabetes increases only modestly the risk for diabetes. Most of these mutations interfere with some aspect of the beta cell function (Perry and Frayling. 2008). For instance mutations impairing the function of the ATP-dependent potassium or the voltage-gated calcium channels lead to the

aberrant first phase of the GIS (Gloyn et al. 2003; Holmkvist et al. 2007). Mutations in the sulphonylnurea receptor gene have been associated with type 2 diabetes and failing second phase of insulin secretion (Hart et al. 2000). Interestingly, in contrast with the glucose-induced secretion, the argine or glucagon-like peptide-stimulated insulin secretion may not be associated with the major risk loci for type 2 diabetes ('t Hart et al. 2010). Mutations predisposing to type 2 diabetes have not been found in the nuclear genes regulating mitochondrial function (Segre et al. 2010). Recently, plasma apolipoprotein B and adiponectin have shown to have a predictive value for diabetes in the general population, but the role of polymorphism in the respective genes for diabetes risk is unclear (Salomaa et al. 2010; Dastani et al. 2012; Lindsay et al. 2002). Importantly, as compared with traditional risk factors, such as family history, body-mass index, liver-enzymes and smoking, or to the measures of insulin secretion and action, the known mutations associated with type 2 diabetes have a poor predictive value for the future diabetes onset (Lyssenko et al. 2008). Therefore, a detection of a single associative mutation has not been very useful in order to find the individuals who would potentially benefit from interventions aiming to maintain beta cell function and mass before diabetes onset (Donath et al. 2005).

2.5.2 Role of mitochondrial function in insulin secretion

Beta cells are the main cell type in the islet of Langerhans accounting for 70% of the human endocrine pancreas (Jain and Lammert. 2009). The beta cells release insulin in response to glucose stimuli in a manner, which is modulated by other nutrients and the route of glucose administration (Faerch et al. 2008; Salinari et al. 2009). Glucose is predominantly transported via the GLUT1 transporters in human beta cells (De Vos et al. 1995). The following phosphorylation step by glucokinase (GK) is the rate limiting step in glucose entry. The overexpression of the GK increases glucose influx. This in turn leads to higher pyruvate availability and oxidation followed by a rise in cytosolic ATP. As a result, the beta cell glucose sensitivity becomes elevated. Due to these observations GK has been considered to be the major glucose sensor of the beta cells (De Vos et al. 1995;

Ishihara et al. 1994; Thorens et al. 2000; Postic et al. 1999; Sayed et al. 2009; Sakura et al. 1998). The elevated ATP is needed to increase the opening probability of the ATP dependent potassium channel, which in turn leads to membrane depolarisation and to the opening of the voltage-gated calcium channel and calcium influx (Cook and Hales. 1984). Finally, elevated calcium triggers the exocytose of insulin (Mariot et al. 1998).

Approximately as much as 90% of the glucose entering the beta cell is oxidized (Schuit et al. 1997). The importance of the direct glucose oxidation to beta cell function can be demonstrated by overexpressing the otherwise neglect lactate dehydrogenase in beta cells. This upregulates anaerobic glycolysis at the expense of glucose oxidation and results in markedly impaired GIS (Zhao and Rutter. 1998). Therefore, the heteroplasmy threshold where the OXPHOS defect becomes manifest might be lower in beta cells than in *in vivo* cybrid cell models or in other tissues with potent lactate dehydrogenase (van den Ouweland et al. 1999; Soejima et al. 1996). It has been clearly shown that during excess substrate availability, it is the generation of mitochondrial membrane potential i.e. OXPHOS capacity, which sets the limit to the rate of the ATP production and the GIS (Antinozzi et al. 2002). Importantly, the mitochondrial level of uncoupling may regulate insulin secretion as uncoupling protein 2-deficient mice show high islet ATP levels and an increased GIS response (Zhang et al. 2001). In addition, mitochondria increase the contrasts in the intracellular calcium oscillation and thereby insulin exocytose by rapidly taking up calcium during cell activation (Quesada et al. 2008). Finally, the potentiation of the GIS is partly independent of calcium concentration in the beta cells, but the role of mitochondria in the calcium independent potentiation of the GIS is unknown (Ravier et al. 2010; Salehi et al. 2010).

2.5.3 Mitochondrial diabetes

2.5.3.1 Clinical presentation

Various mtDNA mutations are associated with monogenetic forms of diabetes (Hirai et al. 1998; Whittaker et al. 2007; Choo-Kang et al. 2002). The m.3243A>G mutation in

mtDNA is the most prevalent cause for mitochondrial diabetes accounting for ~1% of adult onset diabetes (Katulanda et al. 2008; Otabe et al. 1994; Saker et al. 1997; Whittaker et al. 2007; Choo-Kang et al. 2002; Martikainen et al. 2012). The average age of onset is around 40 years although the range is wide. It has been estimated that most carriers of the m.3243A>G mutation develop diabetes by the age of 70 years (Guillausseau et al. 2001; Laloi-Michelin et al. 2009). Patients with m.3243A>G are typically lean and most of them need insulin only a few years after the onset of diabetes (Guillausseau et al. 2001). The prevalence of retinopathy may be lower and the risk of renal complications may be higher than those in patients with the common forms of diabetes (Massin et al. 2008). Hearing impairment co-occurs often with mitochondrial diabetes, and the acronym maternally inherited diabetes and deafness (MIDD) is widely used (Laloi-Michelin et al. 2009).

2.5.3.2 Beta cell failure

In cybrid cells, homoplasmic m.3243A>G mutation leads to respiratory chain deficiency and to over two-fold increase in anaerobic glycolysis. The glucose oxidation is reduced by over 80% and the NADH production and resting mitochondrial membrane potential become decreased as compared to cells with wild type mtDNA. In addition to these key metabolic pathways involved in beta cell function, intracellular calcium concentrations return only slowly to the baseline after stimuli in these cells, probably blunting even more the beta cell response to glucose (Mariotti et al. 1995; de Andrade et al. 2006; Pallotti et al. 2004). However, only a few previous studies assessing insulin secretion in these patients are available. Six studies including 63 subjects with m.3243A>G have revealed impaired GIS, whereas three studies including 41 subjects have not (Brändle et al. 2001; Suzuki et al. 1994; Suzuki et al. 1997; Becker et al. 2002; Holmes-Walker et al. 2001; Salles et al. 2007; Velho et al. 1996; Oka et al. 1996; Maassen et al. 2004). Two of the studies demonstrated defects in the GIS in altogether 10 patients displaying a normal glucose tolerance (Suzuki et al. 1994; Velho et al. 1996). The response to arginine and glutamate has been reported to

be preserved (Brändle et al. 2001). Importantly, no studies have properly assessed the possible association between the insulin secretion and the tissue heteroplasmy.

2.6. The role of skeletal muscle in glucose homeostasis

2.6.1 Skeletal muscle metabolism

2.6.1.1 Nutritive metabolism in the skeletal muscle

The skeletal muscle relies mainly on FFA oxidation in the fasting state. During exercise the proportion of glucose oxidation increases and during high-intensity exercise the glycogen storage may be used for anaerobic glycolysis (Helge et al. 2007). Fatty acids are at least partly transported via transmembrane protein fatty acid translocase into the myocyte for storage and oxidation (Holloway et al. 2006). The magnitude of the intramuscular lipid pool that undergoes oxidation is unclear (Helge et al. 2007). Three fibre types can be delineated in human muscle according to the myosin heavy chain isoforms. Type I fast-twitch fibres are favoured by PGC-1α activation (Lin et al. 2002). The type IIA and IIX/IIB represent slow-twitch fibres. The maximal ATP and glycogen consumption capacity is high in the fast fibres as compared to slow fibres (Greenhaff et al. 1993). The percentage of the muscle fibre volume occupied by mitochondria varies from 6% in type I to 4.5% in type IIA and 2.3% in type IIX/IIB as the respiratory rates in isolated mitochondria are similar in the fibre types (Scheibye-Knudsen and Quistorff. 2009; Howald et al. 1985).

2.6.1.2 Glucose transport to skeletal muscle during hyperinsulinemia

GLUT4 is the predominant glucose transporter in human skeletal muscle (Gaster et al. 2000). The GLUT4-KO completely abolishes the insulin-stimulated glucose uptake and leads to impaired glucose tolerance in mice (Zisman et al. 2000). GLUT4 translocation, hexokinase II (HK II) activity and glycogen synthase are all insulin responsive steps of glucose uptake in the myocyte (Mandarino et al. 1995). However, the GLUT4 translocation appears to be the rate limiting step of glucose transport to

skeletal muscle both during hyperinsulinemia and exercise activation (Wojtaszewski et al. 1999; Cline et al. 1999; Zisman et al. 2000; Fueger et al. 2004; Fueger et al. 2005). The insulin sensitive transmembrane transport step corresponding the sum of GLUT4 and HK II step may be quantified with [^{18}F]FDG-PET. It shows a tight correlation with the whole-body insulin sensitivity (Peltoniemi et al. 2000; Virkamäki et al. 1997). Insulin and also exercise independently increase nutritive perfusion in skeletal muscle, which is mainly regulated according to the metabolic needs (Newman et al. 2007; Hannukainen et al. 2006). Finally, muscle glycogen synthesis is the principal pathway of glucose uptake during hyperinsulinemia (Virkamäki et al. 1997). Insulin also indirectly increases glucose utilization in myocytes as it limits the FFA concentration in the blood by inhibiting the lipolysis in the adipose tissue and possibly within the skeletal muscle (Bolinder et al. 2000).

2.6.1.3 Insulin resistance and oxidative capacity

Peripheral insulin resistance can be quantified by calculating the decrease in whole-body glucose uptake during the hyperinsulinemia (DeFronzo et al. 1982). Due to its availability elevated fasting insulin to glucose ratio has been used as an alternative marker of the insulin resistance. During physiological levels of hyperinsulinemia, the skeletal muscle glucose uptake accounts for the majority of the whole-body glucose uptake (DeFronzo et al. 1982). Some degree of peripheral insulin resistance develops also in type 1 diabetes and thereby it has to be taken into consideration in all patients with diabetes (Peltoniemi et al. 2001). Insulin enhances glucose uptake via insulin receptor substrate 1 tyrosine phosphorylation signalling pathway. This pathway is independent of exercise and insulin sensitizers (Karlsson et al. 2005). The role of insulin signalling pathway in myocytes during glucose intolerance has been challenged by the insulin receptor KO mice, which do not show any glucose intolerance (Bruning et al. 1998). Experiments in these mice, thus lacking the insulin signalling in muscle, have proposed that alternatively the downregulation of mitochondrial respiratory chain might have an initiating role in glucose intolerance (Yechoor et al. 2004). Previous associations between skeletal muscle citrate synthase activity or maximal oxygen

uptake (VO_2 max) and insulin sensitivity in skeletal muscle would be compatible with this proposition (Bruce et al. 2003; Takala et al. 1999a). Large studies have further identified the VO_2 max as an independent predictive factor for metabolic syndrome and diabetes (Hassinen et al. 2010; Eriksson and Lindgarde. 1996). The VO_2 max by itself has been considered to be an inherited feature mainly reflecting the oxidative capacity in the skeletal muscle (Ostergard et al. 2006). Finally, the documentation of the decreased expression of the oxidative metabolism genes, their coactivators, ETC activity and thermodynamic coupling in myocytes in patients with type 2 diabetes as well as impaired mitochondrial activity in the offspring of patients with type 2 diabetes have lead to the suggestion that an initial mitochondrial dysfunction may disturb the insulin responsiveness in skeletal muscle (Patti and Corvera. 2010; Petersen et al. 2004b). In contrast to this, the skeletal muscle specific TFAM KO, mimicking mitochondrial myopathy, leads to respiratory chain failure in muscle without any concomitant decrease in basal or insulin-stimulated glucose uptake in mice (Wredenberg et al. 2006). In summary, the observation of reduced insulin sensitivity and oxidative metabolism in skeletal muscle before type 2 diabetes may remain associative (Phielix et al. 2008).

2.6.2 Metabolic aspects of mitochondrial myopathy

Myopathy is considered to be a late-onset feature among patients with m.3243A>G (Kärppä et al. 2005). The frequency of peripheral neuropathy in patients with the m.3243A>G mutation may be as high as 25% and mild limb weakness or myopathic changes in muscle histology have shown a similar frequency (Kärppä et al. 2003; Kärppä et al. 2005). Ultrastructural variations in mitochondrial size and shape, intramitochondrial crystals and subsarcolemmal and intermyofibrillar collections of mitochondria that is RRFs in trichrome stain are common findings among patients with m.3243A>G and limb weakness, whereas fat infiltration is rare (Kärppä et al. 2005; Stadhouders et al. 1994). A slightly elevated proportion of COX negative fibres is also found in patients with the m.3243A>G myopathy (Kärppä et al. 2005). Interestingly, mild limb weakness is not tightly associated with decreased physical activity, high

lactate, high creatine kinase or high heteroplasmy in skeletal muscle (Kärppä et al. 2003; Karppa et al. 2005). Nevertheless, m.3243A>G mutation load higher than ~50% is associated with low VO_2 max and low maximal workload and prevalent pathological findings in the muscle biopsy (Jeppesen et al. 2006). Oxygen extraction is markedly impaired in exercising forearm as the increase in blood flow is nearly normal (Taivassalo et al. 2002). Single fibre analyses have shown that the m.3243A>G mutation load varies remarkably between and within the cells and that the high heteroplasmy is co-located with prevalent RRFs in the muscle (Kärppä et al. 2005). An excess complex II staining has been reported also in the skeletal muscle blood vessel wall (Hasegawa et al. 1991). Therefore, mitochondrial angiopathy could hypothetically contribute to the insulin resistance in the skeletal muscle. Finally, only two studies have assessed peripheral insulin sensitivity using hyperinsulinemic clamp technique in altogether 17 subjects with m.3243A>G. Mutation heteroplasmy was reported only in leucocytes in one of these two studies. The results showed a trend towards insulin resistance in skeletal muscle but remained inconclusive (Suzuki et al. 1997; Velho et al. 1996).

2.7 Mitochondrial and glucose metabolism in adipose tissue

2.7.1 Insulin action in adipose tissue

Adipose tissue mainly consists of adipocytes which store energy and release fatty acids in fasting conditions (Coppack et al. 1990). The subcutaneous and intra-abdominal fat depots are often further divided into abdominal subcutaneous, retroperitoneal and visceral fat, which all have somewhat different metabolic relevance in human disease (Abate et al. 1995; Virtanen et al. 2005; Lefebvre et al. 1998). In adipocytes insulin stimulates glucose uptake, lipid synthesis and inhibits lipolysis (Coppack et al. 1990; Hagström-Toft et al. 1992). The glucose transporter GLUT4 is the rate limiting step of glucose uptake also in adipocytes. Insulin induces a several-fold increase in translocation of GLUT4 and glucose uptake in adipocytes (James et al. 1988; Green et al. 2006; Kraegen et al. 1986). This leads to a marked increase in glucose uptake in the adipose tissue (Rooyackers et al. 2004). Finally, the largest fat depot, the subcutaneous

adipose tissue accounts for only about 7% of the net glucose uptake during hyperinsulinemia in humans (Virtanen et al. 2002).

2.7.2 Adipogenesis and insulin resistance

Adipose tissue has a turnover rate close to ten years (Arner et al. 2010). The slow generation rate of new adipocytes is independently associated with larger adipocytes and systemic insulin resistance (Arner et al. 2010). Adipogenesis, the differentiation of mesenchymal precursor cells to mature adipocytes, is controlled by insulin through peroxisome proliferator-activated receptor(PPAR)gamma (Zhang et al. 2009). Knocking out PPAR gamma or insulin signalling in fat protects from obesity and glucose intolerance due to caloric excess (Jones et al. 2005; Bluher et al. 2002). In various insulin-resistant states the ability of insulin to stimulate glucose uptake and to suppress lipolysis is decreased in individual adipocytes and per fat tissue depot (Bolinder et al. 2000; Kramer et al. 2001; Virtanen et al. 2005). In obese individuals, the insulin-stimulated glucose uptake per adipocyte and per tissue mass may be restored by caloric restriction (Park et al. 2005; Viljanen et al. 2009). The obese adipose tissue is also infiltrated by macrophages and the secretion of adipocytokines and inflammation mediators are changed (Considine et al. 1996; Weyer et al. 2001; Alessi et al. 2000; Harman-Boehm et al. 2007). Decreased action of adipocytokines, in particular that of leptin and adiponectin, may alone result in insulin resistance (Lindsay et al. 2002). The relevance of healthy adipose tissue in preventing systemic insulin resistance and glucose intolerance becomes strikingly obvious in mice lacking the white adipose tissue (Colombo et al. 2002). Intriguingly, also the GLUT4 KO in adipose tissue alone is sufficient to induce insulin resistance in liver and in skeletal muscle and vice versa its overexpression in adipose tissue is able to reverse insulin resistance outside the adipose tissue (Abel et al. 2001; Carvalho et al. 2005).

2.7.3 Mitochondria in insulin-resistant adipocytes

Adipocytes from obese subjects exhibit a reduced aerobic respiration and uncoupling capacity (Yehuda-Shnaidman et al. 2010). The mtDNA copy number per adipocyte is positively related to lipogenesis and slightly decreased by increasing body mass index (BMI) in healthy humans (Kaaman et al. 2007). The activation of the PPAR gamma in the adipose tissue induces adipogenesis. It corrects the blunted insulin-stimulated glucose uptake and adipocytokine secretion in adipose tissue and finally restores the systemic insulin sensitivity (Jones et al. 2005; Ahmed et al. 2010; Hammarstedt et al. 2005; Viljanen et al. 2005). The levels of mitochondrial DNA, proteins and respiration may be reduced in the adipocytes as obese animals become diabetic (Laye et al. 2009). Accordingly, independent of obesity the genes encoding the ETC are downregulated in adipose tissue in patients with type 2 diabetes (Dahlman et al. 2006). In addition, based on a twin study some authors have proposed that an acquired rather than inherited factor explains many of the obesity-associated differences in the expression of the genes which promote mitochondrial biogenesis in the adipocytes (Pietiläinen et al. 2008). Intruingly, knockdown of TFAM in cultured adipocytes results in an impaired insulin-stimulated GLUT4 translocation to the cell surface and a subsequent decrease in glucose transport (Shi et al. 2008). The impact of mtDNA mutations on human adipose tissue metabolism has not been studied.

2.8 The role of liver metabolism in glucose homeostasis

2.8.1 Hepatic glucose metabolism and insulin resistance

2.8.1.1 Glucose metabolism in liver

Glucose metabolism in the liver is characterized by repartitioning and restoring absorbed nutrients and the release of glucose during fasting conditions (Babcock and Cardell. 1975). Glucose uptake, glycogen synthesis, ATP synthesis and lipogenesis are activated in response to insulin after glucose ingestion or during euglycemic

hyperinsulinemia. The liver produces glucose endogenously (endogenous glucose production [EGP]) by glycogenolysis and via *de novo* gluconeogenesis mainly from lactate, alanine, pyruvate and glycerol (Jenssen et al. 1990). After fasting or exercise, glycolysis and increasingly gluconeogenesis accounts for the hepatic glucose release (Babcock and Cardell. 1975; Wahren et al. 1971; Petersen et al. 2004a). Hepatocyte-specific insulin receptor activation is required for inhibition of hepatic glucose production (Fisher and Kahn. 2003). The basal EGP rate is autoregulated by glucose in the presence of fasting levels of insulin (Jenssen et al. 1990; Puhakainen and Yki-Järvinen. 1993). A moderate postprandial level in circulating insulin is sufficient to block both the basal and glucagon-stimulated EGP in the liver (Barzilai and Rossetti. 1993; Hartmann et al. 1987). During such hyperinsulinemia oxygen consumption is decreased, while glycolysis, gluconeogenesis and lipolysis are inhibited in the liver (Li et al. 2010; Baillet-Blanco et al. 2005; Ortmeyer et al. 1997; Simonsen et al. 2002).

2.8.1.2 Endogenous glucose production and diabetes

Hepatic glucose influx, storing and output are all regulated by insulin and other hormones. Patients with diabetes present with defects in these regulatory pathways (Probst et al. 1985; Giaccari et al. 1998; Petersen et al. 2004a). In human studies the EGP is calculated as a difference between the glucose-tracer plasma disappearance and whole-body glucose uptake. This difference mainly reflects the hepatic glucose production. However, liver is not the only source of the insulin suppressible EGP as the kidney and possibly skeletal muscle may replace the EGP in liver. Therefore the isotope methods assessing gluconeogenesis and glycogenolysis during euglycemic hyperinsulinemia have somewhat uncertain validity and liver tissue specificity (Battezzati et al. 2004; Huidekoper et al. 2010; Meyer et al. 2004; Lamont et al. 2003; Basu et al. 2008; Landau. 2001). Nevertheless, a high EGP is a common feature in both type 1 and type 2 diabetes and may be one of the major determinants of postprandial impairment in glucose tolerance (DeFronzo et al. 1982; Woerle et al. 2006). In patients with type 1 diabetes the basal and insulin suppressed EGP are elevated (Cline et al. 1994; Petersen et al. 2004a; Perseghin et al. 2005). In patients with type 2 diabetes the

autoregulation is preserved but gluconeogenic efficiency, basal and the insulin suppressed gluconeogenesis and thereby EGP are increased (Toft and Jenssen. 2005; Groop et al. 1989).

2.8.1.3 Measuring glucose influx to liver

Liver receives oxygen and nutrients including glucose from hepatic artery and portal vein (Pagliassotti et al. 1992). GLUT2 is the dominant glucose transporter in the liver. Glucose uptake by liver plasma membranes is characterized by features of simple diffusion, i.e. linearity of uptake, lack of stereospecificity, and by facilitated diffusion (Bachmann and Challoner. 1976). Glucose transporter GLUT2 has been considered to be a non-rate-limiting and essentially an insulin receptor activation independent glucose uptake step in the hepatocytes. However, this step is important in regulating hepatic and system glucose homeostasis and in the mobilization of glycogen stores (Burcelin et al. 2000; Santer et al. 1997). The first intracellular step, the dominant liver hexokinase, GK is the rate limiting step in glucose uptake to hepatocytes (Ferre et al. 1996). Extensive animal and human data have shown that the activity of the insulin-sensitive GK enzyme is essential for hepatic glucose uptake. The GK is also an indicator of hepatic glucose production even if the acute changes in its activity account for only a small portion of the in vivo inhibition of hepatic glucose retention by insulin (Barzilai and Rossetti. 1993; Tappy et al. 1997; Velho et al. 1996). Importantly, the restoration of hepatic GK expression corrects hepatic glucose flux and system glucose homeostasis in diabetic rodents (Torres et al. 2009; Okamoto et al. 2007). On the other hand, a long-term GK overexpression is accompanied by an increase in hepatic glucose influx but leads finally to insulin resistance, hypertriglyceridaemia and liver steatosis (Ferre et al. 2003).

Glucose uptake, the glycolytic pathway and the incorporation of glucose into glycogen are all augmented by a rise in insulin and potentiated by concurrent elevation in glucose (Satake et al. 2002; Massillon et al. 1995). Therefore, glucose ingestion increases the hepatic glucose transmembrane transport rate and the direct glycogen

synthesis in human liver (Petersen et al. 2001). Notably, also the glycogen synthase enzyme activity may only be sufficient to restore and maintain a system glucose homeostasis (Ros et al. 2010; Irimia et al. 2010). Dynamic [^{18}F]FDG-PET scanning with arterial blood sampling allows an accurate and organ specific measurement of the glucose influx rate from blood to hepatic tissue through the transmembrane and GK steps and the measured influx should essentially be limited only by the GK activity (Iozzo et al. 2007). [^{18}F]FDG-PET scans show that postprandial level of hyperinsulinemia doubles the hepatic glucose influx in humans. This is more than could be accounted for the concurrent FFA drop in blood (Moore et al. 2004; Iozzo et al. 2003a; Iozzo et al. 2004). The [^{18}F]FDG-PET studies have also shown that the hepatic glucose uptake step is part of the hepatic insulin resistance in patients with type 2 diabetes (Basu et al. 2001; Iozzo et al. 2003; Iozzo et al. 2007).

2.8.2 Liver fat and hepatic failure in mitochondrial disease

The availability of [^{1}H]MRS technique has refined excess liver fat as an independent risk factor for type 2 diabetes and cardiovascular disease (Stefan et al. 2008). Liver fat has been tightly associated with the impaired insulin action on hepatic glucose uptake and output, and also with insulin resistance in skeletal muscle and adipose tissue in patients with type 2 diabetes (Kotronen et al. 2008; Borra et al. 2008). It has been recently suggested that the impaired hepatic ATP turnover and hepatic insulin resistance could precede the development of hepatic steatosis at least in patients with type 2 diabetes (Szendroedi et al. 2009a). On the other hand, increase in the intermediates of the fatty acid oxidation might impair insulin signalling and mitochondrial function in the liver (Patti and Corvera. 2010). From the view of mitochondrial disease several reports have shown microvesicular steatosis and periportal inflammation in the liver of patients with Alpers-Huttenlocher´s syndrome, a fulminate hepato-cerebellar disease. Most of the pathogenic mutations associated with this syndrome are attributed to the POLG gene in the nuclear DNA encoding an mtDNA polymerase protein. The loss of POLG activity leads to depletion of mtDNA and to the loss of OXPHOS and mitochondrial ATP generation due to the decreased

amounts of respiratory chain complexes I, III, IV and ATP synthase in liver (Kurt et al. 2010; Tesarova et al. 2004). In addition, it has been hypothesized that high lactate could lead to high EGP as higher lactate flux to the liver might increase gluconeogenesis in mitochondrial diabetes (Maassen et al. 2004). However, the impact of m.3243A>G and other mitochondrial mutations to liver metabolism have been largely based on sporadic case reports (Takahashi et al. 2008; Szendroedi et al. 2009b).

2.9 Glucose utilization in human heart

2.9.1 Cardiac energetics

2.9.1.1 Myocardial substrate oxidation

Cardiomyocytes are rich in mitochondria (Bodak and Hatt. 1975). In the adult heart more than 90% of the ATP is provided by oxidation of acetyl coenzyme A (acetyl-CoA) in the OXPHOS (Ferrannini et al. 1993). The heart is omnivore that is able to use fatty acids, lactate, glucose and ketone bodies as energy sources (Stanley et al. 2005). The glycogen content of cardiomyocytes is much lower than that in the skeletal muscle emphasizing the importance of direct substrate supply for working myocardium (Russell et al. 1997). Substrate utilization is increased in proportion to cardiac work (Bergman et al. 2009a; Bergman et al. 2009b). At rest about 25% of the capacity of the respiratory chain is being used and this proportion may increase up to 85% during exercise with a concurrent increase in myocardial glucose uptake (Kemppainen et al. 2002; Mootha et al. 1997). Importantly, the intensity of cardiac work does not influence the substrate preference of the healthy heart for it is largely determined by the substrate availability (Ala-Rämi et al. 2005; Neglia et al. 2007). During the immediate postnatal period anaerobic glycolysis and lactate oxidation provide most of the ATP, whereas in the mature heart, fatty acid oxidation and to a lesser extent glucose oxidation are utilized for the ATP synthesis (Stanley et al. 2005). Exceptionally, high lactate oxidation may become a substantial source for ATP in exercising heart (Gertz et al. 1988; Kemppainen et al. 2002). The hyperinsulinemia ensuing carbohydrate consumption suppresses the FFA availability and the majority of

the acetyl-CoAs become derived from the glucose in humans (Ferrannini et al. 1993). Finally, ketones may suppress both glucose and FFA oxidation in myocytes, but under physiological conditions their contribution to the cardiac ATP production is negligible (Stanley et al. 2003).

2.9.1.2 Myocardial glucose uptake during hyperinsulinemia

The circulating fatty acids suppresses the glucose utilization in the heart and this suppression can be blocked by limiting FFAs, fatty acid transmembrane transport or fatty acid oxidation (Nuutila et al. 1994; Nuutila et al. 1992; Hajri et al. 2001; Abdel-aleem et al. 1994). FFAs are taken up in proportion to their circulating levels and their concentration is a linear predictor of glucose uptake in heart also during hyperinsulinemia (Mäki et al. 1998; Ala-Rämi et al. 2005; Knuuti et al. 1995). Insulin decreases fatty acid availability by suppressing lipolysis in adipocytes and also in the heart, but the extent to which intramyocardial lipids are used as a fuel during hyperinsulinemia is unclear (Moberg et al. 2002; Ferrannini et al. 1993). During a standard hyperinsulinemic-euglycemic clamp human myocardial perfusion is increased by ~l0%, glucose uptake is increased by ~400% and FFA levels in blood and the myocardial fatty acid uptake are decreased by ~75%, whereas oxygen consumption is not affected (Ferrannini et al. 1993; Iozzo et al. 2002; Knuuti et al. 1995; Takala et al. 1999b). On the other hand, an acute rise in arterial FFAs is not able to decrease the glucose uptake in heart by more than ~30%, thus part of the several-fold increase in glucose uptake during hyperinsulinemia is possibly a result of decreased lipolysis within the myocardium (Nuutila et al. 1992; Nuutila et al. 1994).

Insulin stimulates the initial incorporation of glucose into glycogen with no change in the glycogen content and thus results in an increased glycogen turnover in the heart (Russell et al. 1997). [^{18}F]FDG uptake parallels glucose uptake also during hyperinsulinemia and it may be used for quantification of glucose uptake in human heart (Ng et al. 1998). The insulin responsive GLUT4 is the predominant form of transmembrane transporter in the heart. However, GLUT1 and to a lesser extent

GLUT3 are also expressed in the human myocardium (Gavete et al. 2002). Studies on rodent hearts have suggested that during hyperinsulinemia the transmembrane transport in general or up to a 85% reduction in the GLUT4 expression are not rate limiting for myocardial glucose uptake (Gavete et al. 2002; Kaczmarczyk et al. 2003). The relatively high importance of FFA availability on glucose uptake as compared to the direct insulin stimulation of the transmembrane glucose transporter translocation has been further demonstrated by the myocyte specific KO of insulin receptor. This leads to a paradoxical increase in the basal cardiac glucose uptake and to a preserved insulin-stimulated glucose uptake rate (Belke et al. 2002).

In the long term, the heart size is reduced and glucose oxidation and insulin-stimulated glucose uptake is increased in rodents in which mitochondrial fatty acid uptake for instance via carnitine palmitoyltransferase 1 is reduced due to acetyl-coenzyme A (CoA) carboxylase KO (Essop et al. 2008). Also, high fat feeding leads first to a decrease in glucose oxidation and to a decreased GLUT4 translocation, which precedes impaired insulin signalling (Wright et al. 2009). Interestingly, also the 85% reduction in GLUT4 leads to cardiac hypertrophy and impaired contractile function in 22 weeks (Kaczmarczyk et al. 2003; Huggins et al. 2008). The studies above may demonstrate the importance of undisturbed glucose transport and oxidation for a long-term cardiac remodelling and function. Nevertheless, the glucose is the most economical fuel for heart in terms of oxidation and ATP yield (Stanley et al. 2005).

2.9.2 Mitochondrial cardiomyopathy

2.9.2.1 General outlines

Mutations in mtDNA or nuclear genes may result in respiratory chain deficiency and mitochondrial cardiomyopathy (Benit et al. 2003; Casali et al. 1999; www.mitomap.org). Mutations in mtDNA have been predominantly associated with hypertrophic concentric cardiomyopathy, even if cases with idiopathic dilated cardiomyopathy have also been reported (Anan et al. 1995; Limongelli et al. 2010;

Wahbi et al. 2010). Cardiac hypertrophy in echocardiography is a common finding in the absence of clinical complaints in the carriers of the mtDNA mutations (Casali et al. 1999).

2.9.2.2 Cardiac manifestations of the m.3243A>G mutation

Cardiac abnormalities have been described in many case series including patients with mitochondrial disease. Sudden and unexpected cardiac death is not uncommon in patients with m.3243A>G, even if non-cardiac causes such as epilepsy may also contribute (Majamaa-Voltti et al. 2008). The m.3243A>G mutation is the most common mutation leading to a maternally inherited form of hypertrophic cardiomyopathy (Majamaa-Voltti et al. 2002). Conduction defects, including Wolff–Parkinson–White (WPW) syndrome, have been reported in patients with the m.3243A>G mutation as also with other relatively prevalent mtDNA mutations such as m.11778G>A and m.8344A>G (Sproule et al. 2007; Nikoskelainen et al. 1994; Wahbi et al. 2010). A population-based study assessing the cardiac symptoms and signs, electrocardiogram, Holter recording and echocardiography in patients with m.3243A>G has shown a LVH in 56% of patients as compared to 15% in matched controls, giving an odds ratio of 7.5. Left ventricular systolic or diastolic dysfunction was observed in 34% of the patients and frequent ventricular extrasystoles in 14%. Still, only one out of 36 patients had a WPW syndrome (Majamaa-Voltti et al. 2002). Follow-up studies have shown that thickening of left ventricle progresses and leads to poor left ventricular contraction and occasionally to dilated cardiomyopathy (Majamaa-Voltti et al. 2006; Okajima et al. 1998).

2.9.2.3 Pathophysiology of mitochondrial cardiomyopathy

The pathogenesis of the LVH has been attributed to the energetic defect due to the failing OXPHOS. Biopsies performed during angiography have revealed abnormal mitochondrial accumulation in cardiomyocytes in patients with m.3243A>G (Sato et al. 1994). Additionally, the phosphocreatine to the ATP ratio as measured with

phosphorus magnetic resonance spectroscopy is decreased as compared to healthy controls and it tends to be inversely associated with the mutation heteroplasmy (Lodi et al. 2004). In mice, the tissue-specific TFAM KO leads to mtDNA depletion and low respiratory chain activity before other cardiac manifestations (Hansson et al. 2004). Likewise, the disruption of mitochondrial adenine nucleotide translocator leads to hypertrophic cardiomyopathy (Graham et al. 1997). Myocardial glucose transport and utilization is decreased in most patients with type 1 and 2 diabetes (Rijzewijk et al. 2009; Herrero et al. 2006). However, it is debatable if hyperglycaemia may, independently from FFA levels, lead to the insulin resistance of glucose transport in human myocytes (Peterson et al. 2008; Sondergaard et al. 2006; vom Dahl et al. 1993; Nuutila et al. 1993; Bugger et al. 2008; Utriainen et al. 1998). No studies on cardiac substrate utilization in patients with mitochondrial disease and with or without diabetes have been performed.

3 AIMS OF THE STUDY

1. To investigate whether glucose oxidation is decreased in the brain in patients harbouring the m.3243A>G mutation.

2. To evaluate the relative importance of the m.3243A>G heteroplasmy, insulin secretion and skeletal muscle insulin action for glucose homeostasis in mitochondrial diabetes.

3 To reveal potential defects in hepatic and subcutaneous adipose tissue metabolism in patients with and without mitochondrial diabetes using imaging techniques.

4. To characterize myocardial glucose metabolism during low fatty acid and high glucose availability using [^{18}F]FDG-PET during euglycemic hyperinsulinemia in patients harbouring the m.3243A>G mutation.

4 SUBJECTS AND STUDY DESIGN

4.1 Study subjects

The study included 29 subjects. Fifteen patients with m.3243A>G were recruited, most of them were previously ascertained in an epidemiological study (Majamaa et al. 1998). It was required that the m.3243A>G mutation heteroplasmy was at least 10% in buccal epithelium or in skeletal muscle. In the case of the 14 controls it was required that no diabetes was present in the first-degree relatives before the age of 55 years. In addition to clinical examination, the absence of m.3243A>G was assessed in buccal epithelium sample in the controls. For studies II-IV only controls with normal glucose (< 7.8 mmol/l at 2 hours) in an oral glucose tolerance test (OGTT) were included. Therefore one healthy control with impaired glucose tolerance 2 hours after the oral glucose load was excluded from studies II-IV.

Inclusion criteria for patients

1) The patient harbours the m.3243A>G mutation in the skeletal muscle or buccal epithelium

Exclusion criteria for all study subjects

1) Age under 20 or over 70 years
2) BMI > 30kg/m^2
3) Severe valvular disease
4) Blood pressure > 160/100 mmHg
5) Hepatic disease; gamma-glutamyltransferase > 120 (U/L), alanine transaminase > 180 (U/L)
6) Any renal disease; creatine > 130 (µmol/l)
7) Metal object in region of imaging

8) Anaemia with haemoglobin < 100 mg/dl in men and < 90 mg/dl in women
9) Oral corticosteroid treatment
10) Untreatable or newly diagnosed malignant disease
11) Pregnancy or lactation
12) Eating disorder or severe mental disorder
13) Clinical heart failure or coronary heart disease
14) Intense exercise training

Additional exclusion criteria for healthy volunteers

1) Diabetes in the 75g OGTT (11.1 mmol/L at 2 hours)
2) Presence of the m.3243A>G mutation in buccal epithelium
3) A family history suggestive for mitochondrial disease

4.2 Study design

4.2.1 General outlines

All subjects were instructed to avoid caffeine, smoking, alcohol, homeopathic preparations and changes in diet or in physical activity for 2 days before the study. Each subject underwent an OGTT and MRI and [^{1}H]MRS protocol on the first study day and indirect calorimetry and hyperinsulinemic-euglycemic clamp procedure with PET imaging on the second study day. Calorimetry, OGTT and the euglycemic clamp with PET imaging were conducted after at least a 10-hour overnight fast and insulin cease. MRI and [^{1}H]MRS studies were performed after at least a 6-hour fast. Metabolically active substances except thyroid hormone were discontinued at least 24 hours before all studies (Table 1). Physical activity was assessed with a validated physical activity questionnaire (Maddison et al. 2007).

4.2.2 Performing PET during euglycemic hyperinsulinemia

Two catheters were inserted, one in an antecubital vein for infusion of glucose and insulin and for injection of [^{15}O]-water ([^{15}O]H_2O) and [^{18}F]FDG, another in the opposite radial artery for blood sampling. Whole-body, skeletal muscle, myocardium, abdominal subcutaneous fat and liver glucose uptake were measured using PET and [^{18}F]FDG during standard euglycemic-hyperinsulinemic clamp. In addition, muscle and brain perfusion and brain oxygen consumption were measured using [^{15}O]H_2O and [^{15}O]O_2 PET tracers during the euglycemic hyperinsulinemia. A skeletal muscle transmission scan and a PET scan in the femoral region were separately performed for the [^{15}O]H_2O and [^{18}F]FDG emission scans. The first PET scan assessed femoral muscle perfusion using [^{15}O]H_2O at 40 min of clamp (Figure 3). The brain transmission scan and emission scans for perfusion, oxygen and glucose uptake were performed consecutively from 70 to 160 min. In order to asses glucose uptake, [^{18}F]FDG (0.23-0.29 GBq) was injected at 120 min. After the brain scan myocardial, subcutaneous fat and the liver glucose uptake was assed with a dynamic PET scan of the lower part of the thorax at 160 min. The last PET scan assessed the glucose uptake in the femoral region at 200 min (Figure 3).

Figure 3. Design of the positron emission tomography study. Each study consisted of a 220-min normoglycemic hyperinsulinemic period. [^{15}O]H_2O was injected twice intravenously, followed by a bolus inhalation of [^{15}O]O_2 which was in turn followed by [^{18}F]FDG injection. During the three dynamic [^{15}O] emission scans a continuous arterial blood sampling was carried out by a pump in order to determine the concurrent arterial input function. During the [^{18}F]FDG emission the arterial samples were drawn manually. A representative study is shown. [^{18}F]FDG arterial time-activity curve was obtained by repetitive arterial blood sampling. Repetitive thoracic scanning was used to measure the tissue activity. The average value within the liver and heart regions of interest (ROI) in each consecutive time frame gave the time-activity points in the tissue time-activity curves. The coronal reconstructions of all thoracal time frames are given at the top of each other. At the fore most frame the liver is under the right lung and the position of the ROI is given with a red square. A green circle indicates myocardium.

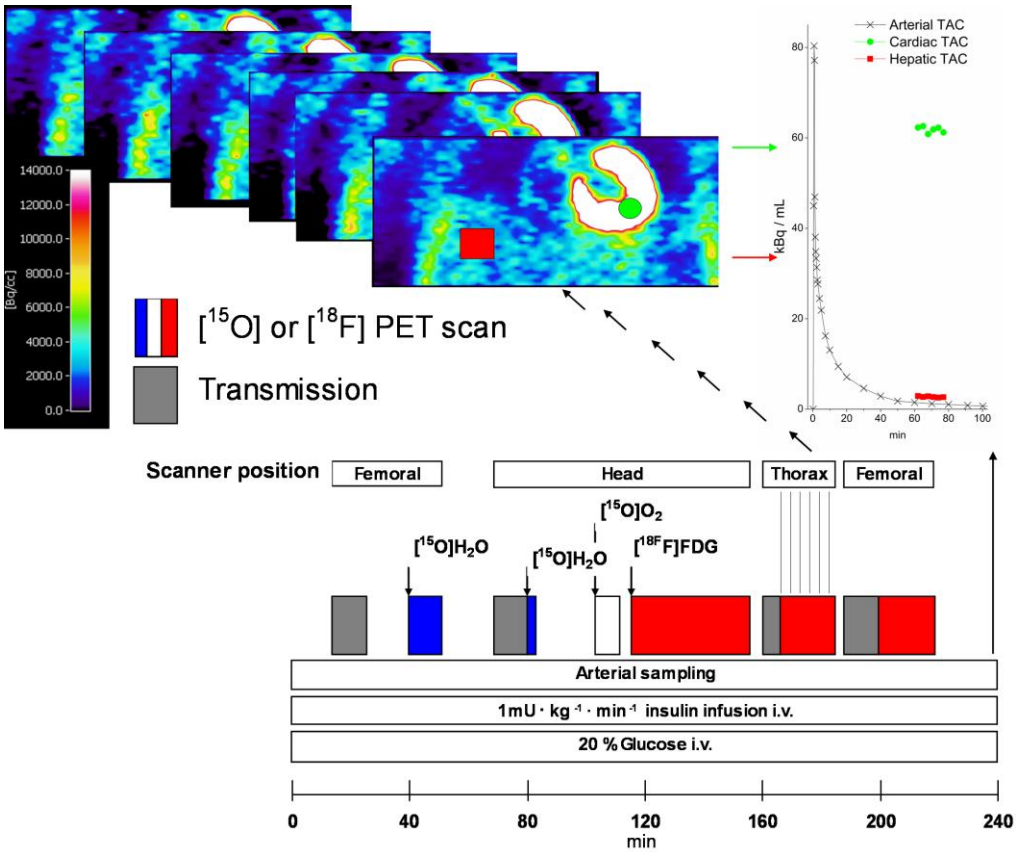

4.2.3 Primary variables and power calculations

Brain, myocardial, skeletal muscle, abdominal subcutaneous fat and liver glucose uptake were predefined as independent primary variables. In addition, regional cerebral metabolic rate of oxygen ($rCMRO_2$), cerebral perfusion (rCBF), liver fat and beta cell glucose sensitivity were considered as such. The sample size was based on power calculations using the standard deviation (SD), sample size and results of the previous studies in patients with defective insulin secretion and action and a previous cerebral PET study in mitochondrial disease (Iozzo et al. 2003; Virtanen et al. 2005; Nuutila et al. 1993; Frackowiak et al. 1988). For example, the glucose disposal rate was estimated to be 30 ± 9 µmol · kg^{-1} · min^{-1} for patients and 43 ± 12 µmol · kg^{-1} · min^{-1} for controls. The other parameters used for power calculation were: $\alpha = 0.05$ and $\beta = 0.1$. Here, it

was estimated that a sample of 11 patients with a control group including 11 subjects would give the power of 80%.

4.3 Safety and ethical considerations

The PET studies were performed using standard procedures. The estimated radiation dose for one individual was 10 mSv, which equals to a 2-year dose of background radiation. Pregnancy was excluded with standard urinary test in all possibly fertile women. If plasma glucose was elevated to over 25 mmol/l during the glucose tolerance test insulin was given. During euglycemic hyperinsulinemia, insulin, glucose and blood pressure were monitored continuously by a physician in the hospital facility. The potential inconvenience related to m.3243A>G testing in healthy controls as well as the risk related to arterial and venous cannula insertion and insulin infusion were explained to all study participants. This study was conducted according to the principles outlined in the Declaration of Helsinki. Written informed consent for the study was obtained from all subjects before any procedures and the study protocol was approved by the local ethics review committee (Ethics Committee of Southwest Finland Hospital District) and by the Turku PET Centre institutional review board, before commencement of the study.

5 METHODS

5.1 Assessment of the mutation heteroplasmy

A buccal epithelial cell sample was obtained from all the subjects (Table 1). The mutation heteroplasmy in skeletal muscle was previously available from 12 of the 15 patients with the m.3243A>G mutation (Majamaa et al. 1998). The amplified fragments were digested with 10U of ApaI (New England Biolabs, Beverly, MA) overnight at 37C°. The digestion products were electrophoresed through a 4% polyacrylamide gel using a model 377 DNA sequencer (Applied Biosystems, Foster City, CA). The acrylamide gel was dried and autoradiographed and analyzed. The reproducibility was controlled by including a sample with the m.3243A>G mutation in each electrophoresis run. The proportions of mutant and wild-type mtDNAs were calculated from the peak areas of cleaved and uncleaved mtDNAs (Moslemi et al. 1998). The heteroplasmy of each sample was determined twice. A standard curve, constructed by mixing different proportions of cloned mutant and wild-type mtDNAs, was linear. The SD of the measurements had been estimated to be 0.6% (Kärppä et al. 2005).

5.2 Glucose tolerance test and the indices of the beta cell function

After an overnight fast subjects ingested 75 g glucose for the OGTT. Blood samples were collected for glucose, insulin and C-peptide at 0, 15, 30, 60, 90 and 120 min. The glucose tolerance was defined based on the glucose value at 2 hours. It was defined normal when < 7.8 mmol/l, impaired when from 7.8 to 11.1 mmol/l and diabetes was diagnosed if the value was over 11.1 mmol/l. The insulinogenic index (IGI), the ratio of the rise of the insulin and glucose concentrations over the basal level at 30 min as well as the ratio of insulin and glucose areas under curve were calculated. Also the basal insulin secretion rate was calculated (BSR, pmol · min^{-1} · m^{-2}). Mathematical modelling based on C-peptide deconvolution was used to describe GIS as the sum of two components: GIS = $S_g(t)$ + $S_d(t)$ reflecting the main components of physiological

beta cell response to glucose (Mari et al. 2001). The first component, Sg(t) expresses a static relationship between beta cell insulin secretion and glucose concentration (G) in a constant manner. It is mainly defined by the dose–response function of the GIS [f(G)]. The steepness of the f(G) slope within the observed glucose range is denoted as the "beta-cell glucose sensitivity" (Mari et al. 2001; Mari et al. 2002). The model further assumes that this beta cell dose–response function is modulated by a time-dependent "potentiation factor" [P(t)] accounting for such modulators of insulin secretion as exposure to hyperglycaemia and the action of gastrointestinal hormones during the glucose tolerance test. Therefore the first component Sg(t) mainly describing the beta cell dose response function is by itself a function of two factors Sg(t) = P(t)f(G). The increment in potentiation during the OGTT was semi-quantified as the ratio of the value of the estimated potentiation at the end of the test to that at the beginning. The second insulin secretion component, Sd(t), represents a dynamic dependence of insulin secretion on the rate of the positive change (rise) in glucose concentration. This constant which describes the additional insulin secretion determined by the rate of blood glucose rise is termed as the "rate sensitivity". The rate sensitivity reflects essentially the same beta cell response, which is provoked by the rapid rise in the intravenous glucose tolerance test, which in turn is commonly ascribed to reflect the rapid insulin granule release (Mari et al. 2002).

5.3 Magnetic resonance imaging and spectroscopy

The subjects were lying in a supine position during the MRI and [^{1}H]MRS. The same superconducting 1.5 T MRI scanner was used for all magnetic resonance measurements (Gyroscan Intera Nova Dual, Philips Medical Systems, Best, The Netherlands).

5.3.1 Brain magnetic resonance imaging and spectroscopy

Axial T2-weighted Turbo Spin Echo [echo time (TE)/repetition time (TR) = 100/4438 ms], coronal Fluid Attenuated Inversion Recovery [TE/TR/inversion time = 140/11

000/2800 ms] and 3D T1-weighted Fast Field Echo (TE/TR = 4.6/25 ms) images were obtained. Two neuroradiologists visually scored brain atrophy (central, cortical and cerebellar) and white matter changes (frontal, temporal, occipito-parietal, basal ganglia and infratentorial) on a four-point scale (Wahlund et al. 2001). The scoring was performed independently and, in the case of disagreement, a consensus was negotiated. The raters were not blind to clinical data. Single-voxel [^{1}H]MRS was performed using Point Resolved Spectroscopy (TE/TR = 144/3000 ms and TE/TR = 288/3000 ms, 128 measurements, voxel size 28 x 10 x 30 mm ^{3}). The 8.4 ml single voxel was placed in the normal appearing white matter and was centred in the middle of capsula interna and inclined parallel to its fibres, avoiding cortical grey matter and CSF spaces (Study 1; Figure 1). All spectra were analysed using the LCModel software package (Provencher. 1993). In each spectrum, the choline, creatine (Cr), N-acetyl-aspartate (NAA) and lactate signals were identified. In order to allow semi-quantitative comparisons of the metabolite data, the ratios for NAA to creatine (Cr), choline to Cr and lactate to Cr (NAA/Cr, choline/Cr and lactate/Cr) are given in the result section.

5.3.2 Cardiac magnetic resonance imaging

Magnetic resonance images were acquired using a 5-element (sensitivity encoding) cardiac coil. The left and right ventricular functions and dimensions were measured from continuous short axis slices by using the balanced turbo field echo sequence (Koskenvuo et al. 2007). Ten to fourteen slices were acquired during serial breath holds and vector cardiographic retrospective gating to cover the ventricles completely from apex to atrium. The slice thickness was 8 mm and with no gaps between the slices (TR = 3.4 ms, TE = 1.7 ms, flip angle 60º and matrix 256 · 256 pixels). Cine loops were reviewed to identify end-diastolic and end-systolic frames. Epicardial and endocardial contours were outlined manually using post-processing software (ViewForum R5.1, Philips Medical Systems; Koskenvuo et al. 2007). Papillary muscles were separately outlined and included in myocardium. End-diastolic and end-systolic volumes were calculated and used to compute cardiac output, stroke volume

(SV) and ejection fraction. The myocardial mass was calculated from diastolic volumes. An experienced observer blinded to clinical data carried out all the tracings.

5.3.3 Abdominal fat depots

A single 10 mm axial T1-weighted fast field echo image was obtained at the level of the intervertebral disc L2-L3 (matrix size 256 · 256 pixels). The images were analyzed on the screen using the region of interest (ROI) facility (Study III; Figure 1). Abdominal subcutaneous and intra-abdominal fat (retroperitoneal and visceral) depot volumes were calculated as previously described (Abate et al. 1997). The adipose tissue density of 0.9196 g/ml was used to convert the measured volumes into weight.

5.3.4 Assessment of liver fat content with [^{1}H]MRS

Liver fat was measured by applying a previously validated [^{1}H]MRS method (Szczepaniak et al. 1999; van Werven et al. 2010). First, a 10 mm thick axial T1 weighted dual fast field echo anatomical reference image of the liver was obtained during breath hold intervals (TE = 2.3 and 4.6 ms, TR = 120 ms). Then, a 27 cm^3 single voxel was positioned in the liver outside the area of the great vessels. Data was acquired during breath-hold intervals using a point-resolved spectroscopy technique (TR = 3000 ms and TE = 25 ms). A quality check was performed manually on each spectrum before the final analysis using user-independent LCModel software. The fat and water amplitudes were corrected for different T2 decay and molar concentrations of ^{1}H nuclei in fat and water as previously described in more detail (Borra et al. 2008). The liver fat content was expressed as fat weight in relation to the total weight of liver tissue (%).

5.4 Indirect calorimetry

The basal whole-body oxygen consumption and the carbon dioxide production were measured in a fasting state with an open-system indirect calorimeter in a quiet dimly-lit

room. The subject's head was placed under a plastic canopy connected to the analyzer. The canopy is a half-ellipsoidal hood made of 1-mm-thick transparent plastic. It is connected with adapters for tubing and with a wide edge of soft plastic cloth to make the construction airtight around the head and neck of the subject (Meriläinen. 1987). The difference between inspired oxygen and expired oxygen was measured with a fast-response paramagnetic differential oxygen sensor (OM-101, Datex/Instrumentarium, Helsinki, Finland, Meriläinen. 1988). The expired CO_2 was measured with an infrared CO_2 sensor. Baseline CO_2 in the air was utilized as a reference. The standard CO_2 production and O_2 consumption rates were calculated. The O_2 consumption rate was calculated using the Haldane transformation: O_2 consumption rate = (Q/ [1-inspired O_2]) x (Disappearance O_2 - Inspired O_2 x [appearance CO_2]) (Meriläinen. 1987). The CO_2 production and O_2 consumption rates were calculated from a 10-minute period after 20 min of initial stabilization. The whole-body energy expenditure (EE) was calculated from the measured rates of O_2 consumption and CO_2 production EE = 3.581 x (O_2 consumption +1.448) x (CO_2 production - 32.4), where EE is given in kcal/d, O_2 consumption and CO_2 production in l/d (Takala et al. 1989).

5.5 Euglycemic hyperinsulinemia

Subjects were lying in a supine position during hyperinsulinemic-euglycemic clamp and the PET-imaging. At 0 min a standard primed hyperinsulinemic-euglycemic clamp was started for at least 220 min using 1mU · kg^{-1} · min^{-1} intravenous insulin infusion (Actrapid, Novo Nordisk A/S, Bagsvaerd, Denmark, DeFronzo et al. 1982). Normoglycemia was maintained using variable rates of 20% glucose infusion, adjusted according to plasma glucose measured in every 5 – 10 minutes in arterial blood. A steady state was reached always before 50 min of the clamp. The whole-body glucose uptake per tissue weight was calculated from the glucose infusion rate between 60 to 180 min. It was expressed as μmol · min^{-1} · kg^{-1}. At 120 min [^{18}F]FDG (0.23-0.29 GBq) was injected for over 15s. The EGP rate was calculated from the plasma [^{18}F]FDG clearance rate as previously validated against d-[6,6-(2)H(2)]glucose tracer method

(Iozzo et al. 2007). Plasma lactate, serum FFA concentrations and insulin were measured in arterial samples obtained at 0, 30, 60, 120 and 180 minutes during hyperinsulinemia (Figure 3).

5.6 PET-imaging

5.6.1 Production of PET tracers

For the production of [^{15}O] (t1/2 = 123 seconds) a low energy deuteron accelerator was used (Cyclone 3, Ion Beam Application Inc., Louvain-la-neuve. Belgium). [^{15}O]O_2 was produced in the ^{14}N(d,n) [^{15}O] reaction using nitrogen gas as target material. The radiochemical purity of [^{15}O]O_2 exceeded 97%. [^{15}O]H_2O was produced based on the membrane technique using sterile exchangeable tubing in the device as previously described (Sipilä et al. 2001). Sterility and pyrogenity tests were performed to verify the purity of the product. [^{18}F]FDG (t1/2 = 110 minutes) was synthesized with a computer-controlled apparatus according to a modified method of Hamacher et al (Hamacher et al. 1986). The specific radioactivity at the end of the synthesis was better than 70 GBq/μmol and the radiochemical purity exceeded 98%.

5.6.2 Image acquisition

All the images were acquired with the same GE Advance PET scanner (General Electric Medical Systems, Milwaukee, WI, U.S.A.), which gives 35 transaxial planes with axial resolution of 4.7 mm and with an in-plane resolution of 5.5 mm. The subjects were lying in a supine position during the PET protocol. After the hyperinsulinemic-euglycemic clamp initiation subjects were positioned and their feet were fixed on the scanner head rest and cushions were applied in order to minimize muscle activation in thighs. The correction for photon attenuation in tissue was determined by using transmission scanning with external circulating ^{68}Ge rod sources. A transmission scan of the femoral region was obtained and after 40 min of clamp [^{15}O]H_2O (0.5-0.8 GBq) was injected in for over 30s using automated administration

(Figure 3). Femoral muscle perfusion was scanned with dynamic 6-min image acquisition (frames 6 · 5s, 6 · 15s and 8 · 30s). Thereafter the subjects were repositioned: the head was fixed to the head rest and a ~ 9-min transmission scan of the head was performed. At 80 min [^{15}O]H_2O (0.22–0.34 GBq) was injected (a 30s injection) and a 90s brain perfusion scan was obtained. After the decay of the previous tracer and a production of a new [^{15}O]O_2 tracer [^{15}O]O_2 (1.13–1.35 GBq) bolus was gathered into a plastic inhalation-bag, released by the investigator and inhaled at command by the study subject at 100 min. Thereafter, tissue O_2 was measured with a 5-min dynamic scan (frames: 6 · 10s, 6 · 20s and 4 · 30s). At 120 min, [^{18}F]FDG (0.23–0.29 GBq) bolus was injected for over 15s and a dynamic 40-min brain scan was started (frames: 4 · 30s, 3 · 60s and 7 · 300s). After a transmission scan a PET scan of lower thorax was performed (frames: 6 · 180s). This scan was performed at 160 min in order to obtain the tissue time activity curve for subcutaneous fat, hepatic tissue and myocardium. The femoral region was again scanned for transmission and at 200 min for [^{18}F]FDG activity (frames: 6 · 180s). Arterial blood samples were drawn in order to calculate the concurrent input function for each tracer and scan. For the same purposes, haematocrit, gas analysis and acid–base status were determined in arterial blood before and after each [^{15}O]O_2 scan (Figure 3).

5.6.3 Quantification of the PET data

5.6.3.1 Tissue glucose uptake rate

The PET scanner and other devices were cross-calibrated. The arterial blood [^{18}F]FDG time activity curve was obtained by analyzing repeated arterial samples using an automated gamma counter (Wizard 1480, Wallac, Turku, Finland). The tissue time activity curve was obtained from [^{18}F]FDG -PET scans with repetitive sampling frames (Figure 3). All [^{18}F]FDG-PET data were normalized, corrected for decay and attenuation and reconstructed as a 128 · 128 pixel matrix using a planar Hann filter and an axial ramp filter. Plasma and tissue time-activity curves were analyzed graphically according to Patlak and Blasberg in order to quantify the fractional rate of tracer uptake

(K_i), which represents the combined tracer transmembrane transport and phosphorylation step from blood to tissue (Patlak and Blasberg. 1985; Nuutila et al. 1992). For the calculation of tissue glucose uptake the three-compartment model of [^{18}F]FDG kinetics was employed (Reivich et al. 1979, Sokoloff et al. 1977). K_i is equal to ($k_1 \cdot k_3 / [k_2 + k_3]$), where k_1 is the transfer coefficient from vascular space into the tissue, k_2 is the initial clearance and efflux coefficient, and k3 is the phosphorylation rate constant. The rate of the glucose uptake within the ROI was obtained by multiplying K_i by the plasma glucose concentration divided by a lumped constant term. The lumped constant accounts for differences in the transport and phosphorylation of [^{18}F]FDG and glucose. Based on previous validation studies in humans, the lumped constant of 1.2 was used for skeletal muscle and 1.14 was used for subcutaneous fat (Peltoniemi et al. 2000; Virtanen et al. 2001). The approximation of 1.00 was used for the myocardium and the liver (Ng et al. 1998; Iozzo et al. 2007). A consensus lumped constant of 0.8 validated against other PET techniques was used to calculate the rGMR (Graham et al. 2002). In skeletal muscle, liver and subcutaneous adipose tissue the Patlak fit was done directly on the tissue activity curve consisting of six consecutive sampling frames using the elapsed time from tracer injection to frames of each six time points (Figure 3). The tissue activity at a certain time point was the mean activity of all pixels within the ROI. The left ventricle myocardium data was corrected for partial volume and for the spillover from the left cavity based on the cardiac dimensions and left ventricle wall thickness in the cardiac MRI. Individual parametric images were computed for the brain glucose uptake giving a quantitative value for each voxel based on the Patlak equitation. The average brain tissue density of 1.04 g/ml was applied to calculate the metabolism per tissue gram (Långsjö et al. 2003).

5.6.3.2 Muscle and brain perfusion

The [^{15}O]H_2O radioactivity were decay-corrected. In order to obtain the arterial time activity curve (input function) the arterial radioactivity was measured. This was done using a two-channel coincidence detection system (GEMS, Uppsala, Sweden) on the

radial artery blood sampling line where 6 ml/min blood outflow was maintained with a pump during the [^{15}O]H_2O scan (Figure 3). The blood flow was calculated pixel-by-pixel into flow images using a quantitative autographic method as previously described and validated (Huang et al. 1983; Iida et al. 1986; Ruotsalainen et al. 1997; Fischman et al. 2002; Howard et al. 1983). A 250s tissue integration time was used for skeletal muscle. In brain, the tissue activity was assessed with a 90s one-frame scan initiated automatically at a rapid increase in the coincidence detection rate. An estimated arterial [^{15}O]H_2O input-activity curve was achieved by correcting the measured blood activity for delay and dispersion (Iida et al. 1986). The quantification is based on a one-compartment model, in which the tissue tracer concentration (Ci) depends only on arterial concentration (Ca), venous concentration (Cv), and flow (f). In the model, the venous concentration is approximated. It is assumed that 1) Tissue-blood water equilibrium is immediate. 2) The tissue-blood water content ratio is stable, represented by partition coefficient (p), with a value of 0.8 in normal brain and 0.99 in skeletal muscle (Huang et al. 1983; Ruotsalainen et al. 1997). As a result, the venous concentration is also always constantly related to the tissue concentration. Using the PET measured tissue activity and the arterial blood activity curve from the sampling line, a lookup table of calculated tissue tracer activity values for a range of imaginary flow values is created. This conversion table is then transformed pixel-by-pixel into quantitative (parametric) flow images (Howard et al. 1983).

5.6.3.3 Brain oxygen metabolism

The oxygen consumption was quantified with non-linear fitting of the dynamic PET scans as previously described (Kaisti et al. 2003). The relationship between oxygen extraction fraction and blood flow, both derived from the [^{15}O]O_2 inhalation PET, arterial oxygen concentration $[O_2]a$ and oxygen uptake ($CMRO_2$) is as follows: $CMRO_2 = [O_2]a \cdot$ oxygen extraction fraction $\cdot$ rCBF. For the calculation of the regional oxygen-to-glucose index, the unit conversion was first performed using the molar

volume of an ideal gas (22.4 l/mol) to obtain the $rCMRO_2$ values in mmol · min^{-1}· $100g^{-1}$ and then these values were divided by the rGMR value (Okazawa et al. 2001).

5.6.4 Tissue analysis

5.6.4.1 Brain

For the quantitative estimation of regional metabolic values (rCBF, $rCMRO_2$ and rGMR), an automated explorative ROI analysis was conducted (Nagano et al. 2000). First a summation image including the total over all frames [^{18}F]FDG activity was calculated for each subject. This summation image was further used to coregistrate and reslice the MRI scans. In order to achieve matching image planes using Statistical Parametric Mapping software (version 2) running under MATLAB 7.5 (The Math Works Inc., Natick, MA, USA). Then, each summation image was normalized using a ligand-specific template for [^{18}F]FDG in order to convert them into the standard stereotactic space used for the statistical analysis. The resulting normalization parameters of each summation image conversion were then further used to convert all the parametric PET images as well as the MRI to PET coregistered MRI scans into the same standard stereotactic space. The quality of the conversion into the standard stereotactic space was manually assured by comparing the converted parametric and anatomical images with each other and with the location of the predefined ROIs. Standardized ROIs were defined on a template image (Montreal Neurological Institute database) using Imadeus software (version 1.50, Forima Inc., Turku, Finland). Eight predefined paired ROIs were drawn encompassing grey matter in posterior cingulate, frontal cortex (anterior cingulate and venterolateral frontal cortex), occipital cortex (extrastriate cortex), temporal cortex (superior, middle and inferior temporal gyri), parietal cortex (angular and supra-marginal gyrus), putamen, thalamus and cerebellum (cerebellar cortex) in the standard stereotactic space. In addition, a pair of ROIs was drawn in the white matter between the lateral ventricles and parieto-frontal cerebral cortex.

5.6.4.2 Myocardium, skeletal muscle, liver and adipose tissue

Myocardium was outlined and the ROIs were defined and reviewed using semi-automated segmentation software (Carimas 2.0, Turku PET Centre, Finland). This segmentation software was preferred as it allowed an automated analysis of the main vascular regions. It was also able to detect and outline a larger proportion of the ventricle wall volume as compared to manual analysis. The average left ventricle glucose uptake was calculated as the mean of the three regions. The tip of the left ventricle apex was not included in this analysis. In skeletal muscle, the regions of interest were drawn both in quadriceps femoris and in hamstring muscles on 3 consecutive planes and on two axial levels of the muscle region carefully avoiding large blood vessels (Nuutila et al. 1993). Due to similar results, the mean of the ROIs in the two legs and regions was used in further analysis. The regional glucose extraction in muscle tissue was calculated by dividing the average glucose uptake with the average perfusion value within the drawn ROI. For adipose tissue a single ROI on three planes was defined in the subcutaneous fat in the upper abdomen (Study III; Figure 1). In liver an ellipsoid ROI on five consecutive planes in the major liver lobe and outside the area of large vessels was used (Figure 3). The localization of the subcutaneous, liver and skeletal muscle ROIs were verified by first defining the ROIs on the respective transmission image and thereafter copying in the positron emission image using Vinci 2.54. software (Max-Planck-Institut für neurologische Forschung, Cologne, Germany).

5.7 Biochemical analyses and cytokines

Plasma glucose was determined with a glucose oxidase method (GM7 Analyser, Analox Instruments, Hammersmith, UK). Glycosylated haemoglobin (Hb-$A1_C$) was measured with an ion-exchange high performance liquid chromatography (Variant II Haemoglobin A1c, Bio-Rad Laboratories, CA, USA). The enzymatic method (IFCC, Roche Modular P analyser, Roche Diagnostics GmbH, Mannheim, Germany) was used

to measure plasma lactate, plasma high-density lipoprotein cholesterol and serum creatine kinase. Blood pyruvate was measured using an enzymatic method (Instruchemie, Delfzijl, The Netherlands). Plasma C-peptide and insulin were assessed by an electrochemiluminescense immunoassay technique (Roche Modular P analyzer, Roche Diagnostics GMbH, Mannheim, Germany). Serum FFA concentrations were measured using an enzymatic colorimetric method, plasma triglycerides with an enzymatic method and plasma cholesterol with an enzymatic method (Roche Modular P analyzer). Fasting serum samples were stored at –70°C and assayed for adiponectin, active plasminogen activator inhibitor-1 (PAI-1) antigen, resistin, interleukin-6 (IL-6), interleukin-8 (IL-8), monocyte chemoattractant protein-1 (MCP-1), nerve growth factor (NGF), tumour necrosis factor-α (TNF-α) and leptin using commercial methods with inter-assay coefficients of variation < 21% as provided by the manufacturer (LINCOplex Kit and Luminex200 instrument, Linco Research, St. Charles, MO, U.S.A.). The measured intra-assay coefficients of variation were < 8.9%. The C-reactive protein (CRP) was determined with a Cobas Modular 6000 analyzer (F. Hoffmann-La Roche Ltd, Diagnostics Division, Basel, Switzerland) using reagents purchased from the same company (C-Reactive Protein, Latex, High Sensitive Assay).

5.8 Statistical methods

5.8.1 General analysis

Before analysis, the normality of variables was assessed with Shapiro–Wilk test. Normalizing procedures were performed in the original publications (I-IV), but they were not applied in the data presented in the results section. Based on the Shapiro–Wilk test, differences among two groups were identified using Student's t-test or Mann–Whitney U-test. In the case of more than two groups, one-way analysis of variance (ANOVA) and Tukey-Kramer post hoc procedure were applied. In the case of at least three groups and continuous variables, which were not normally distributed Kruskal–Wallis test was performed. If the loss of power was suspected, non-parametric tests were performed where appropriate. For the same purpose patients were first

compared with the controls before any subgroup analysis. For non-parametric data post hoc tests were carried out by using the Mann-Whitney U test and P-values were corrected for multiple comparisons by the Benjamini-Hochberg method if not stated otherwise. A P-value of < 0.05 was considered statistically significant. In the result section, significant linear correlations are identified using Spearman's correlation coefficients and Mean ± SD are given if not stated otherwise.

5.8.2 Statistical approach to multiple regions of interest in brain

In brain an explorative ROI analysis was conducted and altogether nine predefined ROIs were applied (Study I). The preliminary analysis revealed only negligible left–right differences and, consequently, all brain ROI variables were presented as the mean of the left and right side. In the case of brain MRI and PET data, special care was taken to eliminate family-wise type I error, which could be introduced by the numerous simultaneous between-group comparisons performed in multiple brain regions. We applied Holm–Bonferroni correction to adjust P-values of all the pair-wise comparisons between groups, which were carried out simultaneously in multiple regions for each outcome. This method controls the family-wise error both for dependent and independent measures. For example, the atrophy scores for three groups were corrected for 9 (groups · regions = 3 · 3) simultaneous hypotheses. For the sake of clarity, an uncorrected post hoc P-value is shown in the analyses of the brain PET and MRI data and the significance remaining after Holm–Bonferroni correction is indicated separately (Study I, result section). In addition, standard z-scores were assigned for each ROI, in each individual, using the SD of the control group in ROIs. Thereafter, an average z-score for each main outcome was obtained in order to give a normal variation context to the detected changes.

Single-measure intraclass correlation coefficients were calculated for the brain ROI data giving $r = 0.85$ for $rCMRO_2$, ($P < 0.001$), $r = 0.69$ for rGMR ($P < 0.001$) and $r = 0.77$ for rCBF ($P < 0.001$). These figures suggested interdependency within the

regional data. This was true also for the regional atrophy scores ($r = 0.75$, $P < 0.001$) and the white matter changes ($r = 0.33$, $P < 0.001$) in the MRI data set. Due to the probable interdependency, the ROI data were first analyzed a priori by repeated-measures ANOVA, using the Huynh–Feldt correction for the sphericity. The nine brain regions were entered as within-subject factors and the group (patients or controls) as the between-subject factor. The main effects and the interaction of these variables were modelled. Repeated-measures ANOVA indicated a major regional variability in all the main outcomes ($P < 0.001$ and Partial $\eta^2 > 0.880$ for $rCMRO_2$ as well as for rGMR and rCBF). Secondly, a similar repeated-measures ANOVA procedure with the presence of symptoms as the between-subject factor was carried out on patient data in order to examine if the presence of symptoms influenced the main outcomes. Thirdly, repeated-measures ANOVA was carried out on all ROI data for confirmatory purposes and to examine the main between-subjects effect (patient subgroups or controls).

5.8.3 Statistical parametric mapping approach

Statistical parametric mapping was carried out as an explorative analysis covering the whole brain, i.e. without an a priori hypothesis concerning the location of potential changes in rCBF, $rCMRO_2$ and rGMR (Study I). Based on the previous autopsy study, the affected cortical areas, i.e. the size of the signal, were expected to be greater than the resolution of the smoothed image (Sparaco et al. 2003). Therefore the normalized parametric images were robustly smoothed by using a 12 mm Gaussian kernel. A subtraction analysis with t-contrasts was used to compare the patients with the controls. Since the rCBF, $rCMRO_2$, and rGMR values of parametric images are quantitative, a subtraction analysis with t-contrast was performed without global normalization. The statistical power of statistical parametric mapping is partly a function of the height threshold and of the signal-size-to-resolution ratio and, therefore, we also used a low height threshold (T) 2.4 as well as the more conventional T 3.5 as previously recommended (Friston et al. 1996). On the other hand, the size of the signal was expected to be greater than the resolution of the smoothed image and even a lower

threshold than 2.4 might have been acceptable. Only clusters with corrected P-values are shown (Study I, Figure 3). Non-significant voxels were discarded from the visualizations by increasing the minimum cluster size (k). In addition, the expected false discovery rates of the voxels were kept always < 0.05 for the whole brain for all visualizations (Study I; Figure 3).

6 RESULTS

6.1 Feasibility of the study protocol (I-IV)

Some minor adverse effects were noted during the two-day study. One control subject had large subcutaneous haematomata few days after the arterial cannulation with spontaneous full recovery. One of the patients had presyncopal symptoms after the initiation of the primed hyperinsulinemic clamp and the brain imaging PET part was not performed for him and due to the lack of the primary variables he was excluded from the brain data analysis (Study I). One of the patients (group 1) failed to lie still due to the back pain during the last hour of the PET protocol and no regional abdominal fat, liver, skeletal muscle or heart [^{18}F]FDG data were obtained for her. Two of the subjects in the symptomatic group failed to inhale correctly and no [^{15}O]O_2 emission or $CMRO_2$ data was obtained. In addition, one patient (group 3) failed to lie still during the MRI due to claustrophobia and the essential part of the functional cardiac data was lost. One frozen plasma cytokine sample in the control group was lost during storing.

6.2 Brain metabolism (I)

6.2.1 Clinical encephalopathy and white matter [^{1}H]MRS

The essential clinical and metabolic characteristics of the patients are given on Table 1. The most common clinical manifestations were diabetes (n = 10) and sensorineural hearing impairment requiring a hearing aid (n = 5). Only one patient fulfilled the criteria for the MELAS syndrome and had had stroke-like episodes. More detailed clinical characteristics of the patients are given in Study I (Study I, Table 1). In six patients the encephalopathy was considered symptomatic as these patients had been diagnosed with stroke-like episodes or epilepsy or central nervous system changes were found in the baseline neurological examination. The remaining eight patients were considered asymptomatic and they all had previously performed a

neuropsychological test with no deviation from the normal range and no focal lesions were found in brain MRI (Majamaa-Voltti et al. 2006).

The single voxel measurement showed that the lactate to creatine ratio was significantly elevated in the white matter in patients 0.43 ± 0.33 as compared to controls 0.11 ± 0.11 ($P < 0.001$). This indicated a shift towards anaerobic glucose metabolism in the tissue. The [^{1}H]MRS and MRI indices of neurodegeneration showed that patients with cerebral symptoms had both significantly lower NAA to creatine ratio 2.02 ± 0.24 than the controls 2.45 ± 0.25 ($P = 0.006$) or the asymptomatic patients 2.41 ± 0.18 ($P = 0.012$) and higher mean atrophy scores 1.2 ± 0.8 than the controls 0.0 ± 0.1 ($P = 0.009$) or the asymptomatic patients 0.0 ± 0.0 ($P = 0.012$).

6.2.3 Oxidative glucose metabolism in the brain

A decrease in cerebral metabolic rate of oxygen was detected in all the regions of interest in the grey matter as well as in the white matter in patients with the m.3243A>G mutation as compared to controls (median -27%, range -18% to -29%). The average $rCMRO_2$ of the patients was 2.19 ml/100 g/min and that of the controls was 2.97 ml/100 g/min ($P < 0.001$, repeated-measures ANOVA, the main effect of the group [patients vs controls] on the regional values). The rGMR in patients (average 30.8 mmol/100 g/min) tended to be slightly lower in most of the regions (Median -10%, range -15% to + 5%) than the rGMR (average 33.8 ± 0.7 mmol/100 g/min) among the controls showing no or weak main effect of the group ($P = 0.056$ for rGMR). Both an absolute and relative decrease in $rCMRO_2$ was detected in asymptomatic as well as in symptomatic patients and in all brain regions as compared to controls (Figure 4 and Study 1 result section). In line with the elevated brain lactate, the regional ogygen-to-glucose index was reduced in patients (median -17%, range -10 to -28%, $P < 0.001$, the main effect of the group) as compared to control subjects. The decrease in the regional oxygen extraction fraction (median - 18%, range -16 to -26%, $P = 0.014$, main effect of the group) and quantitatively normal blood flow in regions

such as cerebellar cortex and periventricular white matter indicated no general perfusion defect in the brain tissue (Figure 4). Even if the groups were found to differ in $rCMRO_2$, rGMR, regional oxygen extraction fraction and ogygen-to-glucose index, the patient or patient subgroup comparison with the controls showed no significant differences in the overall rCBF between the groups (Study I; Table 4).

The decrease in rGMR was restricted to symptomatic patients and to the occipito-tempero-parietal region. The frontal lobe, white matter and cerebellum were relatively spared from the glucose hypometabolism (Figure 4 and Study I; Table 4). Also the statistical parametric mapping showed significant glucose and oxygen hypometabolism in patients with the m.3243A>G mutation. In accordance to the ROI analysis no global change in CBF was detected and the decrease in the metabolic rate of oxygen was confirmed in the grey matter in the whole brain and in both patient groups. Further, as the ROI analysis, the statistical parametric mapping approach did not detect any significant decrease in glucose metabolism in the frontal areas, cerebellum and white matter or in asymptomatic patients (Study I; Figure 3). In addition to the characteristic spatial and clinical patterns of the glucose hypometabolism, the glucose metabolism (average rGMR) correlated both with the NAA to creatine ratio ($r = 0.69$, $P = 0.006$, $n = 14$) and with the average $rCMRO_2$ ($r = 0.77$, $P = 0.003$, $n = 12$) in the patients with the m.3243A>G mutation. No linear coupling could be detected between the average rGMR and rCBF ($r = 0.125$, $P = 0.67$ and $n = 14$).

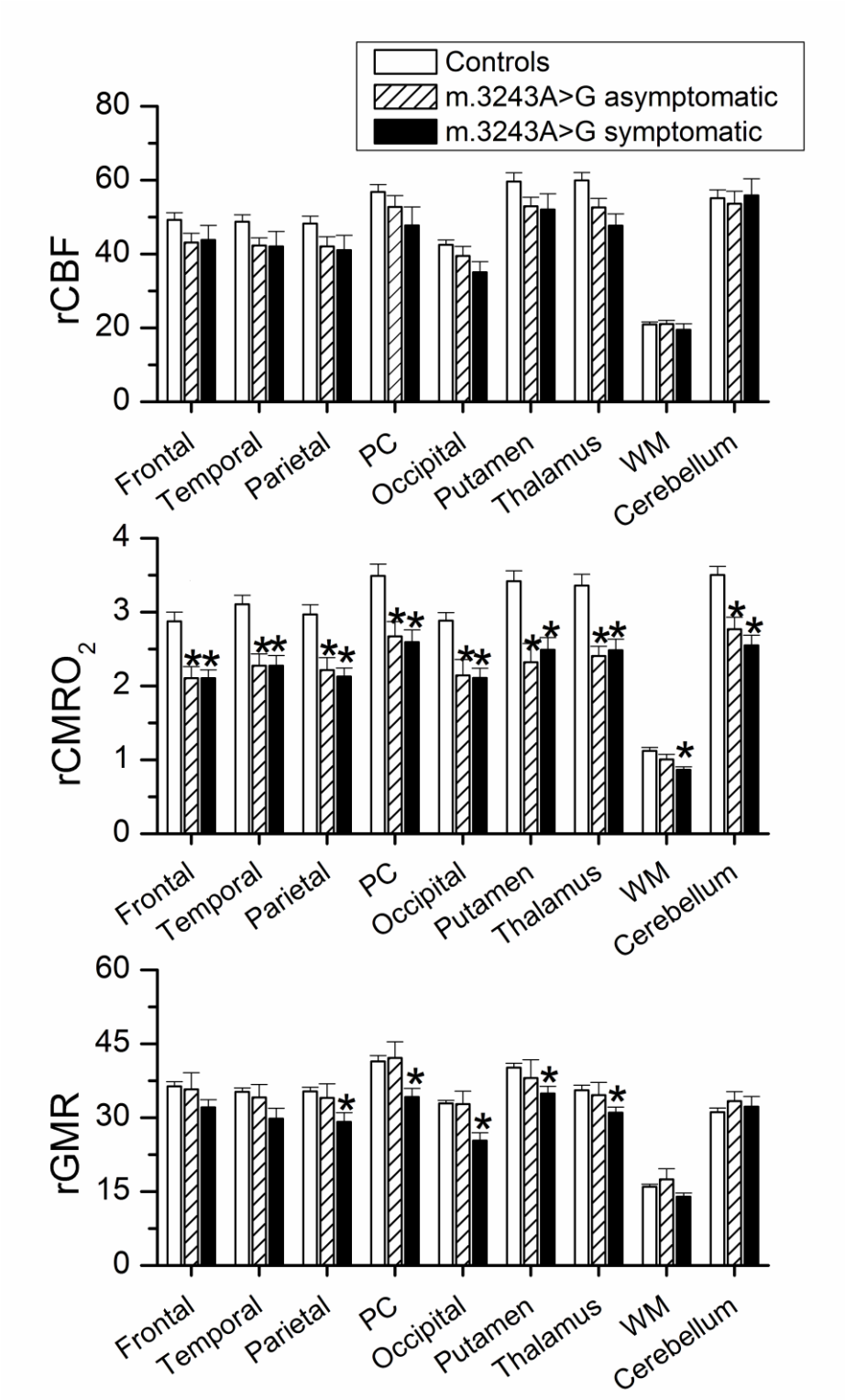
Controls
m.3243A>G asymptomatic
m.3243A>G symptomatic
rCBF
rCMRO2
rGMR
Frontal
Temporal
Parietal
PC
Occipital
Putamen
Thalamus
WM
Cerebellum

Figure 4. Quantitative regional metabolism derived from the PET studies. Absolute values of regional cerebral blood flow (rCBF = ml/100 g/min) and metabolic rate of oxygen ($rCMRO_2$ = ml/100 g/min) and glucose metabolic rate (rGMR = μmol/100 g/min). Data are mean ± SE. Data from the nine region-of-interest-defined structures are shown (PC = posterior cingulate, WM = white matter). For illustrative purposes the nine regions of the asymptomatic and symptomatic patient groups were compared to those of the controls with Mann-Whitney U test and the resulting 18 pair-wise comparisons in the figure were then corrected for the multiple comparisons arising from the two groups and from the multiple regions using the false discovery rate method ($\alpha = 0.05$). * A two-sided *P*-value < 0.05 vs controls after correction for multiple comparisons is given.

6.3 Metabolic characteristics related to insulin secretion and action (II-IV)

In metabolic studies other than the brain metabolism one healthy control subject was excluded due to impaired glucose tolerance in the OGTT. Patients with m.3243A>G were divided into three groups based on the OGTT (Table 1). Group 1: consisted of patients with either normal or impaired glucose tolerance in OGTT (n = 5). Group 2: showed new diagnosis of diabetes on the basis of high 2 hour glucose in OGTT (n = 3). Group 3: patients were all treated for diabetes, which had been diagnosed previously (n = 7). The 15 patients or the patient subgroups did not differ from the 13 healthy controls in age, physical activity, BMI or in resting oxygen consumption (Table 1). Also the fasting C-peptide, uric acid and creatine kinase, serum FFAs, triglycerides, HDL-cholesterol, LDL-cholesterol were similar among all groups (Study 2; Table 1 and Study 3; Table 1). The eight subjects in groups 1 and 2 had a good glycaemic control (Hb-$A1_C \leq 6.1$ %). Some minor differences existed in the number of smokers and men through the study groups (Table 1). As compared to controls fasting glucose, pyruvate and lactate were higher among the patients (Table 1). During the steady state of the euglycemic hyperinsulinemia no difference in the glucose or insulin concentration were noted between the patients and the controls while the FFAs and lactate levels were higher and the whole-body glucose uptake was lower in the patients with the m.3243A>G mutation than in the controls (Table 1).

Table 1.

Clinical and metabolic characteristics

	m.3243A Controls	m.3243G All	P^A	m.3243G Group 1	m.3243G Group 2	m.3243G Group 3
Clinical features				NGT-IGT	DM	tDM
Men / All (N)	2/13	4/15		0/5	0/3	4/7
Age (years)	47 ± 11	47 ± 10	0.91	48 ± 9	46 ± 9	46 ± 12
BMI (kg/m^2)	24 ± 3	23 ± 4	0.38	26 ± 3	24 ± 4	21 ± 3*[1]
m.3243G (%)[B]	0	45 ± 17	n.d.	33 ± 23	47 ± 5	53 ± 10
m.3243G (%)[C]	n.d.	64 ± 21	n.d.	46 ± 19	74 ± 3	80 ± 11*[1]
Physical activity[D]	442 ± 285	492 ± 354	0.69	655 ± 259	548 ± 272	351 ± 419
Medication						
- Insulin	-	6/15		-	-	6/7
- Metformin and Nateglinide	-	1/15		-	-	1/7
- Statins	-	5/15		1/5	-	4/7
- Beta blockers	-	2/15		1/5	-	1/7
- Levothyroxine	1/13	2/15		2/5	-	-
- ACE inhibitors	-	2/15		1/5	-	1/7
- Valsartan	-	2/15		-	-	2/7
Metabolic data						
Hb-A1$_C$ (%)	5.4 ± 0.3	6.6 ± 1.4	0.006	5.4 ± 0.5	6.0 ± 0.2	7.7 ± 1.2***[C]*[1]
Lactate (mmol/l)	0.66 ± 0.25	1.35 ± 0.76	<.001	0.84 ± 0.18	1.23 ± 0.50	1.76 ± 0.91**[C]*[1]
Pyruvate (µmol/l)	54 ± 15	73 ± 30	0.046	52 ± 14	83 ± 25	84 ± 35* [C]
VO_2 (ml·m^{-2})[E]	116 ± 11	117 ± 9	0.77	115 ± 4	117 ± 14	118 ± 10
FFAs (mmol/l)	0.45 ± 0.19	0.59 ± 0.27	0.12	0.46 ± 0.21	0.66 ± 0.40	0.66 ± 0.26
Liver						
Liver fat (%)	1.9 ± 2.8	3.7 ± 5.8	0.037[F]	6.5 ± 9.8	1.6 ± 1.0	2.5 ± 1.7
ALP (U/l)	53 ± 15	62 ± 23	0.240	51 ± 11	51 ± 18	74 ± 28
Clamp-procedure						
Glucose[1-3h] (mmol/l)	5.1 ± 0.2	5.2 ± 0.5	0.90	4.9 ± 0.3	5.1 ± 0.1	5.4 ± 0.7
Insulin[1h] (mU/l)	67 ± 18	69 ± 18	0.74	66 ± 14	63 ± 31	75 ± 17
FFAs[1h] (mmol/l)	0.06 ± 0.04	0.12 ± 0.08	0.002	0.10 ± 0.06	0.09 ± 0.04	0.16 ± 0.09* [C]
Lactate[1h] (mmol/l)	1.0 ± 0.2	1.8 ± 1.0	0.003	1.1 ± 0.2	1.3 ± 0.3	2.4 ± 1.2** [C]
M-value[1-3h] (µmol·min^{-1}·kg^{-1})	33 ± 10	20 ± 8	0.001	24 ± 11	19 ± 6	17 ± 6**[C]

Patients with m.3243A>G and with normal or impaired glucose tolerance (NGT-IGT, Group 1), patients with m.3243A>G and with newly-diagnosed diabetes mellitus (DM, Group 2), patients previously diagnosed and treated for diabetes (tDM, Group 3). BMI = Body-mass index, n.d. = not determined, BSA = body surface area, FFA, Free fatty acids, ALP = alkaline phosphatase. M-value = Whole-body glucose uptake, plasma insulin and plasma glucose were measured during the steady state of euglycemic hyperinsulinemia. [A]*P*-value, all patients with m.3243A>G vs controls. *A post hoc comparison between two groups after a priori $P < 0.05$. *[C],** [C],*** [C] ($P < 0.05$, < 0.01, < 0.001 vs controls [C = controls, 1 = group 1 and 2 = group 2]). [B]The m.3243G heteroplasmy in skeletal muscle. [C]The m.3243G heteroplasmy in buccal epithelium. [D]Daily Metabolic Equivalent estimated with the International Physical Activity Questionnaire. [E]Oxygen consumption per BSA. [F]t-test after log transformation = 0.050. Data are means ± SD.

6.4 Insulin secretion and beta cell function (II)

The basal insulin secretion was preserved in all subjects including the four subjects with over a 10-year diabetes history. The average C-peptide concentrations were identical to that in the controls. The fasting C-peptide lower range was 0.21 nmol/l in patients with m.3243A>G and 0.29 nmol/l in the controls. During the first 30 min of the OGTT absolute glucose, insulin and C-peptide concentrations were identical in the controls and group 1, but at 120 minutes plasma glucose was significantly higher in group 1 patients and the insulin levels tended to surpass those seen in the controls (Figure 5). Insulin secretion indices obtained in the mathematical modelling indicated that the beta cell glucose sensitivity was significantly lower in group 2 and 3 patients than that in the controls. In addition, a significant impairment in the rate sensitivity in group 3 was detected (Table 2). These and other indices of the beta cell function were not impaired in group 1 as compared to the controls. Of the several beta cell indices showing negative linear correlation with mutation heteroplasmy, the correlation between AUC_I/AUC_G and skeletal muscle heteroplasmy was the most robust. This correlation remained significant even if the patients with previous loss of glycaemic control and diabetes diagnosis (Group 3) were excluded ($r = -0.71$, $P = 0.02$, $n = 8$).

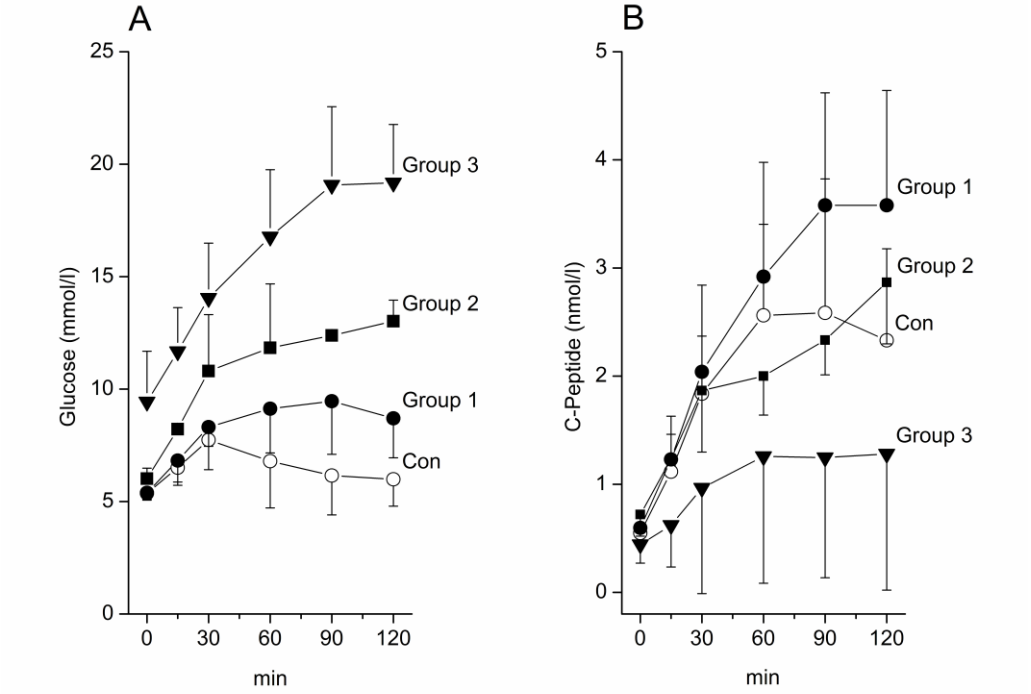

Figure 5. Oral glucose tolerance test in patients with the m.3243A>G mutation. A: Glucose concentration. B: C-peptide concentration. Controls (Con). Patients with m.3243A>G and with normal or impaired glucose tolerance (Group 1), patients with m.3243A>G and with newly-diagnosed diabetes (Group 2), patients previously diagnosed and treated for diabetes (Group 3). Data are mean ± SD.

Table 2.
Beta cell function in subjects with the m.3243A>G mutation during oral glucose tolerance test

	m.3243A	m.3243G	P^A	m.3243G	m.3243G	m.3243G
	Controls	All		Group 1	Group 2	Group 3
Glucose (mmol/l)	5.4 ± 0.3	7.4 ± 2.5	<.001	5.4 ± 0.3	6.0 ± 0.5	9.5 ± 2.2***^{C}**^{1}
Fasting insulin (pmol/l)	39 ± 14	44 ± 22	0.54	46 ± 17	69 ± 32*^{C}	31 ± 11*^{2}
C-peptide (nmol/l)	0.55 ± 0.14	0.55 ± 0.19	0.97	0.60 ± 0.12	0.72 ± 0.20	0.44 ± 0.17
Insulin secretion						
BSR (pmol ·min^{-1}·m^{-2})	71 ± 17	76 ± 25	0.57	78 ± 17	96 ± 25	65 ± 27
IGI (pmol · mmol^{-1})	28 ± 29	8 ±10	0.001	17 ±12	5 ± 1*^{C}	3 ± 4 **^{C}*^{1}
AUC_I/AUC_G (nmol · mol^{-1})	38 ± 16	22 ± 23	0.008	42 ± 27	23 ± 8	7 ± 9 **^{C}*^{1}
Glucose sensitivity (pmol ·min^{-1} ·m^{-2} ·mM^{-1})	137 ± 55	54 ± 50	<.001	106 ± 29	43 ± 34*^{C}	22 ± 37***^{C}*^{1}
Rate sensitivity (pmol · m^{-2} · mM^{-1})	686 ± 297	529 ± 621	0.40	1147 ± 682	493 ± 358	103 ± 132*^{C}***^{1}
End / Start periods potentiation ratio	1.9 ± 0.7	1.2 ± 0.5	0.005	1.4 ± 0.6	1.3 ± 0.6	0.9 ± 0.3*^{C}

Patients with m.3243A>G and with normal or impaired glucose tolerance (Group 1), patients with m.3243A>G and with newly-diagnosed diabetes (Group 2), patients previously diagnosed and treated for diabetes (Group 3). BSR = Basal insulin secretion rate, IGI = insulinogenic index, AUC_I/AUC_G = the ratio of insulin and glucose areas under the curve. ^{A}P-value, all patients with m.3243A>G vs controls. *A post hoc comparison between two groups after a priori $P < 0.05$. *^{C}, **^{C}, ***^{C} ($P < 0.05$, < 0.01, < 0.001 vs controls [C = controls, 1 = group 1 and 2 = group 2]). Data are mean ± SD.

6.5 Skeletal muscle glucose uptake and perfusion (II)

The rate of insulin-stimulated glucose uptake was two-fold lower in the femoral skeletal muscle per unit tissue weight in groups 1, 2 and 3 with the m.3243A>G mutation than in the controls (Figure 6). The skeletal muscle glucose uptake and the whole-body glucose disposal were linearly related in patients with the m.3243A>G mutation ($r = 0.92$, $P < 0.001$, $n = 14$). The skeletal muscle glucose uptake showed also a significant inverse correlation with intra-abdominal fat content in women, liver fat content and fasting triglycerides in patients with m.3243A>G (data not shown). Femoral muscle perfusion per tissue weight was similar in all groups suggesting that muscle insulin resistance was caused by the decreased glucose extraction rate in the patients with m.3243A>G as compared to the controls (Figure 6). A linear correlation between muscle glucose uptake and FFA concentration during hyperinsulinemia was shown in the pooled patient and control population ($r = -0.66$, $P < 0.001$, $n = 27$). No correlation with the muscle heteroplasmy and muscle perfusion ($r= -0.22$, $P = 0.50$, $n = 12$) or glucose uptake was noted ($r = -0.39$, $P = 0.24$, $n = 11$).

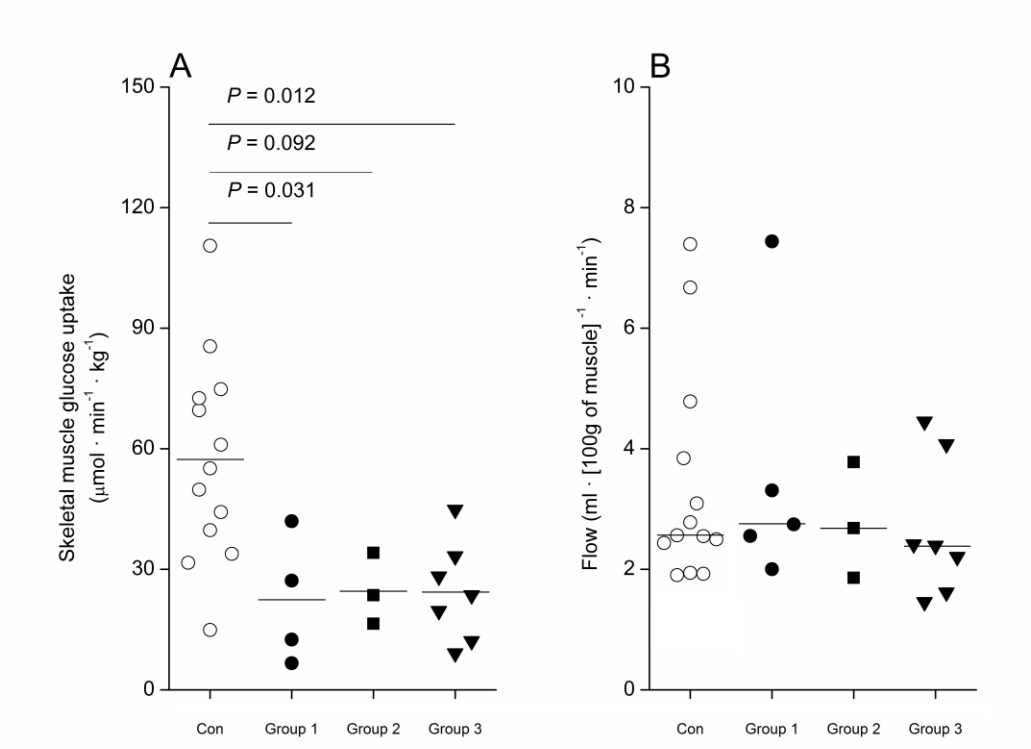

Figure 6. Skeletal muscle glucose uptake and perfusion. A: Skeletal muscle insulin-stimulated glucose uptake. B: Skeletal muscle blood flow per tissue weight. Controls (Con). Patients with m.3243A>G and with normal or impaired glucose tolerance (Group 1), patients with m.3243A>G and with newly-diagnosed diabetes (Group 2), patients previously diagnosed and treated for diabetes (Group 3). Significant post hoc comparisons are given when a priori $P < 0.05$. The horizontal line indicates the mean (A) or median (B).

6.6 Adipose tissue metabolism and adipocytokines (III)

Parallel to the pattern in the skeletal muscle, the insulin-stimulated glucose uptake rate in subcutaneous fat was > 49% decreased in all groups with the m.3243A>G mutation as compared to the controls The differences in the glucose uptake per fat tissue weight remained significant between the controls and the three patient subgroups even if men due to their low total number were excluded (Figure 7). The expected correlation between the glucose uptake rate in fat and the skeletal muscle glucose uptake could be detected in the patients with m.3243A>G ($r = 0.61$, $P = 0.021$, $n = 14$). The size of the abdominal subcutaneous fat depot did not differ between the patient and control women ($P = 0.24$). The insulin-stimulated glucose uptake calculated for the overall abdominal subcutaneous fat depot was lower in women with m.3243A>G than that in healthy women (Figure 7). The waist to hip ratio (0.84 ± 0.05) was greater even if the BMI (23.9 ± 3.4) was similar in women with the m.3243A>G mutation as compared to control women (0.76 ± 0.06, $P = 0.003$; 24.1 ± 3.0, $P = 0.88$). Finally, the intra-abdominal fat depot was 43 % larger in the patient than in the control women ($P = 0.027$, BSA adjusted weight). Adiponectin was significantly lower in the patients than in the controls (Table 3). Both leptin and the BMI were inversely related with mutation heteroplasmy in the buccal epithelium and in muscle ($r = -0.54$ to -0.72 and $P < 0.05$ for all, $n = 15$ for epithelium and $n = 12$ for muscle).

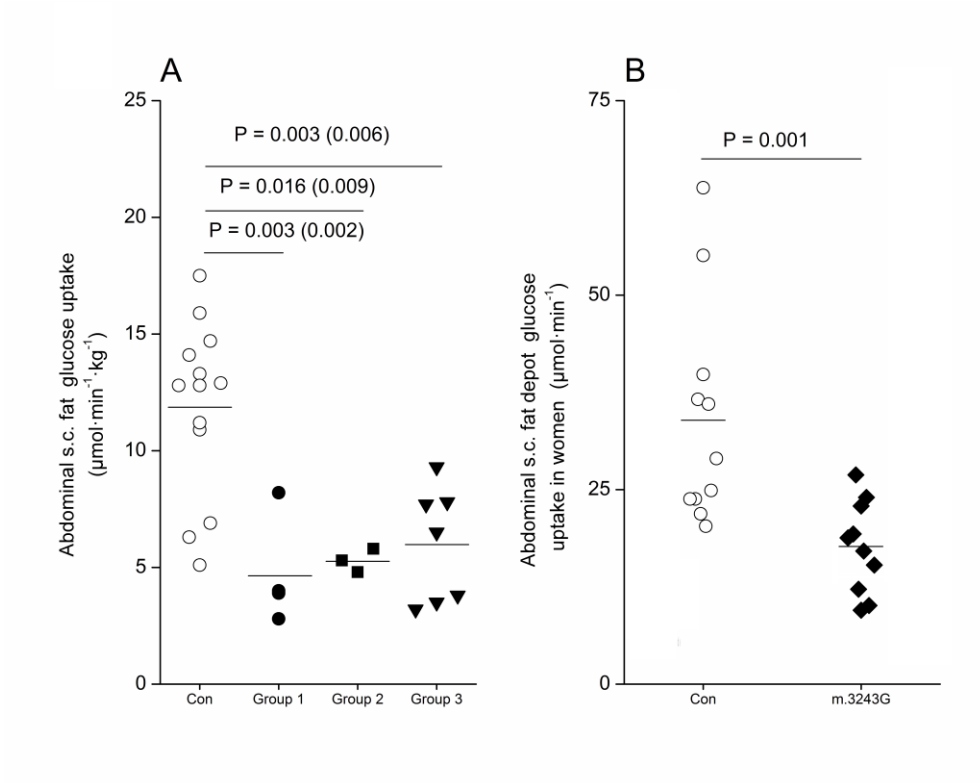

Figure 7. Glucose uptake in subcutaneous fat. A: Glucose uptake (GU) rate per tissue weight in subcutaneous abdominal fat. The P-values are shown for all patients or, in parentheses, for the women only. B: The insulin-stimulated GU per the abdominal fat depot in women. Controls (Con). Patients with m.3243A>G and with normal or impaired glucose tolerance (Group 1), patients with m.3243A>G and with newly-diagnosed diabetes (Group 2), patients previously diagnosed and treated for diabetes (Group 3). Significant post hoc comparisons are given when a priori $P < 0.05$. The horizontal line indicates the mean.

Table 3.

Proteins related to insulin resistance

	m.3243A Controls	m.3243G All	P^A	m.3243G Group 1	m.3243G Group 2	m.3243G Group 3
N	12[B]	15		5	3	7
Adiponectin (mg/l)	16 ± 9	9 ± 7	0.032	10 ± 7	12 ± 11	7 ± 4
Leptin (µg/l)	9 ± 10	10 ± 10	0.94	17 ± 13	13 ± 8	4 ± 3
CRP (mg/l)	0.6 ± 0.4	1.3 ± 1.7	0.86	1.9 ± 1.9	0.3 ± 0.2	1.3 ± 1.9
TNF-α (µg/L)	2.4 ± 1.1	3.3 ± 1.3	0.06	2.6 ± 1.4	3.7 ± 0.5	3.6 ± 1.4
IL-6 (µg/l)	4.2 ± 5.0	6.7 ±12.7	0.83	1.6 ± 1.9	12.3 ± 21.3	7.8 ± 13.6
IL-8 (µg/l)	1.7 ± 1.3	2.2 ± 1.7	0.32	1.5 ± 0.7	2.9 ± 3.2	2.3 ± 1.3
MCP-1 (µg/l)	0.2± 0.1	0.2 ± 0.1	0.23	0.2 ± 0.1	0.2 ± 0.1	0.2 ± 0.1
NGF (ng/l)	18 ± 20	25 ± 41	0.68	6 ± 10	46 ± 74	29 ± 39
PAI-1 (µg/l)	5.2 ± 3.4	6.9 ± 5.4	0.35	8.3 ± 3.5	6.6 ± 4.1	6.0 ± 7.1
Resistin (µg/l)	7.9 ± 3.3	8.5 ± 3.6	0.67	7.4 ± 4.2	5.8 ± 3.7	10.4 ± 2.0

Patients with m.3243A>G and with normal or impaired glucose tolerance (Group 1), patients with m.3243A>G and with newly-diagnosed diabetes (Group 2), patients previously diagnosed and treated for diabetes (Group 3). [A]*P*-value, all patients with m.3243A>G vs controls. A post hoc comparison between two groups was only made when a priori $P < 0.05$. [B]One frozen sample was lost. For abbreviations see methods section (5.7). Data are mean ± SD.

6.7 Liver metabolism (III)

No difference was noted in the liver enzymes between the groups (Table 1, Study 3; Table 1). The insulin-stimulated glucose uptake in the liver did not differ between the patients and the controls (Figure 8). An inverse relationship between intra-abdominal fat mass (BSA adjusted) and hepatic glucose uptake rate was present in women with m.3243A>G (r = -0.66, P = 0.038, n = 10). No differences were detected in the EGP during hyperinsulinemia (Figure 8). Furthermore, only three patients (20%) with m.3243A>G had abnormal high liver fat, defined as higher than the 5.56% cut-off. The median liver fat content was somewhat higher in patients with m.3243A>G than in the controls (P = 0.037). Among the patients or controls, no association between liver fat and hepatic glucose uptake was noted. In the patients with m.3243A>G, EGP correlated with the Hb-$A1_C$ (r = 0.83, < 0.001, n = 15) and heteroplasmy in the skeletal muscle (r = 0.83, P = 0.001, n = 12) and showed a somewhat paradoxical inverse correlation with leptin (r = -0.67, P = 0.007, n = 15).

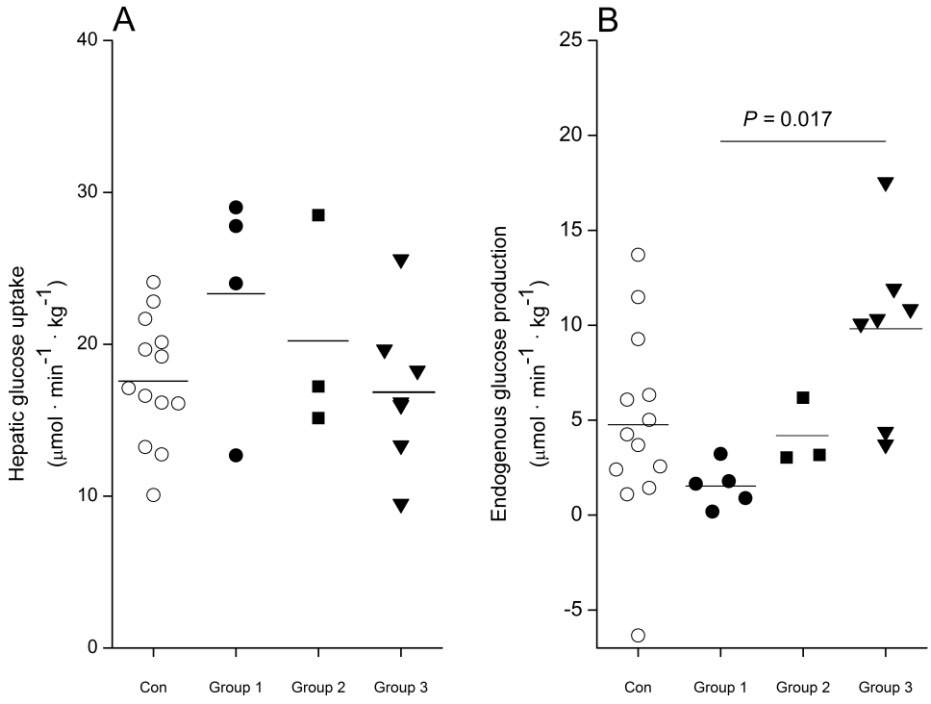

Figure 8. Liver metabolism in patients with the m.3243A>G. A: Hepatic glucose uptake per tissue weight (HGU). B: Endogenous glucose production (EGP). EGP was higher in patients with previously diagnosed diabetes as compared to patients without diabetes. Controls (Con). Patients with m.3243A>G and with normal or impaired glucose tolerance (Group 1), patients with m.3243A>G and with newly-diagnosed diabetes (Group 2), patients previously diagnosed and treated for diabetes (Group 3). Significant post hoc comparisons are given when a priori $P < 0.05$. The horizontal line indicates the mean.

6.8 Cardiac glucose uptake (IV)

The left ventricular glucose uptake per tissue weight (LVGU) was 25% lower in patients with the m.3243A>G than that in the controls ($P = 0.044$ t-test or 0.029 Mann–Whitney U). However, the differences between individual patients and patient subgroups were also evident (Figure 9). Due to the large variation in the LVGU values among the patients, the contribution of parameters commonly associated with the LVGU were assessed in patients with the m.3243A>G mutation. The LVGU was not

associated with the FFAs during the hyperinsulinemia (r = -0. 21, P = 0.46, n = 14) nor forward work (r = 0.45, P = 0.12, n = 13). In addition, the association with LVGU and skeletal muscle insulin sensitivity (r = 0.01, P = 0.98, n = 14) was lacking. Instead, the LVGU was inversely associated with glycosylated haemoglobin (r = -0.58, P = 0.029, n = 14). The LVGU also decreased across the glucose tolerance groups showing a similar pattern as the beta cell function (Figure 9 and Table 2). Unexpectedly, an inverse correlation between the rate pressure product and LVGU was noted (r = -0.60, P = 0.022, n = 14).

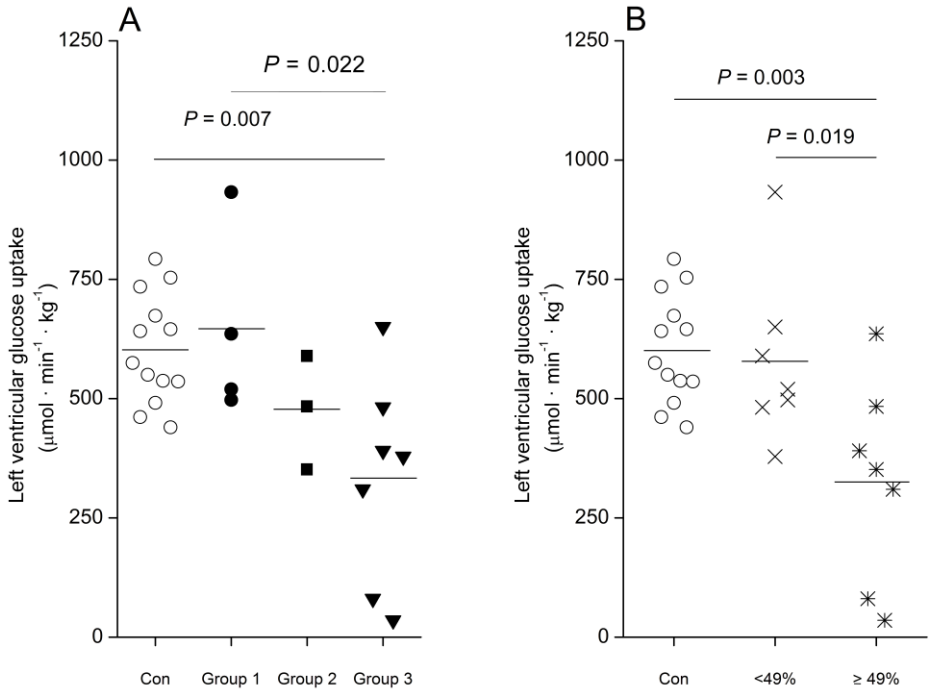

Figure 9. Cardiac glucose uptake. A: The left ventricular glucose uptake per tissue weight (LVGU) in groups defined by glucose tolerance. Controls (Con). Patients with m.3243A>G and with normal or impaired glucose tolerance (Group 1), patients with m.3243A>G and with newly-diagnosed diabetes (Group 2), patients previously diagnosed and treated for diabetes (Group 3). B: Glucose uptake during hyperinsulinemia in myocardium in healthy subjects (Con) and in patients with low or high m.3243A>G mutation load (median 49%). Significant post hoc comparisons are given when a priori $P < 0.05$. The horizontal line indicates the mean.

With respect to the mitochondrial disease, the LVGU was inversely associated with epithelial heteroplasmy (r = -0.53, P = 0.049, n = 14) and muscle heteroplasmy (r = -0.63, P = 0.039, n = 11) and fasting pyruvate (r = -0.62, P = 0.019 n = 14). The effect of the mutation load on LVGU was further assessed by dividing the patients into two groups by the median heteroplasmy 49%. In this analysis, patients with mutation heteroplasmy < 49% in epithelium did not contribute to the low LVGU (Figure 9). This post hoc difference in LVGU between the low and high m.3243A>G heteroplasmy groups remained significant also after adjustment for Hb-A1C (P = 0.029) or FFA during the clamp (P = 0.009) or skeletal muscle glucose uptake (P = 0.03) or all (P = 0.048). No regional variation in LVGU results was detected. The patients with m.3243A>G compensated the low stroke volume with a high heart rate (Table 4). The cardiac morphology and function was essentially similar between the high and low m.3243A>G heteroplasmy groups (data not shown). The difference in LVGU between the high heteroplasmy group and the controls or the high heteroplasmy group and the low heteroplasmy group remained similarly significant if only the patients with available skeletal muscle heteroplasmy value were included and the cut-off was determined by the median heteroplasmy in muscle (data not shown).

Table 4.

Cardiac function and structure assessed with magnetic resonance imaging

	m.3243A Controls	m.3243G All[B]	*P*[A]	m.3243G Group 1	m.3243G Group 2	m.3243G Group 3
N	13	15		5	3	7
BP systolic (mmHg)	125 ± 14	126 ± 15	0.84	131 ± 7	112 ± 15	129 ± 16
BP diastolic (mmHg)	76 ± 7	83 ± 12	0.040	80 ± 6	82 ± 2	85 ± 17
Heart rate (beats/min)	58 ± 6	69 ± 11	0.004	64 ± 14	69 ± 1	73 ± 12*[C]
RPP (mmHg ·beats·min^{-1})	7307 ± 1083	8696 ± 1730	0.029	8283 ± 1475	7742 ± 951	9401 ± 2014
Left Ventricle						
EDV/BSA (ml·m^{-2})	88 ± 10	77 ± 14	0.32	77 ± 16	80 ± 5	76 ± 16
ESV/BSA (ml·m^{-2})	27 ± 6	27 ± 10	0.87	25 ± 10	26 ± 8	28 ± 11
SV/BSA (ml·m^{-2})	61 ± 8	51 ± 7	0.002	53 ± 7	54 ± 3	48 ± 7**[C]
Ejection fraction (%)	69 ± 5	67 ± 9	0.38	69 ± 8	67 ± 9	65 ± 11
Mass/BSA (g·m^{-2})	54 ± 7	59 ±15	0.65	51 ± 6	56 ± 5	67 ± 21
Posterior wall (mm)	6.7 ± 1.1	7.7 ± 1.6	0.057	7.3 ± 0.9	8.0 ± 0.6	8.0 ± 2.4
Septum (mm)	7.8 ± 1.5	8.4 ± 2.0	0.41	7.9 ± 0.3	6.7 ± 0.8	9.8 ± 2.4
CO/BSA (l·min^{-1}·m^{-2})	3.5 ± 0.5	3.4 ± 0.5	0.49	3.3 ± 0.5	3.7 ± 0.3	3.4 ± 0.6
Work power (mmHg·$^{-1}$)	776 ± 179	712 ± 111	0.27	731 ± 117	685 ± 465	707 ± 139
Forward work power (J/g)	8.3 ± 1.1	7.8 ± 1.5	0.32	8.7 ± 1.8	7.6 ± 0.5	7.1 ± 1.4
Right Ventricle						
EDV/BSA (ml·m^{-2})	89 ± 15	80 ± 16	0.16	84 ± 16	81 ± 10	77 ± 21
ESV/BSA (ml·m^{-2})	27 ± 10.0	31 ± 11	0.46	31 ± 11	28 ± 9	31 ± 11

Patients with m.3243A>G and with normal or impaired glucose tolerance (Group 1), patients with m.3243A>G and with newly-diagnosed diabetes (Group 2), patients previously diagnosed and treated for diabetes (Group 3). [A]P-value, all patients with m.3243A>G vs controls. A post hoc comparison between two groups was only made when a priori $P < 0.05$. [B]One patient failed to lie still during the cardiac magnetic resonance imaging and the respective data was lost. RPP = rate pressure product. *A post hoc comparison between two groups after a priori $P < 0.05$. *C and **C ($P < 0.05$ and < 0.01 vs controls [C = controls]) Data are mean ± SD.

7 DISCUSSION

7.1 Synopsis

Twelve of the 15 patients with the m.3243A>G in the present study were ascertained previously in a population-based epidemiological study, thus reducing the selection bias in the present study. The study sample size was small but relevant if compared to the previous metabolic studies. However, I failed to recruit enough adult patients with normal glucose tolerance harbouring the m.3243A>G mutation. Therefore conclusions about the data have to be done accordingly. The novel findings of the present study were that 1) $rCMRO_2$ is globally decreased including frontal lobe and other areas, which have not been traditionally associated with mitochondrial disease. 2) The decreased oxygen to glucose consumption ratio indicated increased lactate production within the brain also in the asymptomatic patients. 3) The insulin secretion parameters correlate with the m.3243A>G heteroplasmy. 4) Insulin resistance in skeletal muscle is a common finding in patients with m.3243A>G. This includes patients with no diabetes and no relevant decrease in the beta cell function or in nutritive muscle perfusion. 5) Insulin-stimulated adipose tissue metabolism in patients with the m.3243A>G mutation is disturbed. 6) A major liver steatosis or hepatic insulin resistance does not characterize patients with mitochondrial diabetes. 7) Cardiac substrate preference is uneconomical in patients with high m.3243A>G mutation heteroplasmy, at least in the presence of diabetes. The PET method was feasible in detecting significant and relevant metabolic differences between small groups of patients and controls in this study. Therefore, it may be a useful tool in future metabolic studies on rare mitochondrial disorders. The available small groups and subgroups resulted in a loss of power in the study and some significant changes may have remained undetected. The small sample size further renders this study as hypothesis generating and some of the new findings require confirmation in future studies.

7.2 Brain glucose oxidation in the presence of the m.3243A>G mutation

A global decrease in cerebral oxygen metabolism and in oxygen to glucose index in patients with the m.3243A>G mutation was found in this study. A global decrease in the mtDNA-encoded proteins has been reported in the affected as well as in the non-affected cerebral cortex in the brain of patients with full-blown MELAS due to the m.3243A>G mutation (Sparaco et al. 2003; Betts et al. 2006). We found that $rCMRO_2$ was decreased in all the grey and white matter regions assessed in patients with m.3243A>G. This was true also for the frontal lobe, which is usually spared in patients with mitochondrial encephalopathy (Betts et al. 2006; Molnar et al. 2000; Sue et al. 1998). This study thus confirmed the presence of an oxidation defect, previously found in the cells harbouring this mutation, now in the living brain. These results extend the similar results in two previous studies performed with a quantitative approach in patients with mitochondrial disease. Firstly, because of the more advanced scanner technology, the concurrent MRI and [^{1}H]MRS data with PET and the inclusion of asymptomatic patients with previous neuropsychological tests made the regional characterization more conclusive as compared to the two previous studies (Frackowiak et al. 1988; Shishido et al. 1996). Secondly, this study contained only patients with confirmed molecular genetic diagnosis and heteroplasmy data. This was not the case in the previous studies making it challenging to draw any parallels between the cerebral and cybrid cell metabolism.

The low OGI ratio was detected together with high lactate in unaffected brain regions suggesting that the previous reports of elevated brain lactate might reflect a high in situ lactate production (Dalsgaard et al. 2004; Dubeau et al. 2000; Kaufmann et al. 2004). However, the decrease in substrate oxidation was not essentially compensated by an anaerobic ATP production as no absolute increase in glucose uptake was detected. Therefore, an increased anaerobic glucose metabolism may have no relevance to the neuronal survival in these patients. The glucose hypometabolism was attributed to patients with CNS symptoms. In general, impaired glucose tolerance is not associated

with glucose hypometabolism during hyperinsulinemic clamp (Hirvonen et al. 2011). However, approximately one third of the observed NAA decrease might have been explained by the presence of chronic hyperglycaemia, which should be taken into consideration in the future studies including patients with m.3243A>G and diabetes (Heikkilä et al. 2009). The overall atrophy score and decreased NAA/Cr ratio in [^{1}H]MRS spectroscopy suggested a higher degree of neurodegeneration in symptomatic patients. The glucose hypometabolism and atrophy were more evident in the posterior part of the brain. The pattern of regional glucose hypometabolism was in accordance with a previously demonstrated hypometabolism non-quantitative [^{18}F]FDG–PET study and previous electrophysiological, imaging and clinical findings in patients with m.3243A>G (Molnar et al. 2000; Damian et al. 1998; Majamaa-Voltti et al. 2006; Sue et al. 1998; Suzuki et al. 1996). Then again, the relative preservation of the glucose metabolism, despite the high atrophy score in the cerebellum seems not to be compatible with an atrophy associated hypometabolism hypothesis. Interestingly, the glucose uptake in the cerebellum may have its own special characteristics such as lack of adaptation to a chronic hyperglycaemia (Heikkilä et al. 2010).

The two previous studies using a multitracer approach reported a decrease in $rCMRO_2$ and rOGI in severely affected patients with mitochondrial disease. The rGMR and rCBF were near normal (Frackowiak et al. 1988; Shishido et al. 1996). The present results show a ~12 % decrease in rCBF in patients with m.3243A>G. This trend of hypoperfusion was significant only in the thalamus. This might have been secondary to degenerative hypodensity and calcifications, which are commonly reported in this area in patients with mitochondrial disease (Sue et al. 1998). Previously, endothelial dysfunction has been suggested to underlie mitochondrial encephalopathy. This has been based mainly on histological analyses of vascular wall and few reports both in muscle and brain in patients with m.3243A>G reporting poor vasodilation. This “mitochondrial angiopathy” has been suggested to underlie both the stroke-like lesions, as well as the encephalopathy (Ohshita et al. 2000; Sparaco et al. 2003; Betts et al. 2006). Previous studies employing non-quantitative single-photon emission computed

tomography have revealed contradictory perfusion patterns. Normal, asymmetric hypoperfusion or hyperperfusion in the brain have been reported in patients with m.3243A>G (Suzuki et al. 1996; Thajeb et al. 2005; Iizuka et al. 2007; Ito et al. 2008). The majority of the patients in these studies have had a history of stroke-like episodes. We did not measure the vascular reserve in the cerebral arteries, but the decreased regional oxygen extraction fraction in brain suggests a relative preservation of the vascular supply of oxygen (Molnar et al. 2000). Notably, the skeletal muscle perfusion was identical to that of the controls during the hyperinsulineamia. The insulin in its turn is a physiological vasodilative stimulant, enhancing the nutritive perfusion in muscle. Thus, the present results do not provide any further support for disturbed endothelial function in mitochondrial encephalopathy or myopathy (Iizuka et al. 2007; Molnar et al. 2000). Finally, I suggest that the primary energy imbalance in neurons rather than ischemia is the major cause for the encephalopathy in patients with the m.3243A>G mutation.

It has been proposed that certain polymorphism in mtDNA and the mitochondrial dysfunction might predispose individuals to neurodegenerative diseases. Some previous epidemiological studies have suggested that variation in mitochondrial genes predispose to Parkinson's disease (Autere et al. 2004). A new interest towards this issue has been evoked after POLG mutations were described to cause Parkinson's disease and due to the discovery of disturbed mitochondrial fission and fusion machinery in the models of monogenetic Parkinson's disease (Davidzon et al. 2006; Deng et al. 2008). At present, there is no firm evidence indicating that defective OXPHOS could be detected in the brains or in other tissues in patients before the onset of common neurodegenerative diseases (Borland et al. 2009; DiDonato et al. 1993; Bindoff et al. 1991). PET studies in patients with Alzheimer's diseases have preferably shown local glucose or oxygen hypometabolism or hypoperfusion or reduced expression of energy metabolism genes (Kuwabara et al. 1995; Liang et al. 2008). In Alzheimer's, Parkinson's or Huntington's disease no decrease in $rCMRO_2$, regional oxygen extraction fraction or rOGI have been found (Kuwabara et al. 1995; Powers et

al. 2007; Powers et al. 2008). Based on the present study, an absolute and relative global decrease in oxidative metabolism characterizes only patients with mitochondrial disease. Thus, no shared pattern in brain metabolism linking patients harbouring the m.3243A>G mutation and common neurodegenerative diseases such as Parkinson's, Alzheimer's or Huntington's disease was found in the present study.

7.3 Insulin secretion in patients with the m.3243A>G mutation

Insulin secretion was measured during OGTT and further analyzed by mathematical modelling based on C-peptide deconvolution. The parameters of beta cell function: the glucose sensitivity and the rate sensitivity were well-preserved in some patients with m.3243A>G. The main parameter "the beta cell glucose sensitivity" derived from this model has previously shown to be at least as sensitive as the intravenous glucose tolerance test based indices, such as acute insulin response in detecting defects in beta cell function in patients with normal to diabetic glucose homeostasis preserving its validity also in hyperglycaemic states (Mari et al. 2001; Mari et al. 2010; Mari et al. 2008). It has also shown a good diabetes prediction potential both in lean and obese patient groups at high risk for diabetes (Walker et al. 2005). The slight non-significant decrease in glucose sensitivity in group 1 was comparable in magnitude to the previously reported decrement in obese subjects with normal glucose tolerance. The tendency to higher rate sensitivity and rate sensitivity disposal index values could also be compared to that of healthy obese subjects (Study2; Table 2)(Ferrannini et al. 2005). Both fasting glucose levels and basal insulin secretion were well-preserved in groups 1 and 2, this also resembling obese individuals with no diabetes (Ferrannini et al. 2005). Studies in cybrid cells have clearly shown that the m.3243A>G mutation impairs both the ATP yield essential for GIS as well as blunts the calcium oscillation through the decreased mitochondrial membrane potential (de Andrade et al. 2006). These two factors may explain the impaired beta cell function in patients with m.3243A>G. Cybrid cell studies have shown that oxygen consumption, which is in turn related to the mitochondrial membrane potential and to the energy generation capacity, is

impaired in the function of the heteroplasmy. In the present study glucose sensitivity and rate sensitivity showed an inverse correlation with the heteroplasmy. Importantly, this correlation was significant for AUC_I/AUC_G index when only patients with no previous diabetes and GHb-$1A_C \leq 6.1\%$ (groups 1 and 2) were included. Possibly, the only available study in patients with m.3243A>G shows no major deviation of the beta cell heteroplasmy in pancreas from the mutation load in other tissues (Otabe et al. 1999). A previous study has also suggested that the level of heteroplasmy may determine the age-of-onset in mitochondrial diabetes (Laloi-Michelin et al. 2009). In summary, the present study is the first to confirm that the insulin secretion capacity is defined by the m.3243A>G heteroplasmy.

Previous studies have shown that insulin secretion is impaired in patients with m.3243A>G and diabetes even if the response to arginine and glutamate is preserved, which is compatible with our data (Suzuki et al. 1997; Suzuki et al. 1994; Brändle et al. 2001). One previous OGTT study has included more m.3243A>G carriers than the present study. It demonstrated that the IGI was decreased in seven m.3243A>G carriers with normal glucose tolerance (Suzuki et al. 1994). This result is compatible with the similar trend seen in group 1. In some studies no defects in insulin secretion have been found (Holmes-Walker et al. 2001; Gebhart et al. 1996). Interestingly, two studies in this context report the OGTT raw data and show a similar insulin and glucose pattern during the 2-hour OGTT at the non-diabetic range as the patients in the present thesis had. Thus, C-peptide and glucose values started from a high normal range and were both relatively higher than the control group values during the last hour of the oral glucose tolerance (Holmes-Walker et al. 2001; Frederiksen et al. 2009). In these two studies the lack of power and modelling efforts have probably resulted in the false negative results and a conclusion about a normal beta cell function. On the other hand, the lack of heteroplasmy in skeletal muscle or epithelial tissue was the major caveat of all the previous studies and may also explain some of the apparently contradicting results. Still, even if the heteroplasmy data are available, the present cross-sectional study fails to explain why none of our subjects were diabetic in their early lives.

Oxidative stress, apoptosis and impaired protein synthesis might lead to a beta cell failure in mitochondrial disease (Abramov et al. 2010; van Eijsden et al. 2008; King et al. 1992). However, a reduced beta cell number and the absence of increased apoptosis have been reported in the pancreatic tissue in patients with m.3243A>G (Otabe et al. 1999). All the seven patients with previously diagnosed diabetes in the thesis had disease duration longer than 5 years. Still, they all had relevant > 0.2 nmol/l fasting C-peptide levels in contrast to ~8% of adult-onset patients with type 1 diabetes with similar disease duration (Sherry et al. 2005). Nevertheless, the residual insulin secretion might potentially reduce hyperglycaemia and possible glucotoxicity to end organs (Sherry et al. 2005; Massin et al. 2008). Further follow-up studies are suggested to enable to characterize the natural course of beta cell function in mitochondrial diabetes.

7.4 Skeletal muscle insulin resistance in mitochondrial diabetes

The present study showed invariably insulin resistance in skeletal muscle (Figure 6). The insulin resistance in skeletal muscle was present already in the early phase of glucose intolerance in subjects with the m.3243A>G mutation even if the beta cell response to glucose and the glycaemic control were essentially preserved. The use of [^{18}F]FDG-PET enabled me to measure glucose uptake directly in the skeletal muscle without any interference from other organs important in glucose homeostasis during hyperinsulinemia, such as adipose tissue and liver. Potentially, a low adipose tissue to muscle mass ratio or a low muscle to liver mass ratio may have decreased the probability to detect insulin resistance in skeletal muscle in the previous studies. The ~50% decrease in skeletal muscle glucose uptake was quantitatively comparable to that previously reported in obese subjects or in patients with type 1 or 2 diabetes (Utriainen et al. 1998; Virtanen et al. 2002; Groop et al. 1989; Nuutila et al. 1993; Iozzo et al. 2003). This study is the first to show that the skeletal muscle insulin sensitivity is decreased in patients with the m.3243A>G mutation. A standard hyperinsulinemic clamp technique has been used to assess skeletal muscle insulin sensitivity in two

previous studies both including less subjects with m.3243A>G than the present study. Such assessments are affected by uptake in other insulin responsive organs and the results in these studies should have been adjusted at least to lean body weight in order to allow conclusion about the skeletal muscle. In the first study seven mutation carriers had lower insulin sensitivity than the controls (Velho et al. 1996). The authors concluded that peripheral insulin resistance did not seem to precede diabetes even if three of the four subjects with no diabetes had insulin sensitivity, which was lower than the mean of the controls. In the other study insulin sensitivity within the low normal range, as compared to historical controls, was reported in eight m.3243A>G patients with diabetes and one with impaired glucose tolerance (Suzuki et al. 1997). The insulin sensitivity has thus been proposed to be unaffected previously. However, the raw data in the two largest studies assessing OGTTs in patients with m.3243A>G and no diabetes might propose another interpretation. These two studies namely show a normal but relatively high insulin secretion and normal but relatively high glucose during the second hour of OGTT as compared to controls. This pattern could be easily explained by the presence of insulin resistance in skeletal muscle (Frederiksen et al. 2009; Holmes-Walker et al. 2001). Thus the data in the previous studies assessing the insulin secretion and action in patients with m.3243A>G seem not to be contradictory to the present thesis reporting insulin resistance in the skeletal muscle.

Insulin resistance is strongly predictive for diabetes in subjects with high hereditary risk. In the light of the previous findings about insulin resistance in both patients with type 1 or 2 diabetes it would have been unexpected not to find it in patients with m.3243A>G and diabetes. Various previous findings in skeletal muscle, such as elevated intramuscular triglycerides, low OXPHOS function, fitness association with reduced OXPHOS gene expression and impaired lipid oxidation or the TFAM gene promoter methylation in blood cells either in patients with diabetes or in subjects with normal glucose tolerance but high predisposition to later diabetes have lead to a suggestion that the defective mitochondrial metabolism might have an initiating role in the development of insulin resistance and diabetes (Patti and Corvera. 2010; Gemma et

al. 2010). Furthermore, insulin sensitivity and substrate oxidation can be increased by overexpressing PGC-1α and PGC-1β in skeletal muscle (Patti and Corvera. 2010). However, the blocking of the mitochondrial respiration in myotubes or the knocking out of PGC-1α leads, at least initially, to increased basal and insulin-stimulated glucose or [^{18}F]FDG uptake due to the elevated glycolysis comparable to the high anaerobic glucose utilization in cybrid cell lines harbouring the m.3243A>G mutation (Patti and Corvera. 2010; Brown et al. 2008; Smith and Blaylock. 2007; de Andrade et al. 2006). Furthermore, a mouse model of mitochondrial myopathy using tissue specific KO of the TFAM leads to myopathy including ragged red fibres, decreased respiratory chain activity in muscle and clinical exercise intolerance. Importantly, these mice show an increase instead of a decrease in insulin-stimulated glucose uptake in skeletal muscle, suggesting that a primary OXPHOS defect does not lead to insulin resistance in the skeletal muscle (Wredenberg et al. 2002; Wredenberg et al. 2006).

The heteroplasmy data in skeletal muscle is reproductive and has a predictive value for instance for the phenotype and VO_2 max in mitochondrial disease (Chinnery et al. 1997; Jeppesen et al. 2006; Janssen et al. 2008). Heteroplasmy in urine sediment, cheek mucosa, and skin fibroblasts correlates with the m.3243A>G heteroplasmy in muscle and may be used as a more accessible alternative for the same purpose. Due to the lack of heteroplasmy data in tissues other than the leucocytes in the study of Velho it is difficult to deduce the contribution of the m.3243A>G mutation to insulin sensitivity in the previous two studies (Whittaker et al. 2009; Frederiksen et al. 2006; Mehrazin et al. 2009; Rajasimha et al. 2008). Importantly, the fate of glucose during the hyperinsulinemia is not oxidation but a glycogen synthesis in skeletal muscle (Virkamäki et al. 1997). Therefore it is not surprising that skeletal muscle glucose uptake and heteroplasmy data did not show any correlation in the present study even if the biochemical OXPHOS defect and the VO_2 max show a good correlation with the heteroplasmy in muscle (Jeppesen et al. 2006; Janssen et al. 2008).

The structured interview on physical activity which we used did not reveal significant differences in the daily physical activity between patients and controls. However, a mild clinical myopathy is common in patients with the m.3242A>G mutation (Kärppä et al. 2005). It is possible that due to the lack of more objective data - that is for instance accelerometer measurements on physical activity, some of the observed differences in the skeletal muscle but probably not in cardiac glucose uptake might be explained by physical deconditioning of the patients in this study (Apabhai S et al.2011 and Takala et al.1999). We found that during physiological insulin stimulus of the blood flow the perfusion was comparable in patients with m.3243A>G and the controls, suggesting no major participation of endothelial function in the glucose uptake results. In conclusion, after the present study it is unclear if and how a primary defect in mitochondrial respiratory chain due to m.3243A>G in myocyte might induce insulin resistance. The now reported combination of insulin resistance with preserved basal insulin secretion and their relation to glycaemic control, epithelial heteroplasmy and BMI suggests further studies on insulin sensitizers in the treatment of mitochondrial diabetes.

7.5 Adipose tissue metabolism during hyperinsulinemia

The patients with the m.3243A>G showed invariably a decreased insulin-stimulated glucose uptake in subcutaneous fat (Figure 7). Using an identical PET technique, it has been previously demonstrated that insulin-stimulated glucose uptake per tissue mass is decreased by 59% in obese subjects and by 41% in obese patients with type 2 diabetes as compared to lean controls. Thus, this change is seemingly independent from the glucose tolerance (Virtanen et al. 2005). In obese patients the insulin-stimulated [^{18}F]FDG uptake per tissue weight decreases with higher depot weight. The low BMI has previously been shown to correlate with the degree of heteroplasmy in patients with the m.3243A>G mutation (Laloi-Michelin et al. 2009). In this thesis both the subcutaneous fat mass, BMI and leptin correlated with the mutation heteroplasmy (Study III, result section). The lower depot weight and possibly the lower adipocyte

size might mask the possibly more pronounced adipocyte dysfunction in patients with high heteroplasmy. Nevertheless, the low adiponectin and impaired insulin suppression of fatty acids in patients with m.3243A>G are in line with impaired [^{18}F]FDG uptake in fat (Viljanen et al. 2009; Groop et al. 1989). Previous studies on adiponectin clearance and production have shown that circulating adiponectin levels are determined by the adipocyte dysfunction and not by the fat tissue mass or the changes in adiponectin clearance (Hoffstedt et al. 2004; Kadowaki et al. 2006). Variation in the BMI or in glucose homeostasis does not determine the adiponectin levels. For instance, physically active healthy lean subjects or patients with type 1 diabetes have relatively high adiponectin levels, whereas healthy obese and patients with type 2 diabetes and lean patients with lipodystrophy show similarly decreased adiponectin levels (Weyer et al. 2001; Perseghin et al. 2003; Sutinen et al. 2003).

Interestingly, a recent report on thymidine kinase 2 deficiency in mice mimicking mitochondrial disease showed mitochondrial DNA depletion, reduced fat accumulation, significant reduction in mtDNA-encoded transcripts, a reduction of thermogenesis related gene expression and a severe reduction in leptin mRNA in white adipose tissue as the circulating levels of leptin and resistin were low (Villarroya et al. 2011). In summary, the insulin resistance in subcutaneous fat, low adiponectin and high insulin suppressed FFAs in patients and the smaller subcutaneous fat depots and leptin levels with increasing heteroplasmy may indicate relevant adipocyte dysfunction in patients harbouring the m.3243A>G mutation.

A role for defective mitochondrial function in obese adipose tissue has been suggested. Firstly, mitochondrial number correlates strongly with lipogenesis in adipocytes and normal energetics are required for insulin signalling suggesting their importance in fat storage (Patti and Corvera. 2010). Secondly, gene expression in twin studies shows relative downregulation of pathways activating mitochondrial biogenesis in acquired obesity (Pietiläinen et al. 2008). Thirdly, relative hypoperfusion in adipose tissue might underlie the deregulated adipocyte metabolism and decreased adiponectin production

due to the hypoxia upregulated C/EBP homologous protein (CHOP) as shown in the adipose tissue of obese mice (Hosogai et al. 2007). Fourthly, PPAR-gamma agonists induce adipocyte FA oxidation and decreased release of FFAs in the circulation and increase the mtDNA copy number and TFAM in fat (Patti and Corvera. 2010). Fifthly adiponectin levels are increased by these drugs, which are considered to be an indicator of normal adipocyte proliferation and maturation (Ahmed et al. 2010; Hammarstedt et al. 2005). The present study was first to evaluate the adipose tissue metabolism in mitochondrial diabetes. Related information about substrate preference is also limited. A single previous study has assessed fatty acid oxidation in patients with mitochondrial mutations including four subjects with m.3243A>G at rest and during exercise. No aberration in the whole-body fatty acid or glucose oxidation was noted as assessed by an indirect calorimeter (Jeppesen et al. 2009). A mouse model for mitochondrial myopathy has recently shown that mitochondrial defects may lead to catechsia and low BMI and adipocyte size (Tyynismaa et al. 2010). Interestingly, also the CHOP seems to be elevated in cells harbouring m.3243A>G (Fujita et al. 2007). However, the most potential model available for mitochondrial diabetes at present is the tissue specific disruption of TFAM, which leads to a mitochondrial translation defect resembling that in patients with the m.3243A>G mutation. Skeletal muscle specific TFAM KO mice show decreased, complex I, III and IV activity, exercise intolerance and RRFs as the insulin-stimulated glucose uptake in muscle is increased in them (Wredenberg et al. 2006). Interestingly, the TFAM knockdown in adipocytes leads to adipocyte insulin resistance including decreased insulin-stimulated GLUT4 translocation and transmembrane glucose transport (Shi et al. 2008). The present results are preliminary and may have been disturbed by small defects in the glucose homeostasis. Still, these results would be strongly compatible with the FFA flux hypothesis, where adipocyte failure leads to insulin resistance in skeletal muscle, now in mitochondrial diabetes (Patti and Corvera. 2010). The FFA flux induction of insulin resistance in skeletal muscle would also potentially reconsolidate the discrepancy between the lack of skeletal muscle insulin resistance in muscle tissue specific TFAM KO mice and patients with insulin resistance and the m.3243A>G mutation.

7.6 The role of liver metabolism in mitochondrial diabetes

The relatively low liver fat content found here in patients with m.3243A>G is in accordance with the more recent of the two case reports available, where one patient with skeletal muscle insulin resistance had no elevation in liver fat as compared to six controls (Szendroedi et al. 2009b). The other case report described a liver failure and steatosis in a patient with the m.3243A>G mutation (Takahashi et al. 2008). The patient having the lowest heteroplasmy in skeletal muscle and a mild PEO phenotype had the highest liver fat. Interestingly, in patients with m.3243A>G and PEO phenotype the fatty acid oxidation proteins might not be upregulated as compared to patients with m.3243A>G and MELAS phenotype and as assessed in myocytes (Crimi et al. 2005). Notably, hepatic failure and steatosis is a common fatal feature in children with Alper's syndrome, which in turn is commonly due to the mtDNA depletion caused by mutations in the POLG gene (Kurt et al. 2010). On the contrary, the fat accumulation in the liver in patients with m.3243A>G was very moderate, especially when keeping in mind that high FFAs during hyperinsulinemia and low fasting adiponectin are commonly associated with high liver fat not only in obesity but also in lean patients with acquired lipodystrophy (Korenblat et al. 2008; Sutinen et al. 2003). In accordance with the present results a recent model for mitochondrial myopathy showed that mitochondrial disease in mice may lead to a low and diet resistant fat content in the liver (Tyynismaa et al. 2010).

The insulin-stimulated hepatic glucose uptake reflects insulin sensitivity in the proximal part of glucose metabolism in liver (Iozzo et al. 2003a; Rijzewijk et al. 2010). Similarly to the ability of insulin to harness EGP, the insulin-stimulated hepatic glucose uptake is usually inversely related to the liver fat content and is augmented by metformin treatment (Rijzewijk et al. 2010; Iozzo et al. 2003b; Borra et al. 2008). Based on the previous studies in patients with type 2 diabetes I would have expected at least a 20% decrease in hepatic glucose uptake partly because of the previous associations between impaired glycaemic control and hepatic glucose uptake, and partly due to the fact that fatty acids impair insulin-mediated glucose uptake in liver

(Iozzo et al. 2003a; Iozzo et al. 2003; Iozzo et al. 2003; Iozzo et al. 2004). However, no impairment in glucose metabolism was present but the correlation between EGP and the Hb-$A1_C$ could be detected in the patients. The well-preserved glucose uptake in liver is, in addition, in accordance with the experimental liver-specific ablation of the mitochondrial apoptosis-inducing factor. These mice show a decrease in complex I activity, and an increased hepatic glucose turnover, which is protective against diet induced diabetes and insulin resistance (Pospisilik et al. 2007). Thus, the present results found no evidence that hepatic insulin resistance or steatosis would be a result of a decreased respiratory OXPHOS in the liver. In conclusion, high liver fat or hepatic metabolic dysfunction do not characterize mitochondrial diabetes.

7.7 Metabolic aspects of mitochondrial cardiomyopathy

The present work demonstrated that patients with the high m.3243A>G heteroplasmy and diabetes utilize less glucose in heart than the healthy controls. As the results about glucose uptake in skeletal muscle, the myocardial results in the thesis are somewhat surprising as compared to the previous results. For instance, the proteins of glycolytic pathway in cardiac TFAM KO mice have been shown to be upregulated before manifest cardiac disease. Furthermore, GLUT4 translocation and glucose uptake are increased in myocytes incubated with inhibitors of mitochondrial respiration (Hansson et al. 2004; Brown et al. 2008). Sedentary lifestyle, or small differences in rate pressure product, blood pressure, left ventricle thickness, the use of angiotensin-converting enzyme inhibitors and angiotensin II type I receptor blockers and beta blockers cannot readily explain the decrease in the myocardial glucose uptake during hyperinsulinemia in patients with m.3243A>G (Takala et al. 1999a; Nuutila et al. 1995; Wang et al. 2003; Bottcher et al. 2002). On the contrary, an increase in cardiac work or rate pressure product is usually associated with an increase in substrate oxidation and uptake rate with no change in substrate preference (Ala-Rämi et al. 2005).

Cardiac disease and condition is often associated with a change in substrate preference. For example, slight cardiac hypertrophy in essential hypertony is associated with a shift from the utilization of fatty acids to increased glucose metabolism while in hypertrophic athlete heart the glucose uptake per tissue weight is decreased (Nuutila et al. 1995; Takala et al. 1999a). As the glucose uptake is unaffected in obese insulin resistant human subjects, the FFA uptake into the heart is markedly increased, a change that may be reversed by loosing weight (Peterson et al. 2004; Viljanen et al. 2009). The diabetic heart in its turn usually utilizes the highly available FFAs at the expense of glucose (Rijzewijk et al. 2009). However, chronic hyperglycaemia alone may not lead to decreased glucose uptake during hyperinsulinemia as shown in patients with type 1 diabetes (Nuutila et al. 1993).

When no changes in cardiac work are observed, the variation in substrate preference is often explained by the Randle's cycle (Nuutila et al. 1992). This metabolic interaction implies that fatty acids have a restrictive effect on glucose oxidation in general in striated muscle. This phenomenon is prominent in cardiac muscle (Ala-Rämi et al. 2005). The myocardial FFA uptake is largely determined by the concentration gradient across the plasma membrane and plasma FFA concentration, which in turn is influenced by the insulin-regulated peripheral lipolysis (Stanley et al. 2005). In the heart, fatty acid β-oxidation increases the NADH/NAD and acetyl-CoA/CoA ratios which transform the pyruvate dehydrogenase (PDH) into its inactive form resulting in a decrease in carbohydrate oxidation and uptake (Stanley et al. 2005). In healthy subjects, >90% of the glucose entering the myocardium is immediately oxidized during the hyperinsulinemia (Ferrannini et al. 1993). Heteroplasmy in skeletal muscle and that in cardiac muscle have been shown to be comparable post mortem (Majamaa-Voltti et al. 2002). Cells harbouring m.3243A>G are unable to oxidize pyruvate derived from the entering glucose due to the failing redox potential of the respiratory chain, thus a step beyond the PDH step leading to the accumulation of pyruvate as a marker of decreased glucose oxidation (Pallotti et al. 2004). A decrease in pyruvate oxidation in cardiomyocytes would explain why the insulin-suppressed FFAs or the skeletal muscle

insulin sensitivity were not coupled with LVGU and why the LVGU was coupled with the blood pyruvate concentrations (reflecting the sum of glucose oxidation capacity in all tissues) and with the tissue heteroplasmy in patients with m.3243A>G. Further, as the cardiac substrate utilization linearly increases, but the substrate preference is unaltered at higher RPP, the observed paradoxically low glucose uptake in the presence of high rate pressure product and m.3243A>G would be reconsolidated if the primary defect would be in the myocardial oxidation of acetyl-CoA (Ala-Rämi et al. 2005). The precence of such a defect is supported by a recent [^{11}C]acetate PET study which suggested a 27% slower citric acid cycle or myocardial oxidation in patients with a median myocyte heteroplasmy of 64% (Arakawa et al. 2010).

The cardiac substrate utilization was shifted away from glucose in patients with the m.3243A>G. This change is commonly considered as an uneconomical substrate preference and it is coupled with a hypertrophic cardiac remodelling. However, as the oxygen metabolism in the heart was not measured, the decreased glucose oxidation hypothesis could not be confirmed in the present thesis. However, I may still conclude that an increased anaerobic glucose utilization, as previously suggested by Arakawa et al, may not compensate the failing cardiac energetics in m.3243A>G cardiomyopathy. FFA and lactate were highly available in the patients as compared to controls. The blood ketone levels were not measured. Therefore, I can only speculate on the matter if a cardiac oxidation defect, increased oxidation of more uneconomical substrates, decreased metabolic flexibility, diabetes or other comorbidities of the mitochondrial disease are the cause of the myocardial glucose hypometabolism. Finally, regardless of the aetiology, patients with a high m.3243A>G mutation load do not prefer to utilize glucose in the heart and they become deprived from the most economical myocardial fuel at postprandial levels of hyperinsulinemia. Therefore, this study adds the uneconomical substrate utilization as a contributing factor in the cardiac vulnerability in patients with mitochondrial disease.

8 CONCLUSIONS

The aim of the thesis was to characterize tissue specific glucose metabolism in patients harbouring the m.3243A>G mutation. The [^{18}F]FDG-PET method allowed a non-invasive measurement of the transmembrane glucose uptake: firstly in brain and heart, where the organ manifestations are associated with the mortality among patients and secondly in the potential tissues maintaining glucose homeostasis before diabetes onset.

The data in the present thesis allows the following conclusions:

1. (Study I) The glucose oxidation and oxygen consumption rate are decreased in brain in patients with m.3243A>G. Low oxygen to glucose index in combination with the increased white matter lactate suggests increased lactate production in situ. This cross-section suggests that a decrease in oxygen metabolism due to the m.3243A>G mutation may precede symptoms of mitochondrial encephalopathy.

2. (Study II) During postprandial levels of euglycemic hyperinsulinemia, a ~50% decrease in glucose uptake with no decrease in bulk perfusion takes place in skeletal muscle in patients with m.3243A>G. This is detected also in patients, who do not fulfil the criteria for diabetes or have previously undiagnosed diabetes. The decline in beta cell function is associated with mutation heteroplasmy. The beta cell dysfunction and the insulin resistance in skeletal muscle together define the degree of glucose intolerance in patients with the m.3243A>G mutation.

3. (Study III) Insulin-stimulated glucose uptake in subcutaneous fat was decreased in patients with m.3243A>G both per tissue weight and per depot. The adipose tissue metabolism is disturbed, before beta cell failure results in mitochondrial diabetes, whereas hepatic metabolism does not contribute to the impaired glucose homeostasis.

4. (Study IV) Patients with m.3243A>G had high variability in the LVGU. Part of this variability is possibly explained by the differences in heteroplasmy and pyruvate oxidation capacity, high availability of alternative substrates or chronic hyperglycaemia or by all. Finally, the most affected patients as defined by the high glycaeted haemoglobin, phenotype or heteroplasmy showed inadequately low glucose utilization, which is likely to contribute to the cardiac vulnerability in such patients.

In summary, the methods of the present study were able to confirm a low *in vivo* glucose oxidation in brain and insulin resistance in skeletal muscle and subcutaneous fat in patients with the m.3243A>G mutation. The heterogenic patient group allowed to conclude that the decline in insulin secretion and cardiac glucose metabolism is predominantly present in patients with high heteroplasmy. This cross-sectional study provides useful data for the planning of follow-up and intervention studies. Further studies are necessary in order to understand and to be able to treat the disturbed metabolism and its multiorgan manifestations in mitochondrial disease.

9 ACKNOWLEDGEMENTS

This study was carried out at the Department of Clinical Physiology and Nuclear Medicine, university of Turku, Finland, during the years 2006-2013. I am grateful to the heads of the department Professor Jaakko Hartiala and director of the Turku PET Centre, Professor Juhani Knuuti, for allowing me to use their department facilities.

I am greatly thankful to my supervisor Pirjo Nuutila. I would like to thank you for your never ending positive attitude, encouragement and executive virtues. I owe my gratitude to my supervisor Kari Majamaa. I am sincerely grateful for your patience in learning me calmness and patience in scientific writing. Thank you both and your teams for your previous inspiring scientific work and efforts that made this distinct project possible.

I sincerely thank the reviewers of this thesis, Professor John Vissing and Professor Ulla Ruotsalainen for their constructive criticism and encouraging comments.

I want especially to thank Professors Andrea Mari, Patricia Iozzo and Juhani Knuuti in showing sincerely altruistic scientific curiosity towards the thesis.

I want to warmly thank my co-authors, Juha Rinne, Terho Lehtimäki, Riitta Parkkola, Ronald Borra, Mikko Kärppä, Kirsi Virtanen, Kari Kalliokoski, Andrea Tura, Jere Virta, Letizia Guiducci, Markku Taittonen, Jussi Pärkkä, Marco Bucci, Virva Lepomäki, Nina Mononen. Grazie. Especially, I want to thank those co-authors that have been struggling with this project in the most inconvenient hours of the day. You know who you are.

I can with no means thank all the past and present members contributing to the excellent geist of the Turku PET centre. Gaber Gomar, Ilkka Heinonen, Vesa Oikonen, Mika Teräs, Jarkko Johansson, Anna Karmi, Antti Viljanen, Iina Laitinen, Irina

Lisinen have directly or undirectly helped me with some important aspect of this project. Hvala. Thank you for being there when I needed help.

Thanks to my very best friends living around the old and new capitals and at antipode.

Finally, I want to express my gratitude to my beloved family. Pia ja Harras sekä Vaari. Parempaa tukea, esimerkkiä ja elämän alkua en olisi voinut saada. Edvin, Linnéa ja pienin pikkuinen, olette isän suurin valo ja ilo, joka pakkasyönä on sytyttänyt uuteen eloon tämänkin kirjan. Det djupaste tack hör till min allra käraste Emma. Jag tackar dig för ditt tålamod och din kärlek under alla dessa år.

"Excelsior"

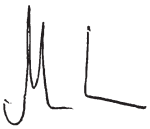

Markus Lindroos

Turku, huhtikuu 2013

10 REFERENCES

Abate N, Garg A, Coleman R, Grundy SM, Peshock RM. Prediction of total subcutaneous abdominal, intraperitoneal, and retroperitoneal adipose tissue masses in men by a single axial magnetic resonance imaging slice. Am J Clin Nutr 1997; 65: 403-8.

Abate N, Garg A, Peshock RM, Stray-Gundersen J, Grundy SM. Relationships of generalized and regional adiposity to insulin sensitivity in men. J Clin Invest 1995; 96: 88-98.

Abdel-aleem S, Li X, Anstadt MP, Perez-Tamayo RA, Lowe JE. Regulation of glucose utilization during the inhibition of fatty acid oxidation in rat myocytes. Horm Metab Res 1994; 26: 88-91.

Abe K, Yoshimura H, Tanaka H, Fujita N, Hikita T, Sakoda S. Comparison of conventional and diffusion-weighted MRI and proton MR spectroscopy in patients with mitochondrial encephalomyopathy, lactic acidosis, and stroke-like events. Neuroradiology 2004; 46: 113-7.

Abel ED, Peroni O, Kim JK, Kim YB, Boss O, Hadro E, et al. Adipose-selective targeting of the GLUT4 gene impairs insulin action in muscle and liver. Nature 2001; 409: 729-33.

Abramov AY, Smulders-Srinivasan TK, Kirby DM, Acin-Perez R, Enriquez JA, Lightowlers RN, et al. Mechanism of neurodegeneration of neurons with mitochondrial DNA mutations. Brain 2010; 133: 797-807.

Adams KL, Palmer JD. Evolution of mitochondrial gene content: Gene loss and transfer to the nucleus. Mol Phylogenet Evol 2003; 29: 380-95.

Ahmed M, Neville MJ, Edelmann MJ, Kessler BM, Karpe F. Proteomic analysis of human adipose tissue after rosiglitazone treatment shows coordinated changes to promote glucose uptake. Obesity (Silver Spring) 2010; 18: 27-34.

Ahren B. Beta- and alpha-cell dysfunction in subjects developing impaired glucose tolerance: Outcome of a 12-year prospective study in postmenopausal caucasian women. Diabetes 2009; 58: 726-31.

Ala-Rämi A, Ylihautala M, Ingman P, Hassinen IE. Influence of calcium-induced workload transitions and fatty acid supply on myocardial substrate selection. Metabolism 2005; 54: 410-20.

Alessi MC, Bastelica D, Morange P, Berthet B, Leduc I, Verdier M, et al. Plasminogen activator inhibitor 1, transforming growth factor-beta1, and BMI are closely associated in human adipose tissue during morbid obesity. Diabetes 2000; 49: 1374-80.

Allen A, Yanushka J, Fitzpatrick JH, Jenkins LW, Gilboe DD. Acute ultrastructural response of hypoxic hypoxia with relative ischemia in the isolated brain. Acta Neuropathol 1989; 78: 637-48.

Amchenkova AA, Bakeeva LE, Chentsov YS, Skulachev VP, Zorov DB. Coupling membranes as energy-transmitting cables. I. filamentous mitochondria in fibroblasts and mitochondrial clusters in cardiomyocytes. J Cell Biol 1988; 107: 481-95.

Anan R, Nakagawa M, Miyata M, Higuchi I, Nakao S, Suehara M, et al. Cardiac involvement in mitochondrial diseases. A study on 17 patients with documented mitochondrial DNA defects. Circulation 1995; 91: 955-61.

Andrews RM, Kubacka I, Chinnery PF, Lightowlers RN, Turnbull DM, Howell N. Reanalysis and revision of the cambridge reference sequence for human mitochondrial DNA. Nat Genet 1999; 23: 147.

Anichini A, Fanin M, Vianey-Saban C, Cassandrini D, Fiorillo C, Bruno C, et al. Genotype-phenotype correlations in a large series of patients with muscle type CPT II deficiency. Neurol Res 2010.

Antinozzi PA, Ishihara H, Newgard CB, Wollheim CB. Mitochondrial metabolism sets the maximal limit of fuel-stimulated insulin secretion in a model pancreatic beta cell: A survey of four fuel secretagogues. J Biol Chem 2002; 277: 11746-55.

Antonicka H, Sasarman F, Kennaway NG, Shoubridge EA. The molecular basis for tissue specificity of the oxidative phosphorylation deficiencies in patients with mutations in the mitochondrial translation factor EFG1. Hum Mol Genet 2006; 15: 1835-46.

Antonicka H, Floryk D, Klement P, Stratilova L, Hermanska J, Houstkova H, et al. Defective kinetics of cytochrome c oxidase and alteration of mitochondrial membrane potential in fibroblasts and cytoplasmic hybrid cells with the mutation for myoclonus epilepsy with ragged-red fibres ('MERRF') at position 8344 nt. Biochem J 1999; 342 Pt 3: 537-44.

Apabhai S, Gorman GS, Sutton L, Elson JL, Plötz T, Turnbull DM, Trenell MI. Habitual physical activity in mitochondrial disease. PLoS One. 2011; 6: e22294.

Arakawa K, Kudo T, Ikawa M, Morikawa N, Kawai Y, Sahashi K, et al. Abnormal myocardial energy-production state in mitochondrial cardiomyopathy and acute response to L-arginine infusion. C-11 acetate

kinetics revealed by positron emission tomography. Circ J 2010; 74: 2702-11.

Arner E, Westermark PO, Spalding KL, Britton T, Ryden M, Frisen J, et al. Adipocyte turnover Relevance to human adipose tissue morphology. Diabetes 2010; 59: 105-9.

Aure K, Ogier de Baulny H, Laforet P, Jardel C, Eymard B, Lombes A. Chronic progressive ophthalmoplegia with large-scale mtDNA rearrangement: Can we predict progression? Brain 2007; 130: 1516-24.

Austin SA, Vriesendorp FJ, Thandroyen FT, Hecht JT, Jones OT, Johns DR. Expanding the phenotype of the 8344 transfer RNAlysine mitochondrial DNA mutation. Neurology 1998; 51: 1447-50.

Autere J, Moilanen JS, Finnilä S, Soininen H, Mannermaa A, Hartikainen P, et al. Mitochondrial DNA polymorphisms as risk factors for parkinson's disease and parkinson's disease dementia. Hum Genet 2004; 115: 29-35.

Azzu V, Brand MD. The on-off switches of the mitochondrial uncoupling proteins. Trends Biochem Sci 2010; 35: 298-307.

Babcock MB, Cardell RR,Jr. Fine structure of hepatocytes from fasted and fed rats. Am J Anat 1975; 143: 399-438.

Bach D, Naon D, Pich S, Soriano FX, Vega N, Rieusset J, et al. Expression of Mfn2, the charcot-marie-tooth neuropathy type 2A gene, in human skeletal muscle: Effects of type 2 diabetes, obesity, weight loss, and the regulatory role of tumor necrosis factor alpha and interleukin-6. Diabetes 2005; 54: 2685-93.

Bachmann W, Challoner D. D-glucose uptake by a rat liver plasma membrane preparation. Biochim Biophys Acta 1976; 443: 254-66.

Baillet-Blanco L, Beauvieux MC, Gin H, Rigalleau V, Gallis JL. Insulin induces a positive relationship between the rates of ATP and glycogen changes in isolated rat liver in presence of glucose; a 31P and 13C NMR study. Nutr Metab (Lond) 2005; 2: 32.

Baron-Van Evercooren A, Olichon-Berthe C, Kowalski A, Visciano G, Van Obberghen E. Expression of IGF-I and insulin receptor genes in the rat central nervous system: A developmental, regional, and cellular analysis. J Neurosci Res 1991; 28: 244-53.

Barrell BG, Bankier AT, Drouin J. A different genetic code in human mitochondria. Nature 1979; 282: 189-94.

Barzilai N, Rossetti L. Role of glucokinase and glucose-6-phosphatase in the acute and chronic regulation of hepatic glucose fluxes by insulin. J Biol Chem 1993; 268: 25019-25.

Basu A, Basu R, Shah P, Vella A, Johnson CM, Jensen M, et al. Type 2 diabetes impairs splanchnic uptake of glucose but does not alter intestinal glucose absorption during enteral glucose feeding: Additional evidence for a defect in hepatic glucokinase activity. Diabetes 2001; 50: 1351-62.

Basu R, Chandramouli V, Dicke B, Landau BR, Rizza RA. Plasma C5 glucose-to-2H2O ratio does not provide an accurate assessment of gluconeogenesis during hyperinsulinemic-euglycemic clamps in either nondiabetic or diabetic humans. Diabetes 2008; 57: 1800-4.

Battezzati A, Caumo A, Martino F, Sereni LP, Coppa J, Romito R, et al. Nonhepatic glucose production in humans. Am J Physiol Endocrinol Metab 2004; 286: E129-35.

Becker R, Laube H, Linn T, Damian MS. Insulin resistance in patients with the mitochondrial tRNA(leu(UUR)) gene mutation at position 3243. Exp Clin Endocrinol Diabetes 2002; 110: 291-7.

Beck-Nielsen H, Vaag A, Poulsen P, Gaster M. Metabolic and genetic influence on glucose metabolism in type 2 diabetic subjects--experiences from relatives and twin studies. Best Pract Res Clin Endocrinol Metab 2003; 17: 445-67.

Belke DD, Betuing S, Tuttle MJ, Graveleau C, Young ME, Pham M, et al. Insulin signaling coordinately regulates cardiac size, metabolism, and contractile protein isoform expression. J Clin Invest 2002; 109: 629-39.

Benit P, Beugnot R, Chretien D, Giurgea I, De Lonlay-Debeney P, Issartel JP, et al. Mutant NDUFV2 subunit of mitochondrial complex I causes early onset hypertrophic cardiomyopathy and encephalopathy. Hum Mutat 2003; 21: 582-6.

Bentourkia M, Tremblay S, Pifferi F, Rousseau J, Lecomte R, Cunnane S. PET study of 11C-acetoacetate kinetics in rat brain during dietary treatments affecting ketosis. Am J Physiol Endocrinol Metab 2009; 296: E796-801.

Bereiter-Hahn J, Voth M. Dynamics of mitochondria in living cells: Shape changes, dislocations, fusion, and fission of mitochondria. Microsc Res Tech 1994; 27: 198-219.

Bergman BC, Tsvetkova T, Lowes B, Wolfel EE. Myocardial FFA metabolism during rest and atrial pacing in humans. Am J Physiol Endocrinol Metab 2009a; 296: E358-66.

Bergman BC, Tsvetkova T, Lowes B, Wolfel EE. Myocardial glucose and lactate metabolism during rest and atrial pacing in humans. J Physiol 2009b; 587: 2087-99.

Betts J, Jaros E, Perry RH, Schaefer AM, Taylor RW, Abdel-All Z, et al. Molecular neuropathology of MELAS: Level of heteroplasmy in individual neurones and evidence of extensive vascular involvement. Neuropathol Appl Neurobiol 2006; 32: 359-73.

Bindoff LA, Birch-Machin MA, Cartlidge NE, Parker WD,Jr, Turnbull DM. Respiratory chain abnormalities in skeletal muscle from patients with parkinson's disease. J Neurol Sci 1991; 104: 203-8.

Blass JP, Avigan J, Uhlendorf BW. A defect in pyruvate decarboxylase in a child with an intermittent movement disorder. J Clin Invest 1970; 49: 423-32.

Bluher M, Michael MD, Peroni OD, Ueki K, Carter N, Kahn BB, et al. Adipose tissue selective insulin receptor knockout protects against obesity and obesity-related glucose intolerance. Dev Cell 2002; 3: 25-38.

Bodak A, Hatt PY. Myocardial lesions induced by rapeseed oil-rich diet in the rat: Ultrastructural aspects. Recent Adv Stud Cardiac Struct Metab 1975; 6: 479-86.

Bogenhagen D, Clayton DA. Mouse L cell mitochondrial DNA molecules are selected randomly for replication throughout the cell cycle. Cell 1977; 11: 719-27.

Bolinder J, Kerckhoffs DA, Moberg E, Hagström-Toft E, Arner P. Rates of skeletal muscle and adipose tissue glycerol release in nonobese and obese subjects. Diabetes 2000; 49: 797-802.

Borland MK, Mohanakumar KP, Rubinstein JD, Keeney PM, Xie J, Capaldi R, et al. Relationships among molecular genetic and respiratory properties of parkinson's disease cybrid cells show similarities to parkinson's brain tissues. Biochim Biophys Acta 2009; 1792: 68-74.

Borra R, Lautamäki R, Parkkola R, Komu M, Sijens PE, Hällsten K, et al. Inverse association between liver fat content and hepatic glucose uptake in patients with type 2 diabetes mellitus. Metabolism 2008; 57: 1445-51.

Bottcher M, Refsgaard J, Gotzsche O, Andreasen F, Nielsen TT. Effect of carvedilol on microcirculatory and glucose metabolic regulation in patients with congestive heart failure secondary to ischemic cardiomyopathy. Am J Cardiol 2002; 89: 1388-93.

Bourgeron T, Rustin P, Chretien D, Birch-Machin M, Bourgeois M, Viegas-Pequignot E, et al. Mutation of a nuclear succinate dehydrogenase gene results in mitochondrial respiratory chain deficiency. Nat Genet 1995; 11: 144-9.

Bourgeron T, Chretien D, Poggi-Bach J, Doonan S, Rabier D, Letouze P, et al. Mutation of the fumarase gene in two siblings with progressive encephalopathy and fumarase deficiency. J Clin Invest 1994; 93: 2514-8.

Brändle M, Lehmann R, Maly FE, Schmid C, Spinas GA. Diminished insulin secretory response to glucose but normal insulin and glucagon secretory responses to arginine in a family with maternally inherited diabetes and deafness caused by mitochondrial tRNA(LEU(UUR)) gene mutation. Diabetes Care 2001; 24: 1253-8.

Brown AE, Elstner M, Yeaman SJ, Turnbull DM, Walker M. Does impaired mitochondrial function affect insulin signaling and action in cultured human skeletal muscle cells? Am J Physiol Endocrinol Metab 2008; 294: E97-102.

Brown AM, Tekkok SB, Ransom BR. Glycogen regulation and functional role in mouse white matter. J Physiol 2003; 549: 501-12.

Brown DT, Samuels DC, Michael EM, Turnbull DM, Chinnery PF. Random genetic drift determines the level of mutant mtDNA in human primary oocytes. Am J Hum Genet 2001; 68: 533-6.

Brown MD, Trounce IA, Jun AS, Allen JC, Wallace DC. Functional analysis of lymphoblast and cybrid mitochondria containing the 3460, 11778, or 14484 leber's hereditary optic neuropathy mitochondrial DNA mutation. J Biol Chem 2000; 275: 39831-6.

Bruce CR, Anderson MJ, Carey AL, Newman DG, Bonen A, Kriketos AD, et al. Muscle oxidative capacity is a better predictor of insulin sensitivity than lipid status. J Clin Endocrinol Metab 2003; 88: 5444-51.

Bruning JC, Michael MD, Winnay JN, Hayashi T, Horsch D, Accili D, et al. A muscle-specific insulin receptor knockout exhibits features of the metabolic syndrome of NIDDM without altering glucose tolerance. Mol Cell 1998; 2: 559-69.

Bruning JC, Gautam D, Burks DJ, Gillette J, Schubert M, Orban PC, et al. Role of brain insulin receptor in control of body weight and reproduction. Science 2000; 289: 2122-5.

Bugger H, Boudina S, Hu XX, Tuinei J, Zaha VG, Theobald HA, et al. Type 1 diabetic akita mouse hearts are insulin sensitive but manifest structurally abnormal mitochondria that remain coupled despite

increased uncoupling protein 3. Diabetes 2008; 57: 2924-32.

Burcelin R, del Carmen Munoz M, Guillam MT, Thorens B. Liver hyperplasia and paradoxical regulation of glycogen metabolism and glucose-sensitive gene expression in GLUT2-null hepatocytes. further evidence for the existence of a membrane-based glucose release pathway. J Biol Chem 2000; 275: 10930-6.

Carta A, D'Adda T, Carrara F, Zeviani M. Ultrastructural analysis of extraocular muscle in chronic progressive external ophthalmoplegia. Arch Ophthalmol 2000; 118: 1441-5.

Carvalho E, Kotani K, Peroni OD, Kahn BB. Adipose-specific overexpression of GLUT4 reverses insulin resistance and diabetes in mice lacking GLUT4 selectively in muscle. Am J Physiol Endocrinol Metab 2005; 289: E551-61.

Casali C, d'Amati G, Bernucci P, DeBiase L, Autore C, Santorelli FM, et al. Maternally inherited cardiomyopathy: Clinical and molecular characterization of a large kindred harboring the A4300G point mutation in mitochondrial deoxyribonucleic acid. J Am Coll Cardiol 1999; 33: 1584-9.

Castillo M, Kwock L, Green C. MELAS syndrome: Imaging and proton MR spectroscopic findings. AJNR Am J Neuroradiol 1995; 16: 233-9.
Chen X, Prosser R, Simonetti S, Sadlock J, Jagiello G, Schon EA. Rearranged mitochondrial genomes are present in human oocytes. Am J Hum Genet 1995; 57: 239-47.

Chinnery PF, Samuels DC. Relaxed replication of mtDNA: A model with implications for the expression of disease. Am J Hum Genet 1999; 64: 1158-65.

Chinnery PF, Howell N, Lightowlers RN, Turnbull DM. Molecular pathology of MELAS and MERRF. the relationship between mutation load and clinical phenotypes. Brain 1997; 120 (Pt 10): 1713-21.

Chinnery PF, Zwijnenburg PJ, Walker M, Howell N, Taylor RW, Lightowlers RN, et al. Nonrandom tissue distribution of mutant mtDNA. Am J Med Genet 1999; 85: 498-501.

Chinnery PF, DiMauro S, Shanske S, Schon EA, Zeviani M, Mariotti C, et al. Risk of developing a mitochondrial DNA deletion disorder. Lancet 2004; 364: 592-6.

Chiry O, Pellerin L, Monnet-Tschudi F, Fishbein WN, Merezhinskaya N, Magistretti PJ, et al. Expression of the monocarboxylate transporter MCT1 in the adult human brain cortex. Brain Res 2006; 1070: 65-70.

Choeiri C, Staines W, Messier C. Immunohistochemical localization and quantification of glucose transporters in the mouse brain. Neuroscience 2002; 111: 19-34.

Chol M, Lebon S, Benit P, Chretien D, de Lonlay P, Goldenberg A, et al. The mitochondrial DNA G13513A MELAS mutation in the NADH dehydrogenase 5 gene is a frequent cause of leigh-like syndrome with isolated complex I deficiency. J Med Genet 2003; 40: 188-91.

Choo-Kang AT, Lynn S, Taylor GA, Daly ME, Sihota SS, Wardell TM, et al. Defining the importance of mitochondrial gene defects in maternally inherited diabetes by sequencing the entire mitochondrial genome. Diabetes 2002; 51: 2317-20.

Cizkova A, Stranecky V, Mayr JA, Tesarova M, Havlickova V, Paul J, et al. TMEM70 mutations cause isolated ATP synthase deficiency and neonatal mitochondrial encephalocardiomyopathy. Nat Genet 2008; 40: 1288-90.

Clayton DA. Transcription and replication of mitochondrial DNA. Hum Reprod 2000; 15 Suppl 2: 11-7.

Cline GW, Rothman DL, Magnusson I, Katz LD, Shulman GI. 13C-nuclear magnetic resonance spectroscopy studies of hepatic glucose metabolism in normal subjects and subjects with insulin-dependent diabetes mellitus. J Clin Invest 1994; 94: 2369-76.

Cline GW, Petersen KF, Krssak M, Shen J, Hundal RS, Trajanoski Z, et al. Impaired glucose transport as a cause of decreased insulin-stimulated muscle glycogen synthesis in type 2 diabetes. N Engl J Med 1999; 341: 240-6.

Cock HR, Tabrizi SJ, Cooper JM, Schapira AH. The influence of nuclear background on the biochemical expression of 3460 leber's hereditary optic neuropathy. Ann Neurol 1998; 44: 187-93.

Coenen MJ, Antonicka H, Ugalde C, Sasarman F, Rossi R, Heister JG, et al. Mutant mitochondrial elongation factor G1 and combined oxidative phosphorylation deficiency. N Engl J Med 2004; 351: 2080-6.

Colombo C, Cutson JJ, Yamauchi T, Vinson C, Kadowaki T, Gavrilova O, et al. Transplantation of adipose tissue lacking leptin is unable to reverse the metabolic abnormalities associated with lipoatrophy. Diabetes 2002; 51: 2727-33.

Considine RV, Sinha MK, Heiman ML, Kriauciunas A, Stephens TW, Nyce MR, et al. Serum immunoreactive-leptin concentrations in normal-weight and obese humans. N Engl J Med 1996; 334: 292-5.

Cook DL, Hales CN. Intracellular ATP directly blocks K+ channels in pancreatic B-cells. Nature 1984; 311: 271-3.

Coppack SW, Fisher RM, Gibbons GF, Humphreys SM, McDonough MJ, Potts JL, et al. Postprandial substrate deposition in human forearm and adipose tissues in vivo. Clin Sci (Lond) 1990; 79: 339-48.

Cortelli P, Montagna P, Avoni P, Sangiorgi S, Bresolin N, Moggio M, et al. Leber's hereditary optic neuropathy: Genetic, biochemical, and phosphorus magnetic resonance spectroscopy study in an italian family. Neurology 1991; 41: 1211-5.

Cortopassi G, Danielson S, Alemi M, Zhan SS, Tong W, Carelli V, et al. Mitochondrial disease activates transcripts of the unfolded protein response and cell cycle and inhibits vesicular secretion and oligodendrocyte-specific transcripts. Mitochondrion 2006; 6: 161-75.

Cranston I, Marsden P, Matyka K, Evans M, Lomas J, Sonksen P, et al. Regional differences in cerebral blood flow and glucose utilization in diabetic man: The effect of insulin. J Cereb Blood Flow Metab 1998; 18: 130-40.

Cree LM, Samuels DC, de Sousa Lopes SC, Rajasimha HK, Wonnapinij P, Mann JR, et al. A reduction of mitochondrial DNA molecules during embryogenesis explains the rapid segregation of genotypes. Nat Genet 2008; 40: 249-54.

Crimi M, Bordoni A, Menozzi G, Riva L, Fortunato F, Galbiati S, et al. Skeletal muscle gene expression profiling in mitochondrial disorders. FASEB J 2005; 19: 866-8.

Cruz NF, Dienel GA. High glycogen levels in brains of rats with minimal environmental stimuli: Implications for metabolic contributions of working astrocytes. J Cereb Blood Flow Metab 2002; 22: 1476-89.

Dahlman I, Forsgren M, Sjögren A, Nordström EA, Kaaman M, Näslund E, et al. Downregulation of electron transport chain genes in visceral adipose tissue in type 2 diabetes independent of obesity and possibly involving tumor necrosis factor-alpha. Diabetes 2006; 55: 1792-9.

Dalsgaard MK, Ide K, Cai Y, Quistorff B, Secher NH. The intent to exercise influences the cerebral O(2)/carbohydrate uptake ratio in humans. J Physiol 2002; 540: 681-9.

Dalsgaard MK, Quistorff B, Danielsen ER, Selmer C, Vogelsang T, Secher NH. A reduced cerebral metabolic ratio in exercise reflects metabolism and not accumulation of lactate within the human brain. J Physiol 2004; 554: 571-8.

Damian MS, Hertel A, Seibel P, Reichmann H, Bachmann G, Schachenmayr W, et al. Follow-up in carriers of the 'MELAS' mutation without strokes. Eur Neurol 1998; 39: 9-15.

Darin N, Oldfors A, Moslemi AR, Holme E, Tulinius M. The incidence of mitochondrial encephalomyopathies in childhood: Clinical features and morphological, biochemical, and DNA anbormalities. Ann Neurol 2001; 49: 377-83.

Dastani Z, Hivert MF, Timpson N, Perry JR, Yuan X, Scott RA, et al. Novel loci for adiponectin levels and their influence on type 2 diabetes and metabolic traits: A multi-ethnic meta-analysis of 45,891 individuals. PLoS Genet 2012; 8: e1002607.

D'Aurelio M, Gajewski CD, Lin MT, Mauck WM, Shao LZ, Lenaz G, et al. Heterologous mitochondrial DNA recombination in human cells. Hum Mol Genet 2004; 13: 3171-9.

Davidzon G, Greene P, Mancuso M, Klos KJ, Ahlskog JE, Hirano M, et al. Early-onset familial parkinsonism due to POLG mutations. Ann Neurol 2006; 59: 859-62.

de Andrade PB, Rubi B, Frigerio F, van den Ouweland JM, Maassen JA, Maechler P. Diabetes-associated mitochondrial DNA mutation A3243G impairs cellular metabolic pathways necessary for beta cell function. Diabetologia 2006; 49: 1816-26.

De Lonlay P, Mugnier C, Sanlaville D, Chantrel-Groussard K, Benit P, Lebon S, et al. Cell complementation using genebridge 4 human:Rodent hybrids for physical mapping of novel mitochondrial respiratory chain deficiency genes. Hum Mol Genet 2002; 11: 3273-81.

De Vos A, Heimberg H, Quartier E, Huypens P, Bouwens L, Pipeleers D, et al. Human and rat beta cells differ in glucose transporter but not in glucokinase gene expression. J Clin Invest 1995; 96: 2489-95.

DeFronzo RA, Simonson D, Ferrannini E. Hepatic and peripheral insulin resistance: A common feature of type 2 (non-insulin-dependent) and type 1 (insulin-dependent) diabetes mellitus. Diabetologia 1982; 23: 313-9.

Del Bo R, Moggio M, Rango M, Bonato S, D'Angelo MG, Ghezzi S, et al. Mutated mitofusin 2 presents with intrafamilial variability and brain mitochondrial dysfunction. Neurology 2008; 71: 1959-66.

Deng H, Dodson MW, Huang H, Guo M. The parkinson's disease genes pink1 and parkin promote mitochondrial fission and/or inhibit fusion in drosophila. Proc Natl Acad Sci U S A 2008; 105: 14503-8.

DiDonato S, Zeviani M, Giovannini P, Savarese N, Rimoldi M, Mariotti C, et al. Respiratory chain and mitochondrial DNA in muscle and brain in parkinson's disease patients. Neurology 1993; 43: 2262-8.

Dienel GA, Ball KK, Cruz NF. A glycogen phosphorylase inhibitor selectively enhances local rates of glucose utilization in brain during sensory stimulation of conscious rats: Implications for glycogen turnover. J Neurochem 2007; 102: 466-78.

DiFrancesco JC, Cooper JM, Lam A, Hart PE, Tremolizzo L, Ferrarese C, et al. MELAS mitochondrial DNA mutation A3243G reduces glutamate transport in cybrids cell lines. Exp Neurol 2008; 212: 152-6.

DiMauro S, DiMauro PM. Muscle carnitine palmityltransferase deficiency and myoglobinuria. Science 1973; 182: 929-31.

Donath MY, Ehses JA, Maedler K, Schumann DM, Ellingsgaard H, Eppler E, et al. Mechanisms of beta-cell death in type 2 diabetes. Diabetes 2005; 54 Suppl 2: S108-13.

Dubeau F, De Stefano N, Zifkin BG, Arnold DL, Shoubridge EA. Oxidative phosphorylation defect in the brains of carriers of the tRNAleu(UUR) A3243G mutation in a MELAS pedigree. Ann Neurol 2000; 47: 179-85.

Durham SE, Samuels DC, Cree LM, Chinnery PF. Normal levels of wild-type mitochondrial DNA maintain cytochrome c oxidase activity for two pathogenic mitochondrial DNA mutations but not for m.3243A-->G. Am J Hum Genet 2007; 81: 189-95.

Elliott HR, Samuels DC, Eden JA, Relton CL, Chinnery PF. Pathogenic mitochondrial DNA mutations are common in the general population. Am J Hum Genet 2008; 83: 254-60.

Elson JL, Andrews RM, Chinnery PF, Lightowlers RN, Turnbull DM, Howell N. Analysis of european mtDNAs for recombination. Am J Hum Genet 2001; 68: 145-53.

Eriksson KF, Lindgärde F. Poor physical fitness, and impaired early insulin response but late hyperinsulinaemia, as predictors of NIDDM in middle-aged swedish men. Diabetologia 1996; 39: 573-9.

Essop MF, Camp HS, Choi CS, Sharma S, Fryer RM, Reinhart GA, et al. Reduced heart size and increased myocardial fuel substrate oxidation in ACC2 mutant mice. Am J Physiol Heart Circ Physiol 2008; 295: H256-65.

Estivill X, Govea N, Barcelo E, Badenas C, Romero E, Moral L, et al. Familial progressive sensorineural deafness is mainly due to the mtDNA A1555G mutation and is enhanced by treatment of aminoglycosides. Am J Hum Genet 1998; 62: 27-35.

Faerch K, Vaag A, Holst JJ, Glumer C, Pedersen O, Borch-Johnsen K. Impaired fasting glycaemia vs impaired glucose tolerance: Similar impairment of pancreatic alpha and beta cell function but differential roles of incretin hormones and insulin action. Diabetologia 2008; 51: 853-61.

Fan W, Waymire KG, Narula N, Li P, Rocher C, Coskun PE, et al. A mouse model of mitochondrial disease reveals germline selection against severe mtDNA mutations. Science 2008; 319: 958-62.

Ferrannini E, Gastaldelli A, Miyazaki Y, Matsuda M, Mari A, DeFronzo RA. Beta-cell function in subjects spanning the range from normal glucose tolerance to overt diabetes: A new analysis. J Clin Endocrinol Metab 2005; 90: 493-500.

Ferrannini E, Santoro D, Bonadonna R, Natali A, Parodi O, Camici PG. Metabolic and hemodynamic effects of insulin on human hearts. Am J Physiol 1993; 264: E308-15.

Ferre T, Riu E, Bosch F, Valera A. Evidence from transgenic mice that glucokinase is rate limiting for glucose utilization in the liver. FASEB J 1996; 10: 1213-8.

Ferre T, Riu E, Franckhauser S, Agudo J, Bosch F. Long-term overexpression of glucokinase in the liver of transgenic mice leads to insulin resistance. Diabetologia 2003; 46: 1662-8.

Finnilä S, Lehtonen MS, Majamaa K. Phylogenetic network for european mtDNA. Am J Hum Genet 2001; 68: 1475-84.

Fischman AJ, Hsu H, Carter EA, Yu YM, Tompkins RG, Guerrero JL, et al. Regional measurement of canine skeletal muscle blood flow by positron emission tomography with H2(15)O. J Appl Physiol 2002; 92: 1709-16.

Fisher SJ, Kahn CR. Insulin signaling is required for insulin's direct and indirect action on hepatic glucose production. J Clin Invest 2003; 111: 463-8.

Flierl A, Reichmann H, Seibel P. Pathophysiology of the MELAS 3243 transition mutation. J Biol Chem 1997; 272: 27189-96.

Frackowiak RS, Herold S, Petty RK, Morgan-Hughes JA. The cerebral metabolism of glucose and oxygen measured with positron tomography in patients with mitochondrial diseases. Brain 1988; 111 (Pt 5): 1009-24.

Fratter C, Gorman GS, Stewart JD, Buddles M, Smith C, Evans J, et al. The clinical, histochemical, and molecular spectrum of PEO1 (twinkle)-linked adPEO. Neurology 2010; 74: 1619-26.

Frederiksen AL, Andersen PH, Kyvik KO, Jeppesen TD, Vissing J, Schwartz M. Tissue specific distribution of the 3243A->G mtDNA mutation. J Med Genet 2006; 43: 671-7.

Frederiksen AL, Jeppesen TD, Vissing J, Schwartz M, Kyvik KO, Schmitz O, et al. High prevalence of impaired glucose homeostasis and myopathy in asymptomatic and oligosymptomatic 3243A>G mitochondrial DNA mutation-positive subjects. J Clin Endocrinol Metab 2009; 94: 2872-9.

Friston KJ, Holmes A, Poline JB, Price CJ, Frith CD. Detecting activations in PET and fMRI: Levels of inference and power. Neuroimage 1996; 4: 223-35.

Fromont I, Nicoli F, Valero R, Felician O, Lebail B, Lefur Y, et al. Brain anomalies in maternally inherited diabetes and deafness syndrome. J Neurol 2009; 256: 1696-704.

Fueger PT, Shearer J, Bracy DP, Posey KA, Pencek RR, McGuinness OP, et al. Control of muscle glucose uptake: Test of the rate-limiting step paradigm in conscious, unrestrained mice. J Physiol 2005; 562: 925-35.

Fueger PT, Hess HS, Bracy DP, Pencek RR, Posey KA, Charron MJ, et al. Regulation of insulin-stimulated muscle glucose uptake in the conscious mouse: Role of glucose transport is dependent on glucose phosphorylation capacity. Endocrinology 2004; 145: 4912-6.

Fujita Y, Ito M, Nozawa Y, Yoneda M, Oshida Y, Tanaka M. CHOP (C/EBP homologous protein) and ASNS (asparagine synthetase) induction in cybrid cells harboring MELAS and NARP mitochondrial DNA mutations. Mitochondrion 2007; 7: 80-8.

Garrido N, Griparic L, Jokitalo E, Wartiovaara J, van der Bliek AM, Spelbrink JN. Composition and dynamics of human mitochondrial nucleoids. Mol Biol Cell 2003; 14: 1583-96.

Gaster M, Handberg A, Beck-Nielsen H, Schroder HD. Glucose transporter expression in human skeletal muscle fibers. Am J Physiol Endocrinol Metab 2000; 279: E529-38.

Gavete ML, Agote M, Martin MA, Alvarez C, Escriva F. Effects of chronic undernutrition on glucose uptake and glucose transporter proteins in rat heart 1. Endocrinology 2002; 143: 4295-303.

Gebhart SS, Shoffner JM, Koontz D, Kaufman A, Wallace D. Insulin resistance associated with maternally inherited diabetes and deafness. Metabolism 1996; 45: 526-31.

Gemma C, Sookoian S, Dieuzeide G, Garcia SI, Gianotti TF, Gonzalez CD, et al. Methylation of TFAM gene promoter in peripheral white blood cells is associated with insulin resistance in adolescents. Mol Genet Metab 2010; 100: 83-7.

Gertz EW, Wisneski JA, Stanley WC, Neese RA. Myocardial substrate utilization during exercise in humans. dual carbon-labeled carbohydrate isotope experiments. J Clin Invest 1988; 82: 2017-25.

Ghosh A, Cheung YY, Mansfield BC, Chou JY. Brain contains a functional glucose-6-phosphatase complex capable of endogenous glucose production. J Biol Chem 2005; 280: 11114-9.

Giaccari A, Morviducci L, Pastore L, Zorretta D, Sbraccia P, Maroccia E, et al. Relative contribution of glycogenolysis and gluconeogenesis to hepatic glucose production in control and diabetic rats. A re-examination in the presence of euglycaemia. Diabetologia 1998; 41: 307-14.

Giles RE, Blanc H, Cann HM, Wallace DC. Maternal inheritance of human mitochondrial DNA. Proc Natl Acad Sci U S A 1980; 77: 6715-9.

Gjedde A, Marrett S. Glycolysis in neurons, not astrocytes, delays oxidative metabolism of human visual cortex during sustained checkerboard stimulation in vivo. J Cereb Blood Flow Metab 2001; 21: 1384-92.

Gloyn AL, Weedon MN, Owen KR, Turner MJ, Knight BA, Hitman G, et al. Large-scale association studies of variants in genes encoding the pancreatic beta-cell KATP channel subunits Kir6.2 (KCNJ11) and SUR1 (ABCC8) confirm that the KCNJ11 E23K variant is associated with type 2 diabetes. Diabetes 2003; 52: 568-72.

Goto Y, Nonaka I, Horai S. A mutation in the tRNA(leu)(UUR) gene associated with the MELAS subgroup of mitochondrial encephalomyopathies. Nature 1990; 348: 651-3.

Goto Y, Horai S, Matsuoka T, Koga Y, Nihei K, Kobayashi M, et al. Mitochondrial myopathy, encephalopathy, lactic acidosis, and stroke-like episodes (MELAS): A correlative study of the clinical features and mitochondrial DNA mutation. Neurology 1992; 42: 545-50.

Graham BH, Waymire KG, Cottrell B, Trounce IA, MacGregor GR, Wallace DC. A mouse model for mitochondrial myopathy and cardiomyopathy resulting from a deficiency in the heart/muscle isoform of the adenine nucleotide translocator. Nat Genet 1997; 16: 226-34.

Graham MM, Muzi M, Spence AM, O'Sullivan F, Lewellen TK, Link JM, et al. The FDG lumped constant in normal human brain. J Nucl Med 2002; 43: 1157-66.

Grant SF, Thorleifsson G, Reynisdottir I, Benediktsson R, Manolescu A, Sainz J, et al. Variant of transcription factor 7-like 2 (TCF7L2) gene confers risk of type 2 diabetes. Nat Genet 2006; 38: 320-3.

Green A, Basile R, Rumberger JM. Transferrin and iron induce insulin resistance of glucose transport in adipocytes. Metabolism 2006; 55: 1042-5.

Greenhaff PL, Soderlund K, Ren JM, Hultman E. Energy metabolism in single human muscle fibres during intermittent contraction with occluded circulation. J Physiol 1993; 460: 443-53.

Groop LC, Bonadonna RC, DelPrato S, Ratheiser K, Zyck K, Ferrannini E, et al. Glucose and free fatty acid metabolism in non-insulin-dependent diabetes mellitus. evidence for multiple sites of insulin resistance. J Clin Invest 1989; 84: 205-13.

Guillausseau PJ, Massin P, Dubois-LaForgue D, Timsit J, Virally M, Gin H, et al. Maternally inherited diabetes and deafness: A multicenter study. Ann Intern Med 2001; 134: 721-8.

Hackenbrock CR. Ultrastructural bases for metabolically linked mechanical activity in mitochondria. I. reversible ultrastructural changes with change in metabolic steady state in isolated liver mitochondria. J Cell Biol 1966; 30: 269-97.

Hagström-Toft E, Arner P, Johansson U, Eriksson LS, Ungerstedt U, Bolinder J. Effect of insulin on human adipose tissue metabolism in situ. interactions with beta-adrenoceptors. Diabetologia 1992; 35: 664-70.

Hajri T, Ibrahimi A, Coburn CT, Knapp FF,Jr, Kurtz T, Pravenec M, et al. Defective fatty acid uptake in the spontaneously hypertensive rat is a primary determinant of altered glucose metabolism, hyperinsulinemia, and myocardial hypertrophy. J Biol Chem 2001; 276: 23661-6.

Hamacher K, Coenen HH, Stocklin G. Efficient stereospecific synthesis of no-carrier-added 2-[18F]-fluoro-2-deoxy-D-glucose using aminopolyether supported nucleophilic substitution. J Nucl Med 1986; 27: 235-8.

Hammarstedt A, Sopasakis VR, Gogg S, Jansson PA, Smith U. Improved insulin sensitivity and adipose tissue dysregulation after short-term treatment with pioglitazone in non-diabetic, insulin-resistant subjects. Diabetologia 2005; 48: 96-104.

Hannukainen JC, Nuutila P, Kaprio J, Heinonen OJ, Kujala UM, Janatuinen T, et al. Relationship between local perfusion and FFA uptake in human skeletal muscle-no effect of increased physical activity and aerobic fitness. J Appl Physiol 2006; 101: 1303-11.

Hansson A, Hance N, Dufour E, Rantanen A, Hultenby K, Clayton DA, et al. A switch in metabolism precedes increased mitochondrial biogenesis in respiratory chain-deficient mouse hearts. Proc Natl Acad Sci U S A 2004; 101: 3136-41.

Harman-Boehm I, Bluher M, Redel H, Sion-Vardy N, Ovadia S, Avinoach E, et al. Macrophage infiltration into omental versus subcutaneous fat across different populations: Effect of regional adiposity and the comorbidities of obesity. J Clin Endocrinol Metab 2007; 92: 2240-7.

Hart LM, Dekker JM, van Haeften TW, Ruige JB, Stehouwer CD, Erkelens DW, et al. Reduced second phase insulin secretion in carriers of a sulphonylurea receptor gene variant associating with type II diabetes mellitus. Diabetologia 2000; 43: 515-9.

Hartmann H, Probst I, Jungermann K, Creutzfeldt W. Inhibition of glycogenolysis and glycogen phosphorylase by insulin and proinsulin in rat hepatocyte cultures. Diabetes 1987; 36: 551-5.

Hasegawa H, Matsuoka T, Goto Y, Nonaka I. Strongly succinate dehydrogenase-reactive blood vessels in muscles from patients with mitochondrial myopathy, encephalopathy, lactic acidosis, and stroke-like episodes. Ann Neurol 1991; 29: 601-5.

Hasselbalch SG, Holm S, Pedersen HS, Svarer C, Knudsen GM, Madsen PL, et al. The (18)F-fluorodeoxyglucose lumped constant determined in human brain from extraction fractions of (18)F-fluorodeoxyglucose and glucose. J Cereb Blood Flow Metab 2001; 21: 995-1002.

Hassinen M, Lakka TA, Hakola L, Savonen K, Komulainen P, Litmanen H, et al. Cardiorespiratory fitness and metabolic syndrome in older men and women: The dose responses to exercise training (DR's EXTRA) study. Diabetes Care 2010; 33: 1655-7.

Heddi A, Stepien G, Benke PJ, Wallace DC. Coordinate induction of energy gene expression in tissues of mitochondrial disease patients. J Biol Chem 1999; 274: 22968-76.

Heikkilä O, Mäkimattila S, Timonen M, Groop PH, Heikkinen S, Lundbom N. Cerebellar glucose during fasting and acute hyperglycemia in nondiabetic men and in men with type 1 diabetes. Cerebellum 2010; 9: 336-44.

Heikkilä O, Lundbom N, Timonen M, Groop PH, Heikkinen S, Mäkimattila S. Hyperglycaemia is associated with changes in the regional concentrations

of glucose and myo-inositol within the brain. Diabetologia 2009; 52: 534-40.

Helge JW, Stallknecht B, Richter EA, Galbo H, Kiens B. Muscle metabolism during graded quadriceps exercise in man. J Physiol 2007; 581: 1247-58.

Herrero P, Peterson LR, McGill JB, Matthew S, Lesniak D, Dence C, et al. Increased myocardial fatty acid metabolism in patients with type 1 diabetes mellitus. J Am Coll Cardiol 2006; 47: 598-604.

Hertz L, Peng L, Dienel GA. Energy metabolism in astrocytes: High rate of oxidative metabolism and spatiotemporal dependence on glycolysis/glycogenolysis. J Cereb Blood Flow Metab 2007; 27: 219-49.

Hirai M, Suzuki S, Onoda M, Hinokio Y, Hirai A, Ohtomo M, et al. Mitochondrial deoxyribonucleic acid 3256C-T mutation in a japanese family with noninsulin-dependent diabetes mellitus. J Clin Endocrinol Metab 1998; 83: 992-4.

Hirano M, Pavlakis SG. Mitochondrial myopathy, encephalopathy, lactic acidosis, and strokelike episodes (MELAS): Current concepts. J Child Neurol 1994; 9: 4-13.

Hirvonen J, Virtanen KA, Nummenmaa L, Hannukainen JC, Honka MJ, Bucci M, et al. Effects of insulin on brain glucose metabolism in impaired glucose tolerance. Diabetes 2011; 60: 443-7.

Hock MB, Kralli A. Transcriptional control of mitochondrial biogenesis and function. Annu Rev Physiol 2009; 71: 177-203.

Hoffstedt J, Arvidsson E, Sjolin E, Wahlen K, Arner P. Adipose tissue adiponectin production and adiponectin serum concentration in human obesity and insulin resistance. J Clin Endocrinol Metab 2004; 89: 1391-6.

Hollenbeck PJ, Saxton WM. The axonal transport of mitochondria. J Cell Sci 2005; 118: 5411-9.

Holloway GP, Bezaire V, Heigenhauser GJ, Tandon NN, Glatz JF, Luiken JJ, et al. Mitochondrial long chain fatty acid oxidation, fatty acid translocase/CD36 content and carnitine palmitoyltransferase I activity in human skeletal muscle during aerobic exercise. J Physiol 2006; 571: 201-10.

Holmes-Walker DJ, Ward GM, Boyages SC. Insulin secretion and insulin sensitivity are normal in non-diabetic subjects from maternal inheritance diabetes and deafness families. Diabet Med 2001; 18: 381-7.

Holmkvist J, Tojjar D, Almgren P, Lyssenko V, Lindgren CM, Isomaa B, et al. Polymorphisms in the gene encoding the voltage-dependent ca(2+) channel ca (V)2.3 (CACNA1E) are associated with type 2 diabetes and impaired insulin secretion. Diabetologia 2007; 50: 2467-75.

Holmkvist J, Cervin C, Lyssenko V, Winckler W, Anevski D, Cilio C, et al. Common variants in HNF-1 alpha and risk of type 2 diabetes. Diabetologia 2006; 49: 2882-91.

Holt IJ, Harding AE, Morgan-Hughes JA. Deletions of muscle mitochondrial DNA in patients with mitochondrial myopathies. Nature 1988; 331: 717-9.

Hosogai N, Fukuhara A, Oshima K, Miyata Y, Tanaka S, Segawa K, et al. Adipose tissue hypoxia in obesity and its impact on adipocytokine dysregulation. Diabetes 2007; 56: 901-11.

Hosszufalusi N, Karcagi V, Horvath R, Palik E, Varkonyi J, Rajczy K, et al. A detailed investigation of maternally inherited diabetes and deafness (MIDD) including clinical characteristics, C-peptide secretion, HLA-DR and -DQ status and autoantibody pattern. Diabetes Metab Res Rev 2009; 25: 127-35.

Hotta O, Inoue CN, Miyabayashi S, Furuta T, Takeuchi A, Taguma Y. Clinical and pathologic features of focal segmental glomerulosclerosis with mitochondrial tRNALeu(UUR) gene mutation. Kidney Int 2001; 59: 1236-43.

Howald H, Hoppeler H, Claassen H, Mathieu O, Straub R. Influences of endurance training on the ultrastructural composition of the different muscle fiber types in humans. Pflugers Arch 1985; 403: 369-76.

Howard BE, Ginsberg MD, Hassel WR, Lockwood AH, Freed P. On the uniqueness of cerebral blood flow measured by the in vivo autoradiographic strategy and positron emission tomography. J Cereb Blood Flow Metab 1983; 3: 432-41.

Huang SC, Carson RE, Hoffman EJ, Carson J, MacDonald N, Barrio JR, et al. Quantitative measurement of local cerebral blood flow in humans by positron computed tomography and 15O-water. J Cereb Blood Flow Metab 1983; 3: 141-53.

Hudson G, Keers S, Yu Wai Man P, Griffiths P, Huoponen K, Savontaus ML, et al. Identification of an X-chromosomal locus and haplotype modulating the phenotype of a mitochondrial DNA disorder. Am J Hum Genet 2005; 77: 1086-91.

Hudson G, Carelli V, Spruijt L, Gerards M, Mowbray C, Achilli A, et al. Clinical expression of leber hereditary optic neuropathy is affected by the mitochondrial DNA-haplogroup background. Am J Hum Genet 2007; 81: 228-33.

Huggins CE, Domenighetti AA, Ritchie ME, Khalil N, Favaloro JM, Proietto J, et al. Functional and metabolic remodelling in GLUT4-deficient hearts confers hyper-responsiveness to substrate intervention. J Mol Cell Cardiol 2008; 44: 270-80.

Huidekoper HH, Visser G, Ackermans MT, Sauerwein HP, Wijburg FA. A potential role for muscle in glucose homeostasis: In vivo kinetic studies in glycogen storage disease type 1a and fructose-1,6-bisphosphatase deficiency. J Inherit Metab Dis 2010; 33: 25-31.

Iida H, Kanno I, Miura S, Murakami M, Takahashi K, Uemura K. Error analysis of a quantitative cerebral blood flow measurement using H2(15)O autoradiography and positron emission tomography, with respect to the dispersion of the input function. J Cereb Blood Flow Metab 1986; 6: 536-45.

Iizuka T, Sakai F, Ide T, Miyakawa S, Sato M, Yoshii S. Regional cerebral blood flow and cerebrovascular reactivity during chronic stage of stroke-like episodes in MELAS -- implication of neurovascular cellular mechanism. J Neurol Sci 2007; 257: 126-38.

Iozzo P, Chareonthaitawee P, Di Terlizzi M, Betteridge DJ, Ferrannini E, Camici PG. Regional myocardial blood flow and glucose utilization during fasting and physiological hyperinsulinemia in humans. Am J Physiol Endocrinol Metab 2002; 282: E1163-71.

Iozzo P, Hällsten K, Oikonen V, Virtanen KA, Kemppainen J, Solin O, et al. Insulin-mediated hepatic glucose uptake is impaired in type 2 diabetes: Evidence for a relationship with glycemic control. J Clin Endocrinol Metab 2003; 88: 2055-60.

Iozzo P, Lautamäki R, Geisler F, Virtanen KA, Oikonen V, Haaparanta M, et al. Non-esterified fatty acids impair insulin-mediated glucose uptake and disposition in the liver. Diabetologia 2004; 47: 1149-56.

Iozzo P, Geisler F, Oikonen V, Mäki M, Takala T, Solin O, et al. Insulin stimulates liver glucose uptake in humans: An 18F-FDG PET study. J Nucl Med 2003a; 44: 682-9.

Iozzo P, Hällsten K, Oikonen V, Virtanen KA, Parkkola R, Kemppainen J, et al. Effects of metformin and rosiglitazone monotherapy on insulin-mediated hepatic glucose uptake and their relation to visceral fat in type 2 diabetes. Diabetes Care 2003b; 26: 2069-74.

Iozzo P, Järvisalo MJ, Kiss J, Borra R, Naum GA, Viljanen A, et al. Quantification of liver glucose metabolism by positron emission tomography: Validation study in pigs. Gastroenterology 2007; 132: 531-42.

Irimia JM, Meyer CM, Peper CL, Zhai L, Bock CB, Previs SF, et al. Impaired glucose tolerance and predisposition to the fasted state in liver glycogen synthase knock-out mice. J Biol Chem 2010; 285: 12851-61.

Ishihara H, Asano T, Tsukuda K, Katagiri H, Inukai K, Anai M, et al. Overexpression of hexokinase I but not GLUT1 glucose transporter alters concentration dependence of glucose-stimulated insulin secretion in pancreatic beta-cell line MIN6. J Biol Chem 1994; 269: 3081-7.

Ito H, Mori K, Harada M, Minato M, Naito E, Takeuchi M, et al. Serial brain imaging analysis of stroke-like episodes in MELAS. Brain Dev 2008; 30: 483-8.

Jain R, Lammert E. Cell-cell interactions in the endocrine pancreas. Diabetes Obes Metab 2009; 11 Suppl 4: 159-67.

James AM, Wei YH, Pang CY, Murphy MP. Altered mitochondrial function in fibroblasts containing MELAS or MERRF mitochondrial DNA mutations. Biochem J 1996; 318 (Pt 2): 401-7.

James DE, Brown R, Navarro J, Pilch PF. Insulin-regulatable tissues express a unique insulin-sensitive glucose transport protein. Nature 1988; 333: 183-5.

Janssen AJ, Schuelke M, Smeitink JA, Trijbels FJ, Sengers RC, Lucke B, et al. Muscle 3243A-->G mutation load and capacity of the mitochondrial energy-generating system. Ann Neurol 2008; 63: 473-81.

Jenssen T, Nurjhan N, Consoli A, Gerich JE. Failure of substrate-induced gluconeogenesis to increase overall glucose appearance in normal humans. demonstration of hepatic autoregulation without a change in plasma glucose concentration. J Clin Invest 1990; 86: 489-97.

Jenuth JP, Peterson AC, Fu K, Shoubridge EA. Random genetic drift in the female germline explains the rapid segregation of mammalian mitochondrial DNA. Nat Genet 1996; 14: 146-51.

Jeppesen TD, Orngreen MC, van Hall G, Haller RG, Vissing J. Fat metabolism during exercise in patients with mitochondrial disease. Arch Neurol 2009; 66: 365-70.

Jeppesen TD, Schwartz M, Frederiksen AL, Wibrand F, Olsen DB, Vissing J. Muscle phenotype and mutation load in 51 persons with the 3243A>G mitochondrial DNA mutation. Arch Neurol 2006; 63: 1701-6.

John GB, Shang Y, Li L, Renken C, Mannella CA, Selker JM, et al. The mitochondrial inner membrane

protein mitofilin controls cristae morphology. Mol Biol Cell 2005; 16: 1543-54.

Jones JR, Barrick C, Kim KA, Lindner J, Blondeau B, Fujimoto Y, et al. Deletion of PPARgamma in adipose tissues of mice protects against high fat diet-induced obesity and insulin resistance. Proc Natl Acad Sci U S A 2005; 102: 6207-12.

Kaaman M, Sparks LM, van Harmelen V, Smith SR, Sjolin E, Dahlman I, et al. Strong association between mitochondrial DNA copy number and lipogenesis in human white adipose tissue. Diabetologia 2007; 50: 2526-33.

Kaczmarczyk SJ, Andrikopoulos S, Favaloro J, Domenighetti AA, Dunn A, Ernst M, et al. Threshold effects of glucose transporter-4 (GLUT4) deficiency on cardiac glucose uptake and development of hypertrophy. J Mol Endocrinol 2003; 31: 449-59.

Kadowaki T, Yamauchi T, Kubota N, Hara K, Ueki K, Tobe K. Adiponectin and adiponectin receptors in insulin resistance, diabetes, and the metabolic syndrome. J Clin Invest 2006; 116: 1784-92.

Kaisti KK, Långsjö JW, Aalto S, Oikonen V, Sipilä H, Teräs M, et al. Effects of sevoflurane, propofol, and adjunct nitrous oxide on regional cerebral blood flow, oxygen consumption, and blood volume in humans. Anesthesiology 2003; 99: 603-13.

Kaneda H, Hayashi J, Takahama S, Taya C, Lindahl KF, Yonekawa H. Elimination of paternal mitochondrial DNA in intraspecific crosses during early mouse embryogenesis. Proc Natl Acad Sci U S A 1995; 92: 4542-6.

Karlsson HK, Ahlsen M, Zierath JR, Wallberg-Henriksson H, Koistinen HA. Insulin signaling and glucose transport in skeletal muscle from first-degree relatives of type 2 diabetic patients. Diabetes 2006; 55: 1283-8.

Karlsson HK, Hällsten K, Björnholm M, Tsuchida H, Chibalin AV, Virtanen KA, et al. Effects of metformin and rosiglitazone treatment on insulin signaling and glucose uptake in patients with newly diagnosed type 2 diabetes: A randomized controlled study. Diabetes 2005; 54: 1459-67.

Karmi A, Iozzo P, Viljanen A, Hirvonen J, Fielding BA, Virtanen K, et al. Increased brain fatty acid uptake in metabolic syndrome. Diabetes 2010; 59: 2171-7.

Kärppä M, Syrjälä P, Tolonen U, Majamaa K. Peripheral neuropathy in patients with the 3243A>G mutation in mitochondrial DNA. J Neurol 2003; 250: 216-21.

Kärppä M, Herva R, Moslemi AR, Oldfors A, Kakko S, Majamaa K. Spectrum of myopathic findings in 50 patients with the 3243A>G mutation in mitochondrial DNA. Brain 2005; 128: 1861-9.

Katulanda P, Groves CJ, Barrett A, Sheriff R, Matthews DR, McCarthy MI, et al. Prevalence and clinical characteristics of maternally inherited diabetes and deafness caused by the mt3243A > G mutation in young adult diabetic subjects in sri lanka. Diabet Med 2008; 25: 370-4.

Kaufmann P, Shungu DC, Sano MC, Jhung S, Engelstad K, Mitsis E, et al. Cerebral lactic acidosis correlates with neurological impairment in MELAS. Neurology 2004; 62: 1297-302.

Kaukonen J, Juselius JK, Tiranti V, Kyttälä A, Zeviani M, Comi GP, et al. Role of adenine nucleotide translocator 1 in mtDNA maintenance. Science 2000; 289: 782-5.

Kekäläinen P, Sarlund H, Pyorälä K, Laakso M. Hyperinsulinemia cluster predicts the development of type 2 diabetes independently of family history of diabetes. Diabetes Care 1999; 22: 86-92.

Kemppainen J, Fujimoto T, Kalliokoski KK, Viljanen T, Nuutila P, Knuuti J. Myocardial and skeletal muscle glucose uptake during exercise in humans. J Physiol 2002; 542: 403-12.

King MP, Koga Y, Davidson M, Schon EA. Defects in mitochondrial protein synthesis and respiratory chain activity segregate with the tRNA(leu(UUR)) mutation associated with mitochondrial myopathy, encephalopathy, lactic acidosis, and strokelike episodes. Mol Cell Biol 1992; 12: 480-90.

Kirino Y, Yasukawa T, Ohta S, Akira S, Ishihara K, Watanabe K, et al. Codon-specific translational defect caused by a wobble modification deficiency in mutant tRNA from a human mitochondrial disease. Proc Natl Acad Sci U S A 2004; 101: 15070-5.

Kirkman MA, Yu-Wai-Man P, Korsten A, Leonhardt M, Dimitriadis K, De Coo IF, et al. Gene-environment interactions in leber hereditary optic neuropathy. Brain 2009; 132: 2317-26.

Knuuti MJ, Mäki M, Yki-Järvinen H, Voipio-Pulkki LM, Härkonen R, Haaparanta M, et al. The effect of insulin and FFA on myocardial glucose uptake. J Mol Cell Cardiol 1995; 27: 1359-67.

Kollberg G, Tulinius M, Melberg A, Darin N, Andersen O, Holmgren D, et al. Clinical manifestation and a new ISCU mutation in iron-sulphur cluster deficiency myopathy. Brain 2009; 132: 2170-9.

Korenblat KM, Fabbrini E, Mohammed BS, Klein S. Liver, muscle, and adipose tissue insulin action is directly related to intrahepatic triglyceride content in obese subjects. Gastroenterology 2008; 134: 1369-75.

Korpelainen H. The evolutionary processes of mitochondrial and chloroplast genomes differ from those of nuclear genomes. Naturwissenschaften 2004; 91: 505-18.

Koskenvuo JW, Karra H, Lehtinen J, Niemi P, Pärkkä J, Knuuti J, et al. Cardiac MRI: Accuracy of simultaneous measurement of left and right ventricular parameters using three different sequences. Clin Physiol Funct Imaging 2007; 27: 385-93.

Kotronen A, Juurinen L, Tiikkainen M, Vehkavaara S, Yki-Järvinen H. Increased liver fat, impaired insulin clearance, and hepatic and adipose tissue insulin resistance in type 2 diabetes. Gastroenterology 2008; 135: 122-30.

Kraegen EW, James DE, Storlien LH, Burleigh KM, Chisholm DJ. In vivo insulin resistance in individual peripheral tissues of the high fat fed rat: Assessment by euglycaemic clamp plus deoxyglucose administration. Diabetologia 1986; 29: 192-8.

Kramer D, Shapiro R, Adler A, Bush E, Rondinone CM. Insulin-sensitizing effect of rosiglitazone (BRL-49653) by regulation of glucose transporters in muscle and fat of zucker rats. Metabolism 2001; 50: 1294-300.

Kraytsberg Y, Schwartz M, Brown TA, Ebralidse K, Kunz WS, Clayton DA, et al. Recombination of human mitochondrial DNA. Science 2004; 304: 981.

Kruse SE, Watt WC, Marcinek DJ, Kapur RP, Schenkman KA, Palmiter RD. Mice with mitochondrial complex I deficiency develop a fatal encephalomyopathy. Cell Metab 2008; 7: 312-20.

Kuroda S, Shiga T, Houkin K, Ishikawa T, Katoh C, Tamaki N, et al. Cerebral oxygen metabolism and neuronal integrity in patients with impaired vasoreactivity attributable to occlusive carotid artery disease. Stroke 2006; 37: 393-8.

Kurt B, Jaeken J, Van Hove J, Lagae L, Löfgren A, Everman DB, et al. A novel POLG gene mutation in 4 children with alpers-like hepatocerebral syndromes. Arch Neurol 2010; 67: 239-44.

Kuwabara Y, Ichiya Y, Ichimiya A, Sasaki M, Akashi Y, Yoshida T, et al. [The relationship between the cerebral blood flow, oxygen consumption and glucose metabolism in primary degenerative dementia]. Kaku Igaku 1995; 32: 253-62.

Laloi-Michelin M, Meas T, Ambonville C, Bellanne-Chantelot C, Beaufils S, Massin P, et al. The clinical variability of maternally inherited diabetes and deafness is associated with the degree of heteroplasmy in blood leukocytes. J Clin Endocrinol Metab 2009; 94: 3025-30.

LaManna JC, Salem N, Puchowicz M, Erokwu B, Koppaka S, Flask C, et al. Ketones suppress brain glucose consumption. Adv Exp Med Biol 2009; 645: 301-6.

Lamont BJ, Andrikopoulos S, Funkat A, Favaloro J, Ye JM, Kraegen EW, et al. Peripheral insulin resistance develops in transgenic rats overexpressing phosphoenolpyruvate carboxykinase in the kidney. Diabetologia 2003; 46: 1338-47.

Landau BR. Methods for measuring glycogen cycling. Am J Physiol Endocrinol Metab 2001; 281: E413-9.

Långsjö JW, Kaisti KK, Aalto S, Hinkka S, Aantaa R, Oikonen V, et al. Effects of subanesthetic doses of ketamine on regional cerebral blood flow, oxygen consumption, and blood volume in humans. Anesthesiology 2003; 99: 614-23.

Långsjö JW, Maksimow A, Salmi E, Kaisti K, Aalto S, Oikonen V, et al. S-ketamine anesthesia increases cerebral blood flow in excess of the metabolic needs in humans. Anesthesiology 2005; 103: 258-68.

Larsson NG, Wang J, Wilhelmsson H, Oldfors A, Rustin P, Lewandoski M, et al. Mitochondrial transcription factor A is necessary for mtDNA maintenance and embryogenesis in mice. Nat Genet 1998; 18: 231-6.

Laye MJ, Rector RS, Warner SO, Naples SP, Perretta AL, Uptergrove GM, et al. Changes in visceral adipose tissue mitochondrial content with type 2 diabetes and daily voluntary wheel running in OLETF rats. J Physiol 2009; 587: 3729-39.

Lefebvre AM, Laville M, Vega N, Riou JP, van Gaal L, Auwerx J, et al. Depot-specific differences in adipose tissue gene expression in lean and obese subjects. Diabetes 1998; 47: 98-103.

Li H, Wang J, Wilhelmsson H, Hansson A, Thoren P, Duffy J, et al. Genetic modification of survival in tissue-specific knockout mice with mitochondrial cardiomyopathy. Proc Natl Acad Sci U S A 2000; 97: 3467-72.

Li J, Cai T, Wu P, Cui Z, Chen X, Hou J, et al. Proteomic analysis of mitochondria from caenorhabditis elegans. Proteomics 2009; 9: 4539-53.

Li R, Guan MX. Human mitochondrial leucyl-tRNA synthetase corrects mitochondrial dysfunctions due to the tRNALeu(UUR) A3243G mutation, associated with mitochondrial encephalomyopathy, lactic

acidosis, and stroke-like symptoms and diabetes. Mol Cell Biol 2010; 30: 2147-54.

Li S, Brown MS, Goldstein JL. Bifurcation of insulin signaling pathway in rat liver: MTORC1 required for stimulation of lipogenesis, but not inhibition of gluconeogenesis. Proc Natl Acad Sci U S A 2010; 107: 3441-6.

Liang WS, Reiman EM, Valla J, Dunckley T, Beach TG, Grover A, et al. Alzheimer's disease is associated with reduced expression of energy metabolism genes in posterior cingulate neurons. Proc Natl Acad Sci U S A 2008; 105: 4441-6.

Lillioja S, Mott DM, Spraul M, Ferraro R, Foley JE, Ravussin E, et al. Insulin resistance and insulin secretory dysfunction as precursors of non-insulin-dependent diabetes mellitus. prospective studies of pima indians. N Engl J Med 1993; 329: 1988-92.

Limongelli A, Schaefer J, Jackson S, Invernizzi F, Kirino Y, Suzuki T, et al. Variable penetrance of a familial progressive necrotising encephalopathy due to a novel tRNA(ile) homoplasmic mutation in the mitochondrial genome. J Med Genet 2004; 41: 342-9.

Limongelli G, Tome-Esteban M, Dejthevaporn C, Rahman S, Hanna MG, Elliott PM. Prevalence and natural history of heart disease in adults with primary mitochondrial respiratory chain disease. Eur J Heart Fail 2010; 12: 114-21.

Lin J, Wu H, Tarr PT, Zhang CY, Wu Z, Boss O, et al. Transcriptional co-activator PGC-1 alpha drives the formation of slow-twitch muscle fibres. Nature 2002; 418: 797-801.

Lindsay RS, Funahashi T, Hanson RL, Matsuzawa Y, Tanaka S, Tataranni PA, et al. Adiponectin and development of type 2 diabetes in the pima indian population. Lancet 2002; 360: 57-8.

Litonin D, Sologub M, Shi Y, Savkina M, Anikin M, Falkenberg M, et al. Human mitochondrial transcription revisited: Only TFAM and TFB2M are required for transcription of the mitochondrial genes in vitro. J Biol Chem 2010; 285: 18129-33.

Lodi R, Rajagopalan B, Blamire AM, Crilley JG, Styles P, Chinnery PF. Abnormal cardiac energetics in patients carrying the A3243G mtDNA mutation measured in vivo using phosphorus MR spectroscopy. Biochim Biophys Acta 2004; 1657: 146-50.
Loeffen J, Smeets R, Smeitink J, Triepels R, Sengers R, Trijbels F, et al. The human NADH: Ubiquinone oxidoreductase NDUFS5 (15 kDa) subunit: CDNA cloning, chromosomal localization, tissue distribution and the absence of mutations in isolated complex I-deficient patients. J Inherit Metab Dis 1999; 22: 19-28.

Loeffen J, Smeets R, Smeitink J, Ruitenbeek W, Janssen A, Mariman E, et al. The X-chromosomal NDUFA1 gene of complex I in mitochondrial encephalomyopathies: Tissue expression and mutation detection. J Inherit Metab Dis 1998a; 21: 210-5.

Loeffen J, Smeitink J, Triepels R, Smeets R, Schuelke M, Sengers R, et al. The first nuclear-encoded complex I mutation in a patient with leigh syndrome. Am J Hum Genet 1998b; 63: 1598-608.

Loiseau D, Chevrollier A, Verny C, Guillet V, Gueguen N, Pou de Crescenzo MA, et al. Mitochondrial coupling defect in charcot-marie-tooth type 2A disease. Ann Neurol 2007; 61: 315-23.

Lopez LC, Schuelke M, Quinzii CM, Kanki T, Rodenburg RJ, Naini A, et al. Leigh syndrome with nephropathy and CoQ10 deficiency due to decaprenyl diphosphate synthase subunit 2 (PDSS2) mutations. Am J Hum Genet 2006; 79: 1125-9.

Lorini R, Klersy C, d'Annunzio G, Massa O, Minuto N, Iafusco D, et al. Maturity-onset diabetes of the young in children with incidental hyperglycemia: A multicenter italian study of 172 families. Diabetes Care 2009; 32: 1864-6.

Love-Gregory LD, Wasson J, Ma J, Jin CH, Glaser B, Suarez BK, et al. A common polymorphism in the upstream promoter region of the hepatocyte nuclear factor-4 alpha gene on chromosome 20q is associated with type 2 diabetes and appears to contribute to the evidence for linkage in an ashkenazi jewish population. Diabetes 2004; 53: 1134-40.

Luft R, Ikkos D, Palmieri G, Ernster L, Afzelius B. A case of severe hypermetabolism of nonthyroid origin with a defect in the maintenance of mitochondrial respiratory control: A correlated clinical, biochemical, and morphological study. J Clin Invest 1962; 41: 1776-804.

Lutz AJ, Pardridge WM. Insulin therapy normalizes GLUT1 glucose transporter mRNA but not immunoreactive transporter protein in streptozocin-diabetic rats. Metabolism 1993; 42: 939-44.

Lyssenko V, Jonsson A, Almgren P, Pulizzi N, Isomaa B, Tuomi T, et al. Clinical risk factors, DNA variants, and the development of type 2 diabetes. N Engl J Med 2008; 359: 2220-32.

Maassen JA, 'T Hart LM, Van Essen E, Heine RJ, Nijpels G, Jahangir Tafrechi RS, et al. Mitochondrial diabetes: Molecular mechanisms and clinical presentation. Diabetes 2004; 53 Suppl 1: S103-9.

Maddison R, Mhurchu CN, Jiang Y, Hoorn SV, Rodgers A, Lawes CMM, et al. International physical activity questionnaire (IPAQ) and new zealand physical activity questionnaire (NZPAQ): A doubly

labelled water validation. International Journal of Behavioral Nutrition and Physical Activity 2007; 4.

Magen D, Georgopoulos C, Bross P, Ang D, Segev Y, Goldsher D, et al. Mitochondrial hsp60 chaperonopathy causes an autosomal-recessive neurodegenerative disorder linked to brain hypomyelination and leukodystrophy. Am J Hum Genet 2008; 83: 30-42.

Majamaa K, Moilanen JS, Uimonen S, Remes AM, Salmela PI, Kärppä M, et al. Epidemiology of A3243G, the mutation for mitochondrial encephalomyopathy, lactic acidosis, and strokelike episodes: Prevalence of the mutation in an adult population. Am J Hum Genet 1998; 63: 447-54.

Majamaa-Voltti K, Turkka J, Kortelainen ML, Huikuri H, Majamaa K. Causes of death in pedigrees with the 3243A>G mutation in mitochondrial DNA. J Neurol Neurosurg Psychiatry 2008; 79: 209-11.

Majamaa-Voltti K, Peuhkurinen K, Kortelainen ML, Hassinen IE, Majamaa K. Cardiac abnormalities in patients with mitochondrial DNA mutation 3243A>G. BMC Cardiovasc Disord 2002; 2: 12.

Majamaa-Voltti KA, Winqvist S, Remes AM, Tolonen U, Pyhtinen J, Uimonen S, et al. A 3-year clinical follow-up of adult patients with 3243A>G in mitochondrial DNA. Neurology 2006; 66: 1470-5.

Mäkelä-Bengs P, Suomalainen A, Majander A, Rapola J, Kalimo H, Nuutila A, et al. Correlation between the clinical symptoms and the proportion of mitochondrial DNA carrying the 8993 point mutation in the NARP syndrome. Pediatr Res 1995; 37: 634-9.

Mäki MT, Haaparanta M, Nuutila P, Oikonen V, Luotolahti M, Eskola O, et al. Free fatty acid uptake in the myocardium and skeletal muscle using fluorine-18-fluoro-6-thia-heptadecanoic acid. J Nucl Med 1998; 39: 1320-7.

Malfatti E, Bugiani M, Invernizzi F, de Souza CF, Farina L, Carrara F, et al. Novel mutations of ND genes in complex I deficiency associated with mitochondrial encephalopathy. Brain 2007; 130: 1894-904.

Man PY, Griffiths PG, Brown DT, Howell N, Turnbull DM, Chinnery PF. The epidemiology of leber hereditary optic neuropathy in the north east of england. Am J Hum Genet 2003; 72: 333-9.

Mandarino LJ, Printz RL, Cusi KA, Kinchington P, O'Doherty RM, Osawa H, et al. Regulation of hexokinase II and glycogen synthase mRNA, protein, and activity in human muscle. Am J Physiol 1995; 269: E701-8.

Mandel H, Szargel R, Labay V, Elpeleg O, Saada A, Shalata A, et al. The deoxyguanosine kinase gene is mutated in individuals with depleted hepatocerebral mitochondrial DNA. Nat Genet 2001; 29: 337-41.

Manwaring N, Jones MM, Wang JJ, Rochtchina E, Howard C, Mitchell P, et al. Population prevalence of the MELAS A3243G mutation. Mitochondrion 2007; 7: 230-3.

Mao CC, Holt IJ. Clinical and molecular aspects of diseases of mitochondrial DNA instability. Chang Gung Med J 2009; 32: 354-69.

Marchington DR, Scott Brown MS, Lamb VK, van Golde RJ, Kremer JA, Tuerlings JH, et al. No evidence for paternal mtDNA transmission to offspring or extra-embryonic tissues after ICSI. Mol Hum Reprod 2002; 8: 1046-9.

Mari A, Tura A, Gastaldelli A, Ferrannini E. Assessing insulin secretion by modeling in multiple-meal tests - role of potentiation. Diabetes 2002; 51: S221-6.

Mari A, Tura A, Pacini G, Kautzky-Willer A, Ferrannini E. Relationships between insulin secretion after intravenous and oral glucose administration in subjects with glucose tolerance ranging from normal to overt diabetes. Diabet Med 2008; 25: 671-7.

Mari A, Pacini G, Murphy E, Ludvik B, Nolan JJ. A model-based method for assessing insulin sensitivity from the oral glucose tolerance test. Diabetes Care 2001; 24: 539-48.

Mari A, Tura A, Natali A, Laville M, Laakso M, Gabriel R, et al. Impaired beta cell glucose sensitivity rather than inadequate compensation for insulin resistance is the dominant defect in glucose intolerance. Diabetologia 2010; 53: 749-56.

Mariot P, Gilon P, Nenquin M, Henquin JC. Tolbutamide and diazoxide influence insulin secretion by changing the concentration but not the action of cytoplasmic Ca2+ in beta-cells. Diabetes 1998; 47: 365-73.

Mariotti C, Savarese N, Suomalainen A, Rimoldi M, Comi G, Prelle A, et al. Genotype to phenotype correlations in mitochondrial encephalomyopathies associated with the A3243G mutation of mitochondrial DNA. J Neurol 1995; 242: 304-12.

Martikainen MH, Rönnemaa T, Majamaa K. Prevalence of mitochondrial diabetes in southwestern finland: A molecular epidemiological study. Acta Diabetol 2012.

Martin BC, Warram JH, Krolewski AS, Bergman RN, Soeldner JS, Kahn CR. Role of glucose and insulin resistance in development of type 2 diabetes mellitus:

Results of a 25-year follow-up study. Lancet 1992; 340: 925-9.

Massillon D, Chen W, Hawkins M, Liu R, Barzilai N, Rossetti L. Quantitation of hepatic glucose fluxes and pathways of hepatic glycogen synthesis in conscious mice. Am J Physiol 1995; 269: E1037-43.

Massin P, Dubois-Laforgue D, Meas T, Laloi-Michelin M, Gin H, Bauduceau B, et al. Retinal and renal complications in patients with a mutation of mitochondrial DNA at position 3,243 (maternally inherited diabetes and deafness). A case-control study. Diabetologia 2008; 51: 1664-70.

McFarland R, Clark KM, Morris AA, Taylor RW, Macphail S, Lightowlers RN, et al. Multiple neonatal deaths due to a homoplasmic mitochondrial DNA mutation. Nat Genet 2002; 30: 145-6.

Mehrazin M, Shanske S, Kaufmann P, Wei Y, Coku J, Engelstad K, et al. Longitudinal changes of mtDNA A3243G mutation load and level of functioning in MELAS. Am J Med Genet A 2009; 149A: 584-7.

Meriläinen PT. A fast differential paramagnetic O2-sensor. Int J Clin Monit Comput 1988; 5: 187-95.

Meriläinen PT. Metabolic monitor. Int J Clin Monit Comput 1987; 4: 167-77.

Meyer C, Woerle HJ, Dostou JM, Welle SL, Gerich JE. Abnormal renal, hepatic, and muscle glucose metabolism following glucose ingestion in type 2 diabetes. Am J Physiol Endocrinol Metab 2004; 287: E1049-56.

Mineri R, Pavelka N, Fernandez-Vizarra E, Ricciardi-Castagnoli P, Zeviani M, Tiranti V. How do human cells react to the absence of mitochondrial DNA? PLoS One 2009; 4: e5713.

Moberg E, Sjöberg S, Hagström-Toft E, Bolinder J. No apparent suppression by insulin of in vivo skeletal muscle lipolysis in nonobese women. Am J Physiol Endocrinol Metab 2002; 283: E295-301.

Molina AJ, Wikström JD, Stiles L, Las G, Mohamed H, Elorza A, et al. Mitochondrial networking protects beta-cells from nutrient-induced apoptosis. Diabetes 2009; 58: 2303-15.

Molnar MJ, Valikovics A, Molnar S, Tron L, Dioszeghy P, Mechler F, et al. Cerebral blood flow and glucose metabolism in mitochondrial disorders. Neurology 2000; 55: 544-8.

Monnot S, Serre V, Chadefaux-Vekemans B, Aupetit J, Romano S, De Lonlay P, et al. Structural insights on pathogenic effects of novel mutations causing pyruvate carboxylase deficiency. Hum Mutat 2009; 30: 734-40.

Moore MC, Satake S, Lautz M, Soleimanpour SA, Neal DW, Smith M, et al. Nonesterified fatty acids and hepatic glucose metabolism in the conscious dog. Diabetes 2004; 53: 32-40.

Mootha VK, Arai AE, Balaban RS. Maximum oxidative phosphorylation capacity of the mammalian heart. Am J Physiol 1997; 272: H769-75.

Mootha VK, Bunkenborg J, Olsen JV, Hjerrild M, Wisniewski JR, Stahl E, et al. Integrated analysis of protein composition, tissue diversity, and gene regulation in mouse mitochondria. Cell 2003; 115: 629-40.

Moran A, Jacobs DR,Jr, Steinberger J, Steffen LM, Pankow JS, Hong CP, et al. Changes in insulin resistance and cardiovascular risk during adolescence: Establishment of differential risk in males and females. Circulation 2008; 117: 2361-8.

Moslemi AR, Tulinius M, Holme E, Oldfors A. Threshold expression of the tRNA(lys) A8344G mutation in single muscle fibres. Neuromuscul Disord 1998; 8: 345-9.

Nagano AS, Ito K, Kato T, Arahata Y, Kachi T, Hatano K, et al. Extrastriatal mean regional uptake of fluorine-18-FDOPA in the normal aged brain--an approach using MRI-aided spatial normalization 1 149 346. Neuroimage 2000; 11: 760-6.

Naini AB, Lu J, Kaufmann P, Bernstein RA, Mancuso M, Bonilla E, et al. Novel mitochondrial DNA ND5 mutation in a patient with clinical features of MELAS and MERRF. Arch Neurol 2005; 62: 473-6.

Narbonne H, Paquis-Fluckinger V, Valero R, Heyries L, Pellissier JF, Vialettes B. Gastrointestinal tract symptoms in maternally inherited diabetes and deafness (MIDD). Diabetes Metab 2004; 30: 61-6.

Nariai T, Ohno K, Ohta Y, Hirakawa K, Ishii K, Senda M. Discordance between cerebral oxygen and glucose metabolism, and hemodynamics in a mitochondrial encephalomyopathy, lactic acidosis, and strokelike episode patient. J Neuroimaging 2001; 11: 325-9.

Nass S, Nass MM. Intramitochondrial fibers with dna characteristics. ii. enzymatic and other hydrolytic treatments. J Cell Biol 1963; 19: 613-29.

Natali A, Muscelli E, Mari A, Balkau B, Walker M, Tura A, et al. Insulin sensitivity and beta-cell function in the offspring of type 2 diabetic patients: Impact of line of inheritance. J Clin Endocrinol Metab 2010; 95: 4703-11.

Naviaux RK, Nguyen KV. POLG mutations associated with alpers' syndrome and mitochondrial DNA depletion. Ann Neurol 2004; 55: 706-12.

Neglia D, De Caterina A, Marraccini P, Natali A, Ciardetti M, Vecoli C, et al. Impaired myocardial metabolic reserve and substrate selection flexibility during stress in patients with idiopathic dilated cardiomyopathy. Am J Physiol Heart Circ Physiol 2007; 293: H3270-8.

Newman JM, Ross RM, Richards SM, Clark MG, Rattigan S. Insulin and contraction increase nutritive blood flow in rat muscle in vivo determined by microdialysis of L-[14C]glucose. J Physiol 2007; 585: 217-29.

Ng CK, Soufer R, McNulty PH. Effect of hyperinsulinemia on myocardial fluorine-18-FDG uptake. J Nucl Med 1998; 39: 379-83.

Nikoskelainen EK, Savontaus ML, Huoponen K, Antila K, Hartiala J. Pre-excitation syndrome in leber's hereditary optic neuropathy. Lancet 1994; 344: 857-8.

Nishimura Y, Yoshinari T, Naruse K, Yamada T, Sumi K, Mitani H, et al. Active digestion of sperm mitochondrial DNA in single living sperm revealed by optical tweezers. Proc Natl Acad Sci U S A 2006; 103: 1382-7.

Nuutila P, Knuuti MJ, Raitakari M, Ruotsalainen U, Teräs M, Voipio-Pulkki LM, et al. Effect of antilipolysis on heart and skeletal muscle glucose uptake in overnight fasted humans. Am J Physiol 1994; 267: E941-6.

Nuutila P, Mäki M, Laine H, Knuuti MJ, Ruotsalainen U, Luotolahti M, et al. Insulin action on heart and skeletal muscle glucose uptake in essential hypertension. J Clin Invest 1995; 96: 1003-9.

Nuutila P, Knuuti J, Ruotsalainen U, Koivisto VA, Eronen E, Teräs M, et al. Insulin resistance is localized to skeletal but not heart muscle in type 1 diabetes. Am J Physiol 1993; 264: E756-62.

Nuutila P, Koivisto VA, Knuuti J, Ruotsalainen U, Teras M, Haaparanta M, et al. Glucose-free fatty acid cycle operates in human heart and skeletal muscle in vivo. J Clin Invest 1992; 89: 1767-74.

Ohshita T, Oka M, Imon Y, Watanabe C, Katayama S, Yamaguchi S, et al. Serial diffusion-weighted imaging in MELAS. Neuroradiology 2000; 42: 651-6.

Oka Y, Katagiri H, Ishihara H, Asano T, Kobayashi T, Kikuchi M. Beta-cell loss and glucose induced signalling defects in diabetes mellitus caused by mitochondrial tRNALeu(UUR) gene mutation. Diabet Med 1996; 13: S98-102.

Okajima Y, Tanabe Y, Takayanagi M, Aotsuka H. A follow up study of myocardial involvement in patients with mitochondrial encephalomyopathy, lactic acidosis, and stroke-like episodes (MELAS). Heart 1998; 80: 292-5.

Okamoto Y, Ogawa W, Nishizawa A, Inoue H, Teshigawara K, Kinoshita S, et al. Restoration of glucokinase expression in the liver normalizes postprandial glucose disposal in mice with hepatic deficiency of PDK1. Diabetes 2007; 56: 1000-9.

Okazawa H, Yamauchi H, Sugimoto K, Takahashi M, Toyoda H, Kishibe Y, et al. Quantitative comparison of the bolus and steady-state methods for measurement of cerebral perfusion and oxygen metabolism: Positron emission tomography study using 15O-gas and water. J Cereb Blood Flow Metab 2001; 21: 793-803.

Ong SB, Hausenloy DJ. Mitochondrial morphology and cardiovascular disease. Cardiovasc Res 2010; 88: 16-29.

Ortmeyer HK, Bodkin NL, Hansen BC. Insulin regulates liver glycogen synthase and glycogen phosphorylase activity reciprocally in rhesus monkeys. Am J Physiol 1997; 272: E133-8.

Ostergard T, Andersen JL, Nyholm B, Lund S, Nair KS, Saltin B, et al. Impact of exercise training on insulin sensitivity, physical fitness, and muscle oxidative capacity in first-degree relatives of type 2 diabetic patients. Am J Physiol Endocrinol Metab 2006; 290: E998-1005.

Otabe S, Yasuda K, Mori Y, Shimokawa K, Kadowaki H, Jimi A, et al. Molecular and histological evaluation of pancreata from patients with a mitochondrial gene mutation associated with impaired insulin secretion. Biochem Biophys Res Commun 1999; 259: 149-56.

Otabe S, Sakura H, Shimokawa K, Mori Y, Kadowaki H, Yasuda K, et al. The high prevalence of the diabetic patients with a mutation in the mitochondrial gene in japan. J Clin Endocrinol Metab 1994; 79: 768-71.

Pagliassotti MJ, Moore MC, Neal DW, Cherrington AD. Insulin is required for the liver to respond to intraportal glucose delivery in the conscious dog. Diabetes 1992; 41: 1247-56.

Pallotti F, Baracca A, Hernandez-Rosa E, Walker WF, Solaini G, Lenaz G, et al. Biochemical analysis of respiratory function in cybrid cell lines harbouring mitochondrial DNA mutations. Biochem J 2004; 384: 287-93.

Pan JW, Rothman TL, Behar KL, Stein DT, Hetherington HP. Human brain beta-hydroxybutyrate and lactate increase in fasting-induced ketosis. J Cereb Blood Flow Metab 2000; 20: 1502-7.

Parini R, Furlan F, Notarangelo L, Spinazzola A, Uziel G, Strisciuglio P, et al. Glucose metabolism and diet-based prevention of liver dysfunction in MPV17 mutant patients. J Hepatol 2009; 50: 215-21.

Park KS, Wiederkehr A, Kirkpatrick C, Mattenberger Y, Martinou JC, Marchetti P, et al. Selective actions of mitochondrial fission/fusion genes on metabolism-secretion coupling in insulin-releasing cells. J Biol Chem 2008a; 283: 33347-56.

Park KS, Chan JC, Chuang LM, Suzuki S, Araki E, Nanjo K, et al. A mitochondrial DNA variant at position 16189 is associated with type 2 diabetes mellitus in asians. Diabetologia 2008b; 51: 602-8.

Park SY, Choi GH, Choi HI, Ryu J, Jung CY, Lee W. Calorie restriction improves whole-body glucose disposal and insulin resistance in association with the increased adipocyte-specific GLUT4 expression in otsuka long-evans tokushima fatty rats. Arch Biochem Biophys 2005; 436: 276-84.

Parsons TJ, Muniec DS, Sullivan K, Woodyatt N, Alliston-Greiner R, Wilson MR, et al. A high observed substitution rate in the human mitochondrial DNA control region. Nat Genet 1997; 15: 363-8.

Pascual JM, Van Heertum RL, Wang D, Engelstad K, De Vivo DC. Imaging the metabolic footprint of Glut1 deficiency on the brain. Ann Neurol 2002; 52: 458-64.

Patlak CS, Blasberg RG. Graphical evaluation of blood-to-brain transfer constants from multiple-time uptake data. generalizations. J Cereb Blood Flow Metab 1985; 5: 584-90.

Patti ME, Corvera S. The role of mitochondria in the pathogenesis of type 2 diabetes. Endocr Rev 2010; 31: 364-95.

Paulson OB, Hasselbalch SG, Rostrup E, Knudsen GM, Pelligrino D. Cerebral blood flow response to functional activation. J Cereb Blood Flow Metab 2010; 30: 2-14.

Pavlakis SG, Phillips PC, DiMauro S, De Vivo DC, Rowland LP. Mitochondrial myopathy, encephalopathy, lactic acidosis, and strokelike episodes: A distinctive clinical syndrome. Ann Neurol 1984; 16: 481-8.

Pearson ER, Flechtner I, Njolstad PR, Malecki MT, Flanagan SE, Larkin B, et al. Switching from insulin to oral sulfonylureas in patients with diabetes due to Kir6.2 mutations. N Engl J Med 2006; 355: 467-77.

Peltoniemi P, Yki-Järvinen H, Oikonen V, Oksanen A, Takala TO, Rönnemaa T, et al. Resistance to exercise-induced increase in glucose uptake during hyperinsulinemia in insulin-resistant skeletal muscle of patients with type 1 diabetes. Diabetes 2001; 50: 1371-7.

Peltoniemi P, Lönnroth P, Laine H, Oikonen V, Tolvanen T, Grönroos T, et al. Lumped constant for [(18)F]fluorodeoxyglucose in skeletal muscles of obese and nonobese humans. Am J Physiol Endocrinol Metab 2000; 279: E1122-30.

Perry JR, Frayling TM. New gene variants alter type 2 diabetes risk predominantly through reduced beta-cell function. Curr Opin Clin Nutr Metab Care 2008; 11: 371-7.

Perseghin G, Lattuada G, Danna M, Sereni LP, Maffi P, De Cobelli F, et al. Insulin resistance, intramyocellular lipid content, and plasma adiponectin in patients with type 1 diabetes. Am J Physiol Endocrinol Metab 2003; 285: E1174-81.

Perseghin G, Lattuada G, De Cobelli F, Esposito A, Costantino F, Canu T, et al. Reduced intrahepatic fat content is associated with increased whole-body lipid oxidation in patients with type 1 diabetes. Diabetologia 2005; 48: 2615-21.

Petersen KF, Price TB, Bergeron R. Regulation of net hepatic glycogenolysis and gluconeogenesis during exercise: Impact of type 1 diabetes. J Clin Endocrinol Metab 2004a; 89: 4656-64.

Petersen KF, Dufour S, Befroy D, Garcia R, Shulman GI. Impaired mitochondrial activity in the insulin-resistant offspring of patients with type 2 diabetes. N Engl J Med 2004b; 350: 664-71.

Petersen KF, Cline GW, Gerard DP, Magnusson I, Rothman DL, Shulman GI. Contribution of net hepatic glycogen synthesis to disposal of an oral glucose load in humans. Metabolism 2001; 50: 598-601.

Peterson LR, Herrero P, McGill J, Schechtman KB, Kisrieva-Ware Z, Lesniak D, et al. Fatty acids and insulin modulate myocardial substrate metabolism in humans with type 1 diabetes. Diabetes 2008; 57: 32-40.

Peterson LR, Herrero P, Schechtman KB, Racette SB, Waggoner AD, Kisrieva-Ware Z, et al. Effect of obesity and insulin resistance on myocardial substrate metabolism and efficiency in young women. Circulation 2004; 109: 2191-6.

Petrova-Benedict R, Robinson BH, Stacey TE, Mistry J, Chalmers RA. Deficient fumarase activity in an infant with fumaricacidemia and its distribution between the different forms of the enzyme seen on isoelectric focusing. Am J Hum Genet 1987; 40: 257-66.

Phielix E, Schrauwen-Hinderling VB, Mensink M, Lenaers E, Meex R, Hoeks J, et al. Lower intrinsic ADP-stimulated mitochondrial respiration underlies in vivo mitochondrial dysfunction in muscle of male type 2 diabetic patients. Diabetes 2008; 57: 2943-9.

Pich S, Bach D, Briones P, Liesa M, Camps M, Testar X, et al. The charcot-marie-tooth type 2A gene product, Mfn2, up-regulates fuel oxidation through expression of OXPHOS system. Hum Mol Genet 2005; 14: 1405-15.

Pierron D, Chang I, Arachiche A, Heiske M, Thomas O, Borlin M, et al. Mutation rate switch inside eurasian mitochondrial haplogroups: Impact of selection and consequences for dating settlement in europe. PLoS One 2011; 6: e21543.

Pietiläinen KH, Naukkarinen J, Rissanen A, Saharinen J, Ellonen P, Keränen H, et al. Global transcript profiles of fat in monozygotic twins discordant for BMI: Pathways behind acquired obesity. PLoS Med 2008; 5: e51.

Plecita-Hlavata L, Lessard M, Santorova J, Bewersdorf J, Jezek P. Mitochondrial oxidative phosphorylation and energetic status are reflected by morphology of mitochondrial network in INS-1E and HEP-G2 cells viewed by 4Pi microscopy. Biochim Biophys Acta 2008; 1777: 834-46.

Pohjoismäki JL, Goffart S, Tyynismaa H, Willcox S, Ide T, Kang D, et al. Human heart mitochondrial DNA is organized in complex catenated networks containing abundant four-way junctions and replication forks. J Biol Chem 2009; 284: 21446-57.

Pohjoismäki JL, Holmes JB, Wood SR, Yang MY, Yasukawa T, Reyes A, et al. Mammalian mitochondrial DNA replication intermediates are essentially duplex but contain extensive tracts of RNA/DNA hybrid. J Mol Biol 2010; 397: 1144-55.

Pospisilik JA, Knauf C, Joza N, Benit P, Orthofer M, Cani PD, et al. Targeted deletion of AIF decreases mitochondrial oxidative phosphorylation and protects from obesity and diabetes. Cell 2007; 131: 476-91.

Postic C, Shiota M, Niswender KD, Jetton TL, Chen Y, Moates JM, et al. Dual roles for glucokinase in glucose homeostasis as determined by liver and pancreatic beta cell-specific gene knock-outs using cre recombinase. J Biol Chem 1999; 274: 305-15.

Poulton J, Deadman ME, Gardiner RM. Duplications of mitochondrial DNA in mitochondrial myopathy. Lancet 1989; 1: 236-40.

Poulton J, Brown MS, Cooper A, Marchington DR, Phillips DI. A common mitochondrial DNA variant is associated with insulin resistance in adult life. Diabetologia 1998; 41: 54-8.

Powers WJ, Videen TO, Markham J, Black KJ, Golchin N, Perlmutter JS. Cerebral mitochondrial metabolism in early parkinson's disease J Cereb Blood Flow Metab 2008; 28: 1754-60.

Powers WJ, Videen TO, Markham J, McGee-Minnich L, Antenor-Dorsey JV, Hershey T, et al. Selective defect of in vivo glycolysis in early huntington's disease striatum. Proc Natl Acad Sci U S A 2007; 104: 2945-9.

Probst I, Hartmann H, Jungermann K, Creutzfeldt W. Insulin-like action of proinsulin on rat liver carbohydrate metabolism in vitro. Diabetes 1985; 34: 415-9.

Provencher SW. Estimation of metabolite concentrations from localized in vivo proton NMR spectra. Magn Reson Med 1993; 30: 672-9.

Puhakainen I, Yki-Järvinen H. Inhibition of lipolysis decreases lipid oxidation and gluconeogenesis from lactate but not fasting hyperglycemia or total hepatic glucose production in NIDDM. Diabetes 1993; 42: 1694-9.

Pulkes T, Eunson L, Patterson V, Siddiqui A, Wood NW, Nelson IP, et al. The mitochondrial DNA G13513A transition in ND5 is associated with a LHON/MELAS overlap syndrome and may be a frequent cause of MELAS. Ann Neurol 1999; 46: 916-9.

Puomila A, Hämäläinen P, Kivioja S, Savontaus ML, Koivumäki S, Huoponen K, et al. Epidemiology and penetrance of leber hereditary optic neuropathy in finland. Eur J Hum Genet 2007; 15: 1079-89.

Pysh JJ, Khan T. Variations in mitochondrial structure and content of neurons and neuroglia in rat brain: An electron microscopic study. Brain Res 1972; 36: 1-18.

Quesada I, Villalobos C, Nunez L, Chamero P, Alonso MT, Nadal A, et al. Glucose induces synchronous mitochondrial calcium oscillations in intact pancreatic islets. Cell Calcium 2008; 43: 39-47.

Raitakari OT, Porkka KV, Rönnemaa T, Knip M, Uhari M, Åkerblom HK, et al. The role of insulin in clustering of serum lipids and blood pressure in children and adolescents. the cardiovascular risk in young finns study. Diabetologia 1995; 38: 1042-50.

Rajasimha HK, Chinnery PF, Samuels DC. Selection against pathogenic mtDNA mutations in a stem cell population leads to the loss of the 3243A-->G mutation in blood. Am J Hum Genet 2008; 82: 333-43.

Rantanen A, Jansson M, Oldfors A, Larsson NG. Downregulation of tfam and mtDNA copy number

during mammalian spermatogenesis. Mamm Genome 2001; 12: 787-92.

Ravier MA, Cheng-Xue R, Palmer AE, Henquin JC, Gilon P. Subplasmalemmal ca(2+) measurements in mouse pancreatic beta cells support the existence of an amplifying effect of glucose on insulin secretion. Diabetologia 2010; 53: 1947-57.

Rayner DV, Thomas ME, Trayhurn P. Glucose transporters (GLUTs 1-4) and their mRNAs in regions of the rat brain: Insulin-sensitive transporter expression in the cerebellum. Can J Physiol Pharmacol 1994; 72: 476-9.

Reivich M, Alavi A, Wolf A, Fowler J, Russell J, Arnett C, et al. Glucose metabolic rate kinetic model parameter determination in humans: The lumped constants and rate constants for [18F]fluorodeoxyglucose and [11C]deoxyglucose. J Cereb Blood Flow Metab 1985; 5: 179-92.

Reivich M, Kuhl D, Wolf A, Greenberg J, Phelps M, Ido T, et al. The [18F]fluorodeoxyglucose method for the measurement of local cerebral glucose utilization in man. Circ Res 1979; 44: 127-37.

Remes AM, Majamaa-Voltti K, Kärppä M, Moilanen JS, Uimonen S, Helander H, et al. Prevalence of large-scale mitochondrial DNA deletions in an adult finnish population. Neurology 2005; 64: 976-81.

Rich PR. The molecular machinery of keilin's respiratory chain. Biochem Soc Trans 2003; 31: 1095-105.

Rijzewijk LJ, van der Meer RW, Lubberink M, Lamb HJ, Romijn JA, de Roos A, et al. Liver fat content in type 2 diabetes: Relationship with hepatic perfusion and substrate metabolism. Diabetes 2010.

Rijzewijk LJ, van der Meer RW, Lamb HJ, de Jong HW, Lubberink M, Romijn JA, et al. Altered myocardial substrate metabolism and decreased diastolic function in nonischemic human diabetic cardiomyopathy: Studies with cardiac positron emission tomography and magnetic resonance imaging. J Am Coll Cardiol 2009; 54: 1524-32.

Roland PE, Eriksson L, Stone-Elander S, Widen L. Does mental activity change the oxidative metabolism of the brain? J Neurosci 1987; 7: 2373-89.

Rooyackers O, Myrenfors P, Nygren J, Thorell A, Ljungqvist O. Insulin stimulated glucose disposal in peripheral tissues studied with microdialysis and stable isotope tracers. Clin Nutr 2004; 23: 743-52.

Ros S, Zafra D, Valles-Ortega J, Garcia-Rocha M, Forrow S, Dominguez J, et al. Hepatic overexpression of a constitutively active form of liver glycogen synthase improves glucose homeostasis. J Biol Chem 2010.

Ruiz-Pesini E, Mishmar D, Brandon M, Procaccio V, Wallace DC. Effects of purifying and adaptive selection on regional variation in human mtDNA. Science 2004; 303: 223-6.

Ruiz-Pesini E, Lott MT, Procaccio V, Poole JC, Brandon MC, Mishmar D, et al. An enhanced MITOMAP with a global mtDNA mutational phylogeny. Nucleic Acids Res 2007; 35: D823-8.

Ruotsalainen U, Raitakari M, Nuutila P, Oikonen V, Sipila H, Teras M, et al. Quantitative blood flow measurement of skeletal muscle using oxygen-15-water and PET. J Nucl Med 1997; 38: 314-9.

Russell RR,3rd, Cline GW, Guthrie PH, Goodwin GW, Shulman GI, Taegtmeyer H. Regulation of exogenous and endogenous glucose metabolism by insulin and acetoacetate in the isolated working rat heart. A three tracer study of glycolysis, glycogen metabolism, and glucose oxidation. J Clin Invest 1997; 100: 2892-9.

Saada A, Shaag A, Mandel H, Nevo Y, Eriksson S, Elpeleg O. Mutant mitochondrial thymidine kinase in mitochondrial DNA depletion myopathy. Nat Genet 2001; 29: 342-4.

Saker PJ, Hattersley AT, Barrow B, Hammersley MS, Horton V, Gillmer MD, et al. UKPDS 21: Low prevalence of the mitochondrial transfer RNA gene (tRNA(leu(UUR))) mutation at position 3243bp in UK caucasian type 2 diabetic patients. Diabet Med 1997; 14: 42-5.

Sakura H, Ashcroft SJ, Terauchi Y, Kadowaki T, Ashcroft FM. Glucose modulation of ATP-sensitive K-currents in wild-type, homozygous and heterozygous glucokinase knock-out mice. Diabetologia 1998; 41: 654-9.

Salehi M, Aulinger B, Prigeon RL, D'Alessio DA. Effect of endogenous GLP-1 on insulin secretion in type 2 diabetes. Diabetes 2010; 59: 1330-7.

Salinari S, Bertuzzi A, Asnaghi S, Guidone C, Manco M, Mingrone G. First-phase insulin secretion restoration and differential response to glucose load depending on the route of administration in type 2 diabetic subjects after bariatric surgery. Diabetes Care 2009; 32: 375-80.

Salles JE, Kasamatsu TS, Dib SA, Moises RS. Beta-cell function in individuals carrying the mitochondrial tRNA leu (UUR) mutation. Pancreas 2007; 34: 133-7.

Salomaa V, Havulinna A, Saarela O, Zeller T, Jousilahti P, Jula A, et al. Thirty-one novel

biomarkers as predictors for clinically incident diabetes. PLoS One 2010; 5: e10100.

Sandhu JK, Sodja C, McRae K, Li Y, Rippstein P, Wei YH, et al. Effects of nitric oxide donors on cybrids harbouring the mitochondrial myopathy, encephalopathy, lactic acidosis and stroke-like episodes (MELAS) A3243G mitochondrial DNA mutation. Biochem J 2005; 391: 191-202.

Santer R, Schneppenheim R, Dombrowski A, Gotze H, Steinmann B, Schaub J. Mutations in GLUT2, the gene for the liver-type glucose transporter, in patients with fanconi-bickel syndrome. Nat Genet 1997; 17: 324-6.

Santorelli FM, Tanji K, Kulikova R, Shanske S, Vilarinho L, Hays AP, et al. Identification of a novel mutation in the mtDNA ND5 gene associated with MELAS. Biochem Biophys Res Commun 1997; 238: 326-8.

Saraste M. Oxidative phosphorylation at the fin de siecle. Science 1999; 283: 1488-93.

Sasarman F, Antonicka H, Shoubridge EA. The A3243G tRNALeu(UUR) MELAS mutation causes amino acid misincorporation and a combined respiratory chain assembly defect partially suppressed by overexpression of EFTu and EFG2. Hum Mol Genet 2008; 17: 3697-707.

Satake S, Moore MC, Igawa K, Converse M, Farmer B, Neal DW, et al. Direct and indirect effects of insulin on glucose uptake and storage by the liver. Diabetes 2002; 51: 1663-71.

Sato W, Tanaka M, Sugiyama S, Nemoto T, Harada K, Miura Y, et al. Cardiomyopathy and angiopathy in patients with mitochondrial myopathy, encephalopathy, lactic acidosis, and strokelike episodes. Am Heart J 1994; 128: 733-41.

Sayed S, Langdon DR, Odili S, Chen P, Buettger C, Schiffman AB, et al. Extremes of clinical and enzymatic phenotypes in children with hyperinsulinism caused by glucokinase activating mutations. Diabetes 2009; 58: 1419-27.

Sazanov LA, Jackson JB. Proton-translocating transhydrogenase and NAD- and NADP-linked isocitrate dehydrogenases operate in a substrate cycle which contributes to fine regulation of the tricarboxylic acid cycle activity in mitochondria. FEBS Lett 1994; 344: 109-16.

Scalettar BA, Abney JR, Hackenbrock CR. Dynamics, structure, and function are coupled in the mitochondrial matrix. Proc Natl Acad Sci U S A 1991; 88: 8057-61.

Schaefer AM, McFarland R, Blakely EL, He L, Whittaker RG, Taylor RW, et al. Prevalence of mitochondrial DNA disease in adults. Ann Neurol 2008; 63: 35-9.

Scheibye-Knudsen M, Quistorff B. Regulation of mitochondrial respiration by inorganic phosphate; comparing permeabilized muscle fibers and isolated mitochondria prepared from type-1 and type-2 rat skeletal muscle. Eur J Appl Physiol 2009; 105: 279-87.

Schuit F, De Vos A, Farfari S, Moens K, Pipeleers D, Brun T, et al. Metabolic fate of glucose in purified islet cells. glucose-regulated anaplerosis in beta cells. J Biol Chem 1997; 272: 18572-9.

Sebastian D, Hernandez-Alvarez MI, Segales J, Sorianello E, Munoz JP, Sala D, et al. Mitofusin 2 (Mfn2) links mitochondrial and endoplasmic reticulum function with insulin signaling and is essential for normal glucose homeostasis. Proc Natl Acad Sci U S A 2012; 109: 5523-8.

Segre AV, DIAGRAM Consortium, MAGIC investigators, Groop L, Mootha VK, Daly MJ, et al. Common inherited variation in mitochondrial genes is not enriched for associations with type 2 diabetes or related glycemic traits. PLoS Genet 2010; 6: e1001058.

Sherry NA, Tsai EB, Herold KC. Natural history of beta-cell function in type 1 diabetes. Diabetes 2005; 54 Suppl 2: S32-9.

Shi X, Burkart A, Nicoloro SM, Czech MP, Straubhaar J, Corvera S. Paradoxical effect of mitochondrial respiratory chain impairment on insulin signaling and glucose transport in adipose cells. J Biol Chem 2008; 283: 30658-67.

Shishido F, Uemura K, Inugami A, Tomura N, Higano S, Fujita H, et al. Cerebral oxygen and glucose metabolism and blood flow in mitochondrial encephalomyopathy: A PET study 1 159 356. Neuroradiology 1996; 38: 102-7.

Shoffner JM, Lott MT, Lezza AM, Seibel P, Ballinger SW, Wallace DC. Myoclonic epilepsy and ragged-red fiber disease (MERRF) is associated with a mitochondrial DNA tRNA(lys) mutation. Cell 1990; 61: 931-7.

Silander K, Mohlke KL, Scott LJ, Peck EC, Hollstein P, Skol AD, et al. Genetic variation near the hepatocyte nuclear factor-4 alpha gene predicts susceptibility to type 2 diabetes. Diabetes 2004; 53: 1141-9.

Silva JP, Kohler M, Graff C, Oldfors A, Magnuson MA, Berggren PO, et al. Impaired insulin secretion and beta-cell loss in tissue-specific knockout mice

with mitochondrial diabetes. Nat Genet 2000; 26: 336-40.

Silvestri G, Rana M, Odoardi F, Modoni A, Paris E, Papacci M, et al. Single-fiber PCR in MELAS(3243) patients: Correlations between intratissue distribution and phenotypic expression of the mtDNA(A3243G) genotype. Am J Med Genet 2000; 94: 201-6.

Simonsen L, Coker R, A L Mulla N, Kjaer M, Bulow J. The effect of insulin and glucagon on splanchnic oxygen consumption. Liver 2002; 22: 459-66.

Sirrenberg C, Bauer MF, Guiard B, Neupert W, Brunner M. Import of carrier proteins into the mitochondrial inner membrane mediated by Tim22. Nature 1996; 384: 582-5.

Smeitink JA, Elpeleg O, Antonicka H, Diepstra H, Saada A, Smits P, et al. Distinct clinical phenotypes associated with a mutation in the mitochondrial translation elongation factor EFTs. Am J Hum Genet 2006; 79: 869-77.

Smith TA, Blaylock MG. Treatment of breast tumor cells in vitro with the mitochondrial membrane potential dissipater valinomycin increases 18F-FDG incorporation. J Nucl Med 2007; 48: 1308-12.

Soejima A, Inoue K, Takai D, Kaneko M, Ishihara H, Oka Y, et al. Mitochondrial DNA is required for regulation of glucose-stimulated insulin secretion in a mouse pancreatic beta cell line, MIN6. J Biol Chem 1996; 271: 26194-9.

Sokoloff L, Reivich M, Kennedy C, Des Rosiers MH, Patlak CS, Pettigrew KD, et al. The [14C]deoxyglucose method for the measurement of local cerebral glucose utilization: Theory, procedure, and normal values in the conscious and anesthetized albino rat. J Neurochem 1977; 28: 897-916.

Sondergaard HM, Bottcher M, Marie MM, Schmitz O, Hansen SB, Nielsen TT, et al. Impact of type 2 diabetes on myocardial insulin sensitivity to glucose uptake and perfusion in patients with coronary artery disease. J Clin Endocrinol Metab 2006; 91: 4854-61.

Sparaco M, Simonati A, Cavallaro T, Bartolomei L, Grauso M, Piscioli F, et al. MELAS: Clinical phenotype and morphological brain abnormalities. Acta Neuropathol 2003; 106: 202-12.

Sproule DM, Kaufmann P, Engelstad K, Starc TJ, Hordof AJ, De Vivo DC. Wolff-parkinson-white syndrome in patients with MELAS. Arch Neurol 2007; 64: 1625-7.

Srivastava S, Diaz F, Iommarini L, Aure K, Lombes A, Moraes CT. PGC-1alpha/beta induced expression partially compensates for respiratory chain defects in cells from patients with mitochondrial disorders. Hum Mol Genet 2009; 18: 1805-12.

Stadhouders AM, Jap PH, Winkler HP, Eppenberger HM, Wallimann T. Mitochondrial creatine kinase: A major constituent of pathological inclusions seen in mitochondrial myopathies. Proc Natl Acad Sci U S A 1994; 91: 5089-93.

Stanley WC, Recchia FA, Lopaschuk GD. Myocardial substrate metabolism in the normal and failing heart. Physiol Rev 2005; 85: 1093-129.

Stanley WC, Meadows SR, Kivilo KM, Roth BA, Lopaschuk GD. Beta-hydroxybutyrate inhibits myocardial fatty acid oxidation in vivo independent of changes in malonyl-CoA content. Am J Physiol Heart Circ Physiol 2003; 285: H1626-31.

Stefan N, Kantartzis K, Haring HU. Causes and metabolic consequences of fatty liver. Endocr Rev 2008; 29: 939-60.

Steinthorsdottir V, Thorleifsson G, Reynisdottir I, Benediktsson R, Jonsdottir T, Walters GB, et al. A variant in CDKAL1 influences insulin response and risk of type 2 diabetes. Nat Genet 2007; 39: 770-5.

Stewart JB, Freyer C, Elson JL, Wredenberg A, Cansu Z, Trifunovic A, et al. Strong purifying selection in transmission of mammalian mitochondrial DNA. PLoS Biol 2008; 6: e10.

Stride A, Hattersley AT. Different genes, different diabetes: Lessons from maturity-onset diabetes of the young. Ann Med 2002; 34: 207-16.

Sue CM, Crimmins DS, Soo YS, Pamphlett R, Presgrave CM, Kotsimbos N, et al. Neuroradiological features of six kindreds with MELAS tRNA(leu) A2343G point mutation: Implications for pathogenesis. J Neurol Neurosurg Psychiatry 1998; 65: 233-40.

Sue CM, Tanji K, Hadjigeorgiou G, Andreu AL, Nishino I, Krishna S, et al. Maternally inherited hearing loss in a large kindred with a novel T7511C mutation in the mitochondrial DNA tRNA(ser(UCN)) gene. Neurology 1999; 52: 1905-8.

Suomalainen A, Majander A, Pihko H, Peltonen L, Syvänen AC. Quantification of tRNA3243(leu) point mutation of mitochondrial DNA in MELAS patients and its effects on mitochondrial transcription. Hum Mol Genet 1993; 2: 525-34.

Sutinen J, Korsheninnikova E, Funahashi T, Matsuzawa Y, Nyman T, Yki-Jarvinen H. Circulating concentration of adiponectin and its expression in subcutaneous adipose tissue in patients with highly active antiretroviral therapy-associated lipodystrophy. J Clin Endocrinol Metab 2003; 88: 1907-10.

Suzuki S, Hinokio Y, Hirai S, Onoda M, Matsumoto M, Ohtomo M, et al. Pancreatic beta-cell secretory defect associated with mitochondrial point mutation of the tRNA(LEU(UUR)) gene: A study in seven families with mitochondrial encephalomyopathy, lactic acidosis and stroke-like episodes (MELAS). Diabetologia 1994; 37: 818-25.

Suzuki Y, Hata T, Miyaoka H, Atsumi Y, Kadowaki H, Taniyama M, et al. Diabetes with the 3243 mitochondrial tRNALeu(UUR) mutation. characteristic neuroimaging findings. Diabetes Care 1996; 19: 739-43.

Suzuki Y, Iizuka T, Kobayashi T, Nishikawa T, Atsumi Y, Kadowaki T, et al. Diabetes mellitus associated with the 3243 mitochondrial tRNA(leu)(UUR) mutation: Insulin secretion and sensitivity. Metabolism 1997; 46: 1019-23.

Szczepaniak LS, Babcock EE, Schick F, Dobbins RL, Garg A, Burns DK, et al. Measurement of intracellular triglyceride stores by H spectroscopy: Validation in vivo. Am J Physiol 1999; 276: E977-89.

Szendroedi J, Chmelik M, Schmid AI, Nowotny P, Brehm A, Krssak M, et al. Abnormal hepatic energy homeostasis in type 2 diabetes. Hepatology 2009a; 50: 1079-86.

Szendroedi J, Schmid AI, Meyerspeer M, Cervin C, Kacerovsky M, Smekal G, et al. Impaired mitochondrial function and insulin resistance of skeletal muscle in mitochondrial diabetes. Diabetes Care 2009b; 32: 677-9.

't Hart LM, Simonis-Bik AM, Nijpels G, van Haeften TW, Schafer SA, Houwing-Duistermaat JJ, et al. Combined risk allele score of eight type 2 diabetes genes is associated with reduced first-phase glucose-stimulated insulin secretion during hyperglycemic clamps. Diabetes 2010; 59: 287-92.

Taivassalo T, Abbott A, Wyrick P, Haller RG. Venous oxygen levels during aerobic forearm exercise: An index of impaired oxidative metabolism in mitochondrial myopathy. Ann Neurol 2002; 51: 38-44.

Takahashi Y, Iida K, Takeno R, Kitazawa R, Kitazawa S, Kitamura H, et al. Hepatic failure and enhanced oxidative stress in mitochondrial diabetes. Endocr J 2008; 55: 509-14.

Takakubo F, Cartwright P, Hoogenraad N, Thorburn DR, Collins F, Lithgow T, et al. An amino acid substitution in the pyruvate dehydrogenase E1 alpha gene, affecting mitochondrial import of the precursor protein. Am J Hum Genet 1995; 57: 772-80.

Takala J, Keinänen O, Väisänen P, Kari A. Measurement of gas exchange in intensive care: Laboratory and clinical validation of a new device. Crit Care Med 1989; 17: 1041-7.

Takala TO, Nuutila P, Knuuti J, Luotolahti M, Yki-Järvinen H. Insulin action on heart and skeletal muscle glucose uptake in weight lifters and endurance athletes. Am J Physiol 1999a; 276: E706-11.

Takala TO, Nuutila P, Katoh C, Luotolahti M, Bergman J, Mäki M, et al. Myocardial blood flow, oxygen consumption, and fatty acid uptake in endurance athletes during insulin stimulation. Am J Physiol 1999b; 277: E585-90.

Tanahashi C, Nakayama A, Yoshida M, Ito M, Mori N, Hashizume Y. MELAS with the mitochondrial DNA 3243 point mutation: A neuropathological study. Acta Neuropathol 2000; 99: 31-8.

Tappy L, Dussoix P, Iynedjian P, Henry S, Schneiter P, Zahnd G, et al. Abnormal regulation of hepatic glucose output in maturity-onset diabetes of the young caused by a specific mutation of the glucokinase gene. Diabetes 1997; 46: 204-8.

Tatuch Y, Christodoulou J, Feigenbaum A, Clarke JT, Wherret J, Smith C, et al. Heteroplasmic mtDNA mutation (T----G) at 8993 can cause leigh disease when the percentage of abnormal mtDNA is high. Am J Hum Genet 1992; 50: 852-8.

Taylor RW, McDonnell MT, Blakely EL, Chinnery PF, Taylor GA, Howell N, et al. Genotypes from patients indicate no paternal mitochondrial DNA contribution. Ann Neurol 2003a; 54: 521-4.

Taylor RW, Giordano C, Davidson MM, d'Amati G, Bain H, Hayes CM, et al. A homoplasmic mitochondrial transfer ribonucleic acid mutation as a cause of maternally inherited hypertrophic cardiomyopathy. J Am Coll Cardiol 2003b; 41: 1786-96.

Tesarova M, Mayr JA, Wenchich L, Hansikova H, Elleder M, Blahova K, et al. Mitochondrial DNA depletion in alpers syndrome. Neuropediatrics 2004; 35: 217-23.

Thajeb P, Wu MC, Shih BF, Tzen CY, Chiang MF, Yuan RY. Brain single photon emission computed tomography in patients with A3243G mutation in mitochondrial DNA tRNA. Ann N Y Acad Sci 2005; 1042: 48-54.

Thorens B, Guillam MT, Beermann F, Burcelin R, Jaquet M. Transgenic reexpression of GLUT1 or GLUT2 in pancreatic beta cells rescues GLUT2-null mice from early death and restores normal glucose-stimulated insulin secretion. J Biol Chem 2000; 275: 23751-8.

Toft I, Jenssen T. Type 2 diabetic patients have increased gluconeogenic efficiency to substrate availability, but intact autoregulation of endogenous glucose production. Scand J Clin Lab Invest 2005; 65: 307-20.

Torres TP, Catlin RL, Chan R, Fujimoto Y, Sasaki N, Printz RL, et al. Restoration of hepatic glucokinase expression corrects hepatic glucose flux and normalizes plasma glucose in zucker diabetic fatty rats. Diabetes 2009; 58: 78-86.

Torroni A, Campos Y, Rengo C, Sellitto D, Achilli A, Magri C, et al. Mitochondrial DNA haplogroups do not play a role in the variable phenotypic presentation of the A3243G mutation. Am J Hum Genet 2003; 72: 1005-12.

Tranebjaerg L, Jensen PK, Van Ghelue M, Vnencak-Jones CL, Sund S, Elgjo K, et al. Neuronal cell death in the visual cortex is a prominent feature of the X-linked recessive mitochondrial deafness-dystonia syndrome caused by mutations in the TIMM8a gene. Ophthalmic Genet 2001; 22: 207-23.

Triepels R, van den Heuvel L, Loeffen J, Smeets R, Trijbels F, Smeitink J. The nuclear-encoded human NADH:Ubiquinone oxidoreductase NDUFA8 subunit: CDNA cloning, chromosomal localization, tissue distribution, and mutation detection in complex-I-deficient patients. Hum Genet 1998; 103: 557-63.

Tsao K, Aitken PA, Johns DR. Smoking as an aetiological factor in a pedigree with leber's hereditary optic neuropathy. Br J Ophthalmol 1999; 83: 577-81.

Tyynismaa H, Carroll CJ, Raimundo N, Ahola-Erkkilä S, Wenz T, Ruhanen H, et al. Mitochondrial myopathy induces a starvation-like response. Hum Mol Genet 2010.

Utriainen T, Takala T, Luotolahti M, Rönnemaa T, Laine H, Ruotsalainen U, et al. Insulin resistance characterizes glucose uptake in skeletal muscle but not in the heart in NIDDM. Diabetologia 1998; 41: 555-9.

Uusimaa J, Moilanen JS, Vainionpää L, Tapanainen P, Lindholm P, Nuutinen M, et al. Prevalence, segregation, and phenotype of the mitochondrial DNA 3243A>G mutation in children. Ann Neurol 2007; 62: 278-87.

van den Ouweland JM, Maechler P, Wollheim CB, Attardi G, Maassen JA. Functional and morphological abnormalities of mitochondria harbouring the tRNA(leu)(UUR) mutation in mitochondrial DNA derived from patients with maternally inherited diabetes and deafness (MIDD) and progressive kidney disease. Diabetologia 1999; 42: 485-92.

van Eijsden RG, Eijssen LM, Lindsey PJ, van den Burg CM, de Wit LE, Rubio-Gozalbo ME, et al. Termination of damaged protein repair defines the occurrence of symptoms in carriers of the m.3243A > G tRNA(leu) mutation. J Med Genet 2008; 45: 525-34.

Van Goethem G, Dermaut B, Lofgren A, Martin JJ, Van Broeckhoven C. Mutation of POLG is associated with progressive external ophthalmoplegia characterized by mtDNA deletions. Nat Genet 2001; 28: 211-2.

van Werven JR, Marsman HA, Nederveen AJ, Smits NJ, ten Kate FJ, van Gulik TM, et al. Assessment of hepatic steatosis in patients undergoing liver resection: Comparison of US, CT, T1-weighted dual-echo MR imaging, and point-resolved 1H MR spectroscopy. Radiology 2010; 256: 159-68.

Vänttinen M, Nuutila P, Pihlajamäki J, Hällsten K, Virtanen KA, Lautamäki R, et al. The effect of the Ala12 allele of the peroxisome proliferator-activated receptor-gamma2 gene on skeletal muscle glucose uptake depends on obesity: A positron emission tomography study. J Clin Endocrinol Metab 2005; 90: 4249-54.

Velho G, Petersen KF, Perseghin G, Hwang JH, Rothman DL, Pueyo ME, et al. Impaired hepatic glycogen synthesis in glucokinase-deficient (MODY-2) subjects. J Clin Invest 1996; 98: 1755-61.

Velho G, Froguel P, Clement K, Pueyo ME, Rakotoambinina B, Zouali H, et al. Primary pancreatic beta-cell secretory defect caused by mutations in glucokinase gene in kindreds of maturity onset diabetes of the young. Lancet 1992; 340: 444-8.

Velho G, Byrne MM, Clement K, Sturis J, Pueyo ME, Blanche H, et al. Clinical phenotypes, insulin secretion, and insulin sensitivity in kindreds with maternally inherited diabetes and deafness due to mitochondrial tRNALeu(UUR) gene mutation. Diabetes 1996; 45: 478-87.

Viljanen AP, Lautamäki R, Järvisalo M, Parkkola R, Huupponen R, Lehtimäki T, et al. Effects of weight loss on visceral and abdominal subcutaneous adipose tissue blood-flow and insulin-mediated glucose uptake in healthy obese subjects. Ann Med 2009; 41: 152-60.

Viljanen AP, Virtanen KA, Järvisalo MJ, Hällsten K, Parkkola R, Rönnemaa T, et al. Rosiglitazone treatment increases subcutaneous adipose tissue glucose uptake in parallel with perfusion in patients with type 2 diabetes: A double-blind, randomized study with metformin. J Clin Endocrinol Metab 2005; 90: 6523-8.

Viljanen AP, Karmi A, Borra R, Pärkkä JP, Lepomäki V, Parkkola R, et al. Effect of caloric restriction on

myocardial fatty acid uptake, left ventricular mass, and cardiac work in obese adults. Am J Cardiol 2009; 103: 1721-6.

Villarroya J, Dorado B, Vila MR, Garcia-Arumi E, Domingo P, Giralt M, et al. Thymidine kinase 2 deficiency-induced mitochondrial DNA depletion causes abnormal development of adipose tissues and adipokine levels in mice. PLoS One 2011; 6: e29691.

Virkamäki A, Rissanen E, Hämäläinen S, Utriainen T, Yki-Järvinen H. Incorporation of [3-3H]glucose and 2-[1-14C]deoxyglucose into glycogen in heart and skeletal muscle in vivo: Implications for the quantitation of tissue glucose uptake. Diabetes 1997; 46: 1106-10.

Virtanen KA, Peltoniemi P, Marjamäki P, Asola M, Strindberg L, Parkkola R, et al. Human adipose tissue glucose uptake determined using [(18)F]-fluoro-deoxy-glucose ([(18)F]FDG) and PET in combination with microdialysis. Diabetologia 2001; 44: 2171-9.

Virtanen KA, Lönnroth P, Parkkola R, Peltoniemi P, Asola M, Viljanen T, et al. Glucose uptake and perfusion in subcutaneous and visceral adipose tissue during insulin stimulation in nonobese and obese humans. J Clin Endocrinol Metab 2002; 87: 3902-10.

Virtanen KA, Iozzo P, Hällsten K, Huupponen R, Parkkola R, Janatuinen T, et al. Increased fat mass compensates for insulin resistance in abdominal obesity and type 2 diabetes: A positron-emitting tomography study. Diabetes 2005; 54: 2720-6.

vom Dahl J, Herman WH, Hicks RJ, Ortiz-Alonso FJ, Lee KS, Allman KC, et al. Myocardial glucose uptake in patients with insulin-dependent diabetes mellitus assessed quantitatively by dynamic positron emission tomography. Circulation 1993; 88: 395-404.

Vydt TC, de Coo RF, Soliman OI, Ten Cate FJ, van Geuns RJ, Vletter WB, et al. Cardiac involvement in adults with m.3243A>G MELAS gene mutation. Am J Cardiol 2007; 99: 264-9.

Wahbi K, Larue S, Jardel C, Meune C, Stojkovic T, Ziegler F, et al. Cardiac involvement is frequent in patients with the m.8344A>G mutation of mitochondrial DNA. Neurology 2010; 74: 674-7.

Wahlund LO, Barkhof F, Fazekas F, Bronge L, Augustin M, Sjogren M, et al. A new rating scale for age-related white matter changes applicable to MRI and CT 13. Stroke 2001; 32: 1318-22.

Wahren J, Felig P, Ahlborg G, Jorfeldt L. Glucose metabolism during leg exercise in man. J Clin Invest 1971; 50: 2715-25.

Wai T, Teoli D, Shoubridge EA. The mitochondrial DNA genetic bottleneck results from replication of a subpopulation of genomes. Nat Genet 2008; 40: 1484-8.

Walker M, Mari A, Jayapaul MK, Bennett SM, Ferrannini E. Impaired beta cell glucose sensitivity and whole-body insulin sensitivity as predictors of hyperglycaemia in non-diabetic subjects. Diabetologia 2005; 48: 2470-6.

Wallace DC, Singh G, Lott MT, Hodge JA, Schurr TG, Lezza AM, et al. Mitochondrial DNA mutation associated with leber's hereditary optic neuropathy. Science 1988; 242: 1427-30.

Wang CH, Leung N, Lapointe N, Szeto L, Uffelman KD, Giacca A, et al. Vasopeptidase inhibitor omapatrilat induces profound insulin sensitization and increases myocardial glucose uptake in zucker fatty rats: Studies comparing a vasopeptidase inhibitor, angiotensin-converting enzyme inhibitor, and angiotensin II type I receptor blocker. Circulation 2003; 107: 1923-9.

Wang J, Wilhelmsson H, Graff C, Li H, Oldfors A, Rustin P, et al. Dilated cardiomyopathy and atrioventricular conduction blocks induced by heart-specific inactivation of mitochondrial DNA gene expression. Nat Genet 1999; 21: 133-7.

Weyer C, Funahashi T, Tanaka S, Hotta K, Matsuzawa Y, Pratley RE, et al. Hypoadiponectinemia in obesity and type 2 diabetes: Close association with insulin resistance and hyperinsulinemia. J Clin Endocrinol Metab 2001; 86: 1930-5.

Whittaker RG, Schaefer AM, McFarland R, Taylor RW, Walker M, Turnbull DM. Prevalence and progression of diabetes in mitochondrial disease. Diabetologia 2007; 50: 2085-9.

Whittaker RG, Blackwood JK, Alston CL, Blakely EL, Elson JL, McFarland R, et al. Urine heteroplasmy is the best predictor of clinical outcome in the m.3243A>G mtDNA mutation. Neurology 2009; 72: 568-9.

Wibrand F, Jeppesen TD, Frederiksen AL, Olsen DB, Duno M, Schwartz M, et al. Limited diagnostic value of enzyme analysis in patients with mitochondrial tRNA mutations. Muscle Nerve 2010; 41: 607-13.

Willems JL, Monnens LA, Trijbels JM, Veerkamp JH, Meyer AE, van Dam K, et al. Leigh's encephalomyelopathy in a patient with cytochrome c oxidase deficiency in muscle tissue. Pediatrics 1977; 60: 850-7.

Woerle HJ, Szoke E, Meyer C, Dostou JM, Wittlin SD, Gosmanov NR, et al. Mechanisms for abnormal postprandial glucose metabolism in type 2 diabetes. Am J Physiol Endocrinol Metab 2006; 290: E67-77.

Wojtaszewski JF, Higaki Y, Hirshman MF, Michael MD, Dufresne SD, Kahn CR, et al. Exercise modulates postreceptor insulin signaling and glucose transport in muscle-specific insulin receptor knockout mice. J Clin Invest 1999; 104: 1257-64.

Wredenberg A, Freyer C, Sandström ME, Katz A, Wibom R, Westerblad H, et al. Respiratory chain dysfunction in skeletal muscle does not cause insulin resistance. Biochem Biophys Res Commun 2006; 350: 202-7.

Wredenberg A, Wibom R, Wilhelmsson H, Graff C, Wiener HH, Burden SJ, et al. Increased mitochondrial mass in mitochondrial myopathy mice. Proc Natl Acad Sci U S A 2002; 99: 15066-71.

Wright JJ, Kim J, Buchanan J, Boudina S, Sena S, Bakirtzi K, et al. Mechanisms for increased myocardial fatty acid utilization following short-term high-fat feeding. Cardiovasc Res 2009; 82: 351-60.

Wyss MT, Weber B, Treyer V, Heer S, Pellerin L, Magistretti PJ, et al. Stimulation-induced increases of astrocytic oxidative metabolism in rats and humans investigated with 1-11C-acetate. J Cereb Blood Flow Metab 2009; 29: 44-56.

Yamagata K, Furuta H, Oda N, Kaisaki PJ, Menzel S, Cox NJ, et al. Mutations in the hepatocyte nuclear factor-4alpha gene in maturity-onset diabetes of the young (MODY1). Nature 1996; 384: 458-60.

Yamasoba T, Goto Y, Oka Y, Nishino I, Tsukuda K, Nonaka I. Atypical muscle pathology and a survey of cis-mutations in deaf patients harboring a 1555 A-to-G point mutation in the mitochondrial ribosomal RNA gene. Neuromuscul Disord 2002; 12: 506-12.

Yechoor VK, Patti ME, Ueki K, Laustsen PG, Saccone R, Rauniyar R, et al. Distinct pathways of insulin-regulated versus diabetes-regulated gene expression: An in vivo analysis in MIRKO mice. Proc Natl Acad Sci U S A 2004; 101: 16525-30.

Yehuda-Shnaidman E, Buehrer B, Pi J, Kumar N, Collins S. Acute stimulation of white adipocyte respiration by PKA-induced lipolysis. Diabetes 2010.

Yi M, Weaver D, Hajnoczky G. Control of mitochondrial motility and distribution by the calcium signal: A homeostatic circuit. J Cell Biol 2004; 167: 661-72.

Yoneda M, Maeda M, Kimura H, Fujii A, Katayama K, Kuriyama M. Vasogenic edema on MELAS: A serial study with diffusion-weighted MR imaging. Neurology 1999; 53: 2182-4.

Zanna C, Ghelli A, Porcelli AM, Karbowski M, Youle RJ, Schimpf S, et al. OPA1 mutations associated with dominant optic atrophy impair oxidative phosphorylation and mitochondrial fusion. Brain 2008; 131: 352-67.

Zeviani M, Di Donato S. Mitochondrial disorders 1 59. Brain 2004; 127: 2153-72.

Zhang CY, Baffy G, Perret P, Krauss S, Peroni O, Grujic D, et al. Uncoupling protein-2 negatively regulates insulin secretion and is a major link between obesity, beta cell dysfunction, and type 2 diabetes. Cell 2001; 105: 745-55.

Zhang HH, Huang J, Duvel K, Boback B, Wu S, Squillace RM, et al. Insulin stimulates adipogenesis through the akt-TSC2-mTORC1 pathway. PLoS One 2009; 4: e6189.

Zhang J, Li X, Mueller M, Wang Y, Zong C, Deng N, et al. Systematic characterization of the murine mitochondrial proteome using functionally validated cardiac mitochondria. Proteomics 2008; 8: 1564-75.

Zhao C, Rutter GA. Overexpression of lactate dehydrogenase A attenuates glucose-induced insulin secretion in stable MIN-6 beta-cell lines. FEBS Lett 1998; 430: 213-6.

Zhu Z, Yao J, Johns T, Fu K, De Bie I, Macmillan C, et al. SURF1, encoding a factor involved in the biogenesis of cytochrome c oxidase, is mutated in leigh syndrome. Nat Genet 1998; 20: 337-43.

Zisman A, Peroni OD, Abel ED, Michael MD, Mauvais-Jarvis F, Lowell BB, et al. Targeted disruption of the glucose transporter 4 selectively in muscle causes insulin resistance and glucose intolerance. Nat Med 2000; 6: 924-8.